ELECTRON TRANSFER MECHANISM AND POTENTIAL APPLICATIONS OF α-HELICAL PEPTIDES

A Thesis Submitted to the College of

Graduate Studies and Research

In Partial Fulfillment of the Requirements

For the Degree of Doctor of Philosophy

In the Department of Chemistry

University of Saskatchewan

Saskatoon

By

HIMADRI SHEKHAR MANDAL

Keywords: peptide, electron transfer, electrochemistry, photocurrent, nanoparticles

PERMISSION TO USE

Presenting this thesis in partial fulfillment of the requirements for a degree of Doctorate of Philosophy from the University of Saskatchewan, I agree that the libraries of this university may make it available for inspection. I further agree that permission for copying of this thesis in any manner, in whole or in part, for scholarly purposes may be granted by the professor or professors who supervised my thesis work or, in their absence, by the Head of the Department of Chemistry or the Dean of the College of Graduate Studies and Research. It is understood that any copying or publication or use of this thesis or parts thereof, for financial gain shall not be allowed without my written permission. It is also understood that due recognition shall be given to me and to the University of Saskatchewan in any scholarly use which may be made of any material in this thesis.

Requests for permission to copy or to make other use of material in this thesis in whole or part should be addressed to:

Head of the Department of Chemistry

University of Saskatchewan

Saskatoon, Saskatchewan,

S7K 5C9

ABSTRACT

Understanding long range electron transfer (ET) in proteins is of fundamental interest to elucidate the complex nature of many biological processes. The mechanistic discussion is highly debated in the literature and the factors that control this process are still not clear. Because of the structural complexity and dynamic nature, it is very difficult to correctly evaluate long range ET in proteins. The study of simple model peptides having specific secondary structures is useful for a systematic and accurate evaluation. The polypeptide matrix in the photosynthetic reaction centre is rich in helices and this particular structural motif is believed to play an important role in ET in nature. In this thesis, ET study through some synthetic α-helical model peptides is described. The model peptides studied herein contain the redox-active ferrocene at one end and the thiol-functionalised Cys residue at the other. Films of these peptides were formed on the surface of gold electrodes via the Au-S bond, and by employing cyclic voltammetry, the rate of ET between the pendant ferrocene and the gold electrode through the peptide spacer has been evaluated. My study indicates that ET in α-helical peptides is a function of molecular dynamics and occurs via a tunnelling mechanism. These findings are significant and expected to offer new directions in the highly controversial discussion on ET in proteins.

This thesis also describes investigations in two important areas of applications of the α-helices. The first is "photocurrent generation upon laser excitation of light-harvesting chromophore-functionalised peptides" which mimics the natural photosynthetic centre. This important area of research can promote development of nano-scaled photovoltaic devices. Surprisingly, following the conventional experimental protocols, a photocurrent was observed in the absence of a chromophore and even by the

irradiation of a bare gold electrode with laser light. It is suggested that an important consequence of laser irradiation has been overlooked in several publications and the so-called photocurrent phenomenon may be a consequence of laser heating.

"Peptide-protected nanoparticles" is another area of research receiving significant attention these days due to its potential relevance in biomedical applications. However, peptides are highly flexible and their structure can change depending on the nature of the environment. Since the reactivity of a peptide is related to its secondary structure, any conformational change could seriously alter the overall activity of the peptide-protected nanoparticles. In this thesis, the structural investigation of an α-helical peptide was carried out and it was found that the radius of curvature of nanoparticles has a profound effect on the structure of the adsorbate peptides and thereby, may affect the overall activity of the peptide-protected nanoparticles.

.

ACKNOWLEDGMENTS

I sincerely express my gratitude to my supervisor Dr. H.-B. Kraatz for his continuous support and guidance throughout the progress of this work. I'm also extremely grateful to my Advisory Committee members: Dr. Stephen G. Urquhart, Dr. Stephen Foley and Dr. Susan Kaminskyj. I sincerely acknowledge the help from Dr. Ian Burgess, Dr. Todd Sutherland, Ken Thoms, Jason Maley, Sarah Caldwell and the members of our group. The Department of Chemistry, the University of Saskatchewan and the Natural Sciences and Engineering Research Council of Canada (NSERC) are gratefully acknowledged for financial support.

DEDICATION

This work is dedicated to my Parents:

Kishori Mohan Mandal

&

Pratima Rani Mandal

TABLE OF CONTENT

LIST OF FIGURES

LIST OF SCHEMES

LIST OF TABLES

LIST OF ABBREVIATIONS

A	acceptor
AA	amino acid
Å	angstrom
AFM	atomic force microscopy
Ala	alanine
Asn	aspartine
B	bridge
BOP	benzotriazol-1-yl-*N*-oxy-tris(dimethylamino)-phosphonium hexafluoro-phosphate
CD	circular dichroism
CV	cyclic voltammetry
Cys	cystein
D	donor
DCM	dichloromethane
DBU	1,8-diazabicyclo[5.4.0]undec-7-ene
DIPEA	diisopropylethylamine
DM	dipole moment
EDC	1-ethyl-3-(3-dimethylaminopropyl)-carbodiimide
Fc	ferrocene
EIS	electrochemical impedance spectroscopy
ET	electron transfer
$E^{0'}$	formal potential
FT-IR	Fourier transform infrared spectroscopy
FT-RAIRS	Fourier transform-reflection absorption infrared spectroscopy
HOBt	hydroxybenzotriazole
Leu	leucine
Lys	lysine
MD	molecular dynamics
ps	picosecond

Pro	proline
SAM	self-assembled monolayer
STM	scanning tunneling microscopy
STS	scanning tunneling spectroscopy
SPPS	solid phase peptide synthesis
TFA	trifluroacetic acid
Thr	threonine
TFE	trifluoroethanol
TEM	transmission electron microscopy
XPS	X-ray photoelectron spectroscopy

Chapter 1

Introduction

1.1. Overview

Electron transfer (ET) study of proteins is of fundamental interest to understand the complex nature of photosynthesis, respiration and other important biological processes.[1] To date, there are several reports[2-8] in the literature that have investigated this phenomenon, but the interpretations are controversial and the actual mechanism of ET and the factors that control this highly efficient process in nature are still elusive. One of the major problems in this regard is that proteins are structurally complex: they have multiple structural motifs (α-helix, β-sheet, etc.).[9] In addition, proteins are dynamic and the time-scale for this dynamics can vary from ps to many seconds,[10-13] resulting in potentially numerous structural conformers during the experimental measurement of long range ET. Thus, studying ET in simple synthetic model peptides having specific secondary structures is very useful to know the role of each motif in ET and to have a correct interpretation of the experimental observation. Besides, the study is also important for using peptide-based structures as possible candidates for molecular electronics, which, because of the versatility of peptide syntheses and ease of functionalization, are becoming increasingly popular. This thesis describes the study of ET through some α-helical model peptides, motivated by the fact that the proteins involved in biological ET is rich in helical content (Figure 1.1) and this particular structural motif is believed to play an important role in ET in proteins.[14] The potential

of using the α-helical peptides for two nano-scaled applications (photocurrent generation with chromophore-functionalized helical peptides and peptide-protected nanoparticles) is also described in this thesis.

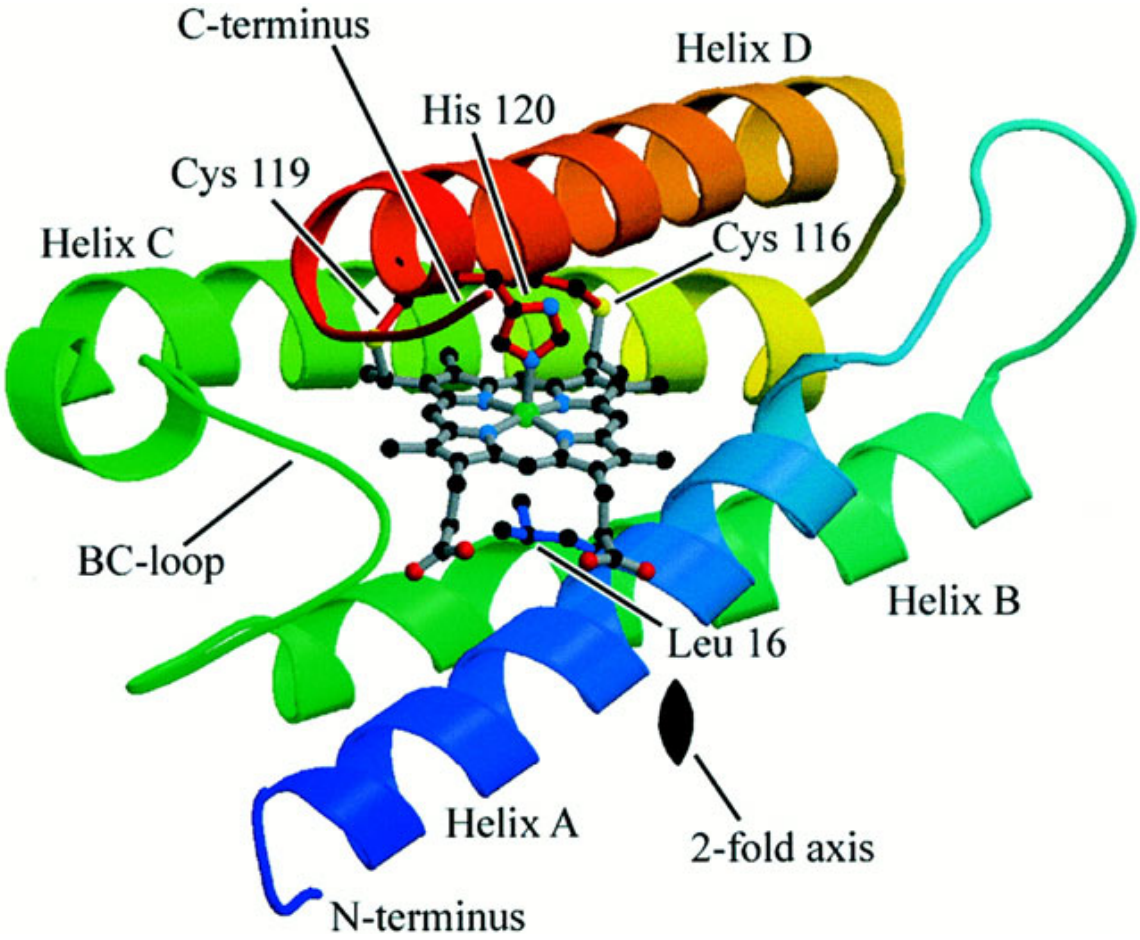

Figure 1.1. Helical peptides surrounding the heme group in a single subunit of the reduced *Alcaligenes xylosoxidans* cytochrome *c*.[14b] Figure reproduced with the permission from Lawson et al, *The EMBO Journal* **2000**, 19, 5661. Copyright © 2000 by the European Molecular Biology Organization.

1.2. The α-Helix

1.2.1. Structure

Proteins are polymers of the twenty common amino acids (AAs) which are linked to each other by the amide bond (Figure 1.2). The number of AA in natural proteins ranges from dozens to thousands.[9]

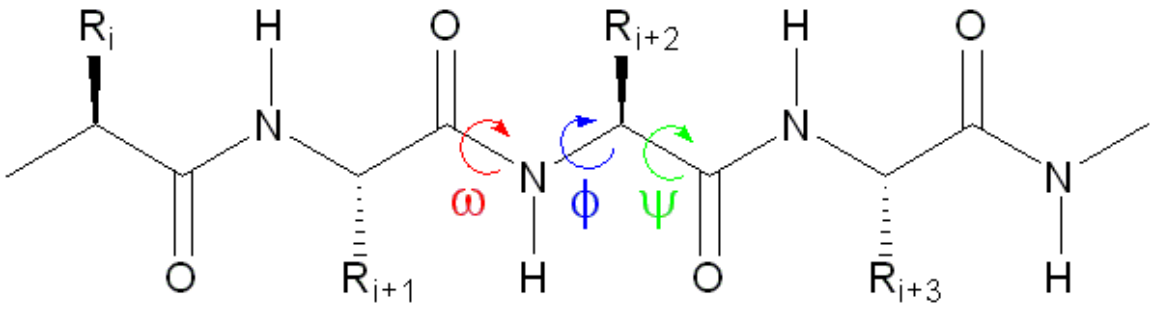

Figure 1.2. The amide bond and the related torsion angles.[9]

Each AA can locally change the peptide backbone (depending on the bulkiness and the geometry of the side chain) and based on the sequence of the AAs, the backbone adopts different secondary structures like helices, sheets and turns. Three torsion angles (ω, Φ and Ψ) are used to describe the polypeptide backbone in a particular secondary structure (Table 1.1).[15] Due to the partial double bond nature of the amide group, ω is always around 180° (proline is the only exception, where ω ≈ 0°), whereas Φ and Ψ vary depending on the secondary structure.[9, 15]

Table 1.1. Torsion angles (º) for the major secondary structures observed in proteins. [15]

	Φ	Ψ	ω
α-helix	180	-57	-47
3_{10}-helix	180	-49	-27
β-sheet	180	-119	-47
Antiparallel β-sheet	180	-139	135
Polyproline I	0	-83	158
Polyproline II	180	-78	149

The α-helix is the most frequently observed secondary structure observed in proteins,[16] where ω, Φ and Ψ are 180º, -57º and -47º, respectively.[15] In the α-helix, the polypeptide backbone adopts a coiled conformation. Each turn consists of 3.6 amino acid residues with a pitch length of 5.4 Å.[9,15] One of the special features of the α-helix is that this structure orients the N-H of a particular amide group (i^{th}) to the C=O of another that is situated four residues away ($i+4^{th}$) in such a fashion that they can form an intra-molecular hydrogen bond, resulting in a network of H-bonds throughout the helical backbone (Figure 1.3).[9,15]

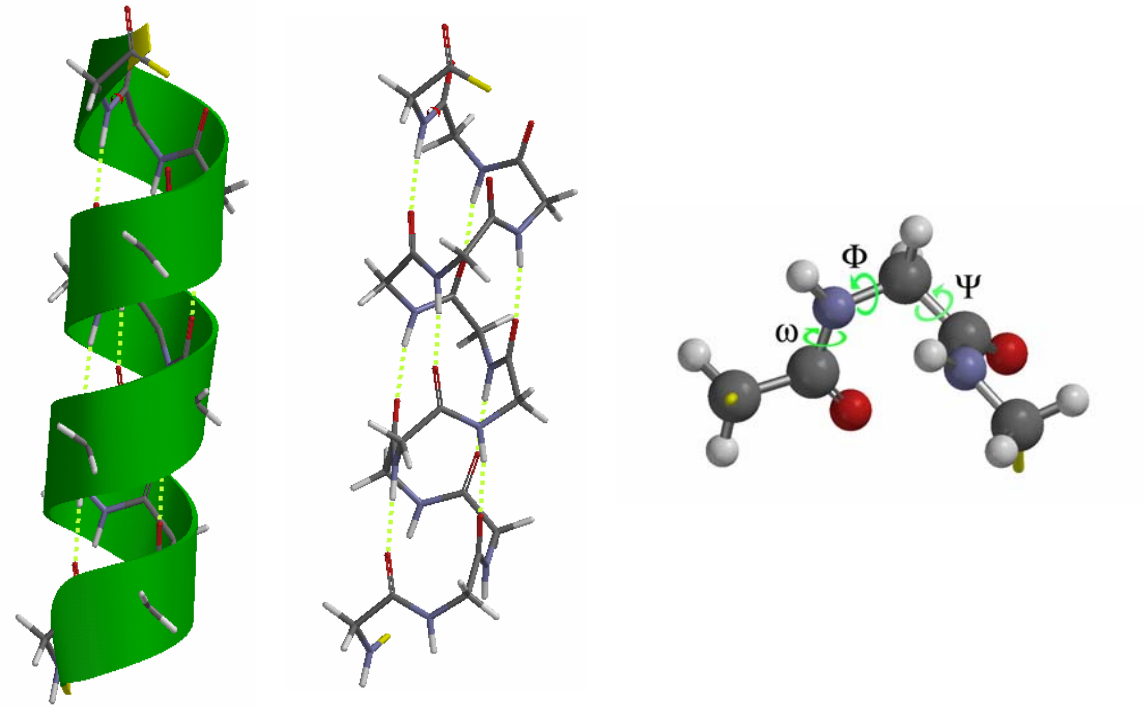

Figure 1.3. Structure of the α-helix showing intra-molecular H-bonding network and the related dihedrals.

Another important feature of the α-helix is the presence of a strong and permanent dipole moment (DM) along the helical axis.[17] Each amide has a DM (about 3.5 D) and in the α-helix, the amides are oriented in the same direction (Figure 1.4). The positive and the negative ends of the dipole are at the N- and C-terminals respectively. This DM produces a strong electrostatic field along the helical axis and is believed to play an important role in ET.[18-20]

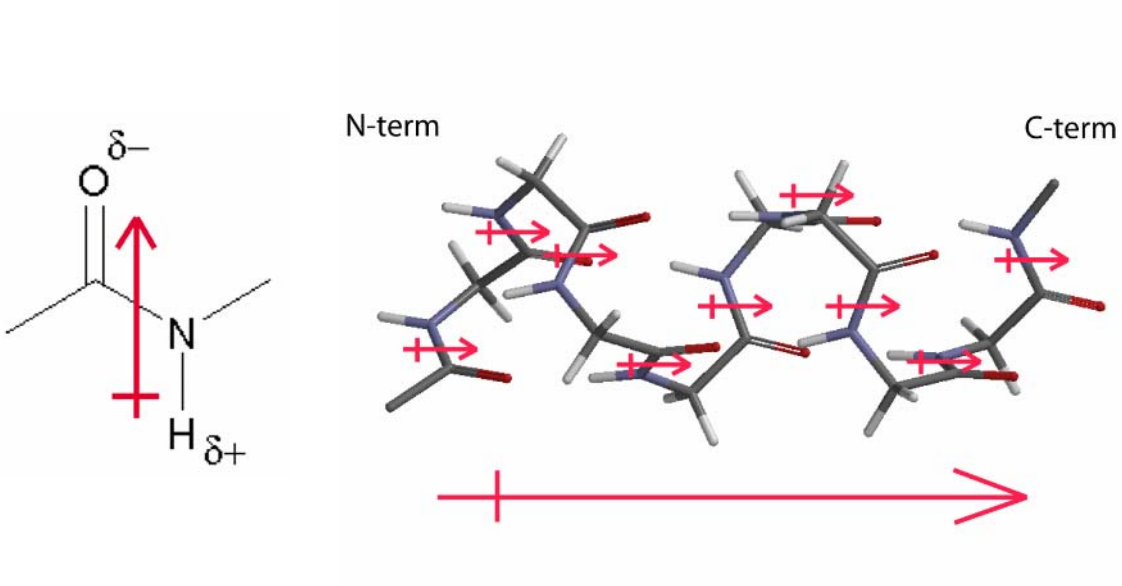

Figure 1.4. Dipole moment in an amide bond (left) and the arrangement of the individual dipoles in the α-helix, resulting in a net dipole moment along the helical axis (right).

1.2.2. Design of Synthetic α-Helices

The design of short synthetic model α-helical peptides is challenging. If the α-helical peptide is removed from the protective environment of the protein, its secondary structure may not be stable.[21,22] An extensive array of literature demonstrates the many and varied methods by which isolated α-helices may be stabilized: (i) the use of salt bridges as non-covalent side-chain restraints,[23] (ii) a variety of covalent side-chain linking agents[24-31] and metal ions that can be ligated to specific side-chains,[32] (iii) π-π interaction among the side chains of AAs[33] (Figure 1.5).

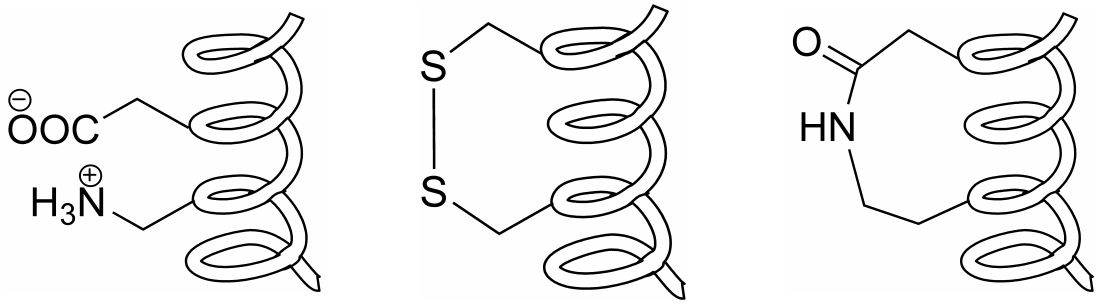

Figure 1.5. Few examples to stabilize the α-helix.[15] Figures redrawn from ref. 15.

Leu-based peptides are well-known for adopting α-helical conformation. Leu has the highest helix forming potential of all the naturally occurring AAs[34-36] and in nature, Leu is frequently observed in the helical motifs of proteins.[34,35] Synthetic Leu-rich peptides are stabilized by the hydrophobic interactions among the branched side chain of Leu residues.[34,37]

1.2.3. Dynamics of the α-Helix

One of the important features of short synthetic helices is that they exist as an equilibrium mixture of α- and 3_{10}-helical conformers in solution (Figure 1.6).[38] The 3_{10} conformer is more stretched (the corresponding dihedrals are 180, −49 and −27° for ω, Φ and Ψ, respectively) and generally less stable (because of the steric repulsions among the side chains of AA residues) compared to the α-helical conformer although the number of H-bonds is greater in the former (the intra-molecular H-bonding pattern is different in the 3_{10} conformer; i^{th} residue forms H-bond with the $i+3^{th}$ one).[38-45] Extensive molecular dynamics (MD) simulations showed that the time-scale for this equilibrium is ~ ps[46,47] and experimental studies indicated that dynamics of this equilibrium is affected by the nature of the AA residues, length of the peptide, solvent

and temperature.[38-45] With the increase of the chain length and decrease of the temperature, the equilibrium shifts to the α-helical conformer.[38,48]

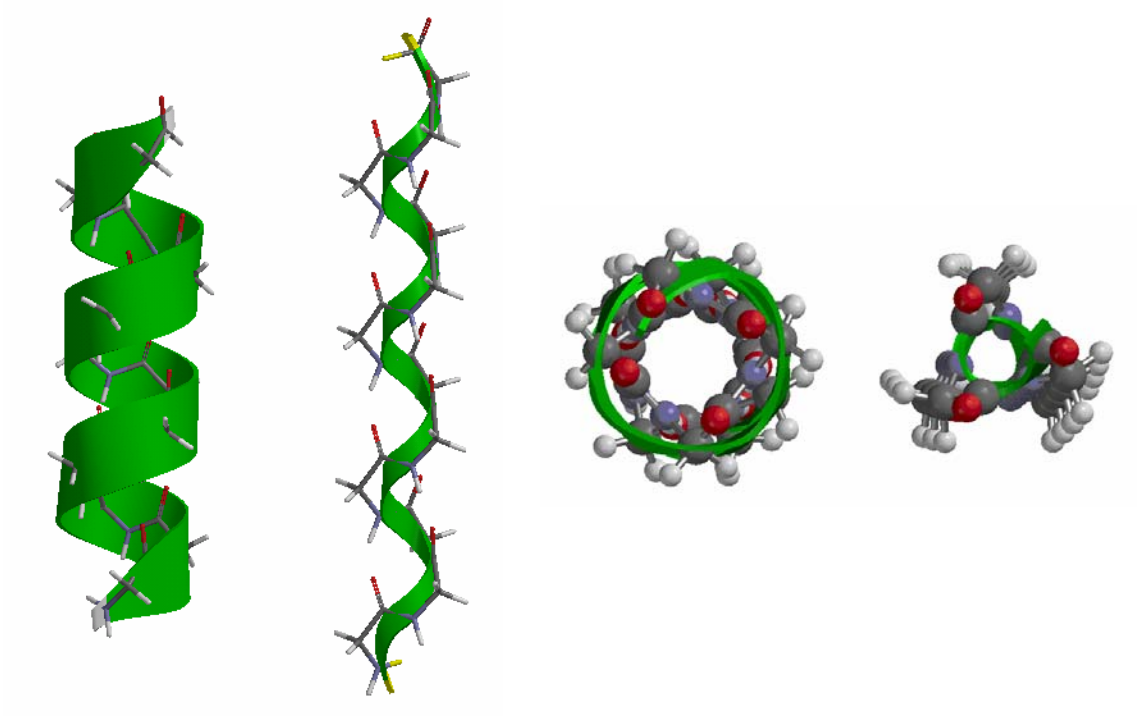

Figure 1.6. α- and 3_{10}–helical conformers.

1.3. General Electron Transfer Theory

According to Marcus, the rate of ET from a donor (D) to an acceptor (A) separated by a bridge (B) (Scheme 1.1) is expressed by Equation 1.1.[2]

Scheme 1.1. ET from a donor (D) to an acceptor (A) through a bridge (B).

$$k_{et} = \left(\frac{4\pi^3}{h^2 \lambda k_B T}\right)^{1/2} (H_{DA}) \exp\left(-\frac{\Delta G^{\neq}}{k_B T}\right) \quad \text{.....} \quad \textbf{1.1}$$

$$\Delta G^{\neq} = \frac{(\Delta G^0 + \lambda)^2}{4\lambda} \quad \text{.....} \quad \textbf{1.2}$$

Where, h = the Planck's constant,

k_B = the Boltzmann constant,

H_{DA} = the electronic coupling matrix between the D and A. Its value depends on the D-A separation and the nature of the bridge; with the increase of the separation, H_{AD} generally decreases exponentially resulting in an exponential decrease of ET rate from the D to the A.

$\Delta G^{\neq}$ = the reaction activation energy, and

λ = the reorganization energy which is associated with the nuclear rearrangement upon ET.

The potential energy of both the reactant (D-B-A) and the product (D^+-B-A^-) states is a function of the change in all the coordinates associated with the nuclei within the D-B-A and the surrounding medium, and hence the associated potential energy surfaces (PESs) are multidimensional.[2,49] For the reactant (D-B-A), there is a particular conformation which has the lowest potential energy and similarly, there is another minimum for the product state (D^+-B-A^-). The complex multidimensional scenario can be visualized by a simple one-dimensional PES along the coordinate connecting the D-B-A and D^+-B-A^- minima. From Equation 1.1, we can see that when $\Delta G^0 < \lambda$, the rate of ET increases with the increase of ΔG^0 (the normal region), and reaches a maximum at $\Delta G^0 = \lambda$ (the reaction becomes activation-less at this point). But when $\Delta G^0 > \lambda$, k_{et}

is predicted to decrease again (the "inverted region"), giving overall a parabolic dependence of k_{et} on ΔG^0 (Figure 1.7).[2,50] This prediction has been shown to be true for proteins[6] by measuring k_{et} at different ΔG^0, validating the Marcus theory of ET.

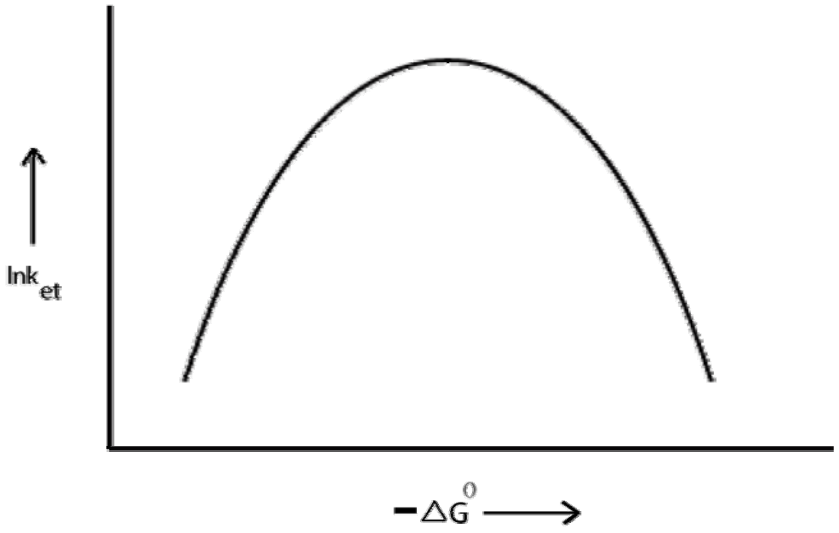

Figure 1.7. Graphical representation of the driving force dependency of the ET rate.[2,50] Figure redrawn from ref. 50.

1.4. Determination of the Electron Transfer Rate by Electrochemical Methods

For the electrochemical determination of the ET rates, a clean gold electrode is soaked in a solution of the compound of interest which typically has a thiol group at one end and a redox-active group (usually ferrocene, Fc) at the other.[51] Gold has a strong tendency to react with the thiol and the compound is bound covalently on the surface of gold electrode via the formation of the Au-S bond. After five days (conventionally), the electrode is taken out from the solution and washed thoroughly with the solvent to remove any physisorbed compounds. The procedure is very straightforward and is called

"self-assembly".[52] In the literature, there are numerous reports that used this procedure to form organic monolayers (self-assembled monolayers or SAMs) on gold surface (Scheme 1.2).[19,20,51-53]

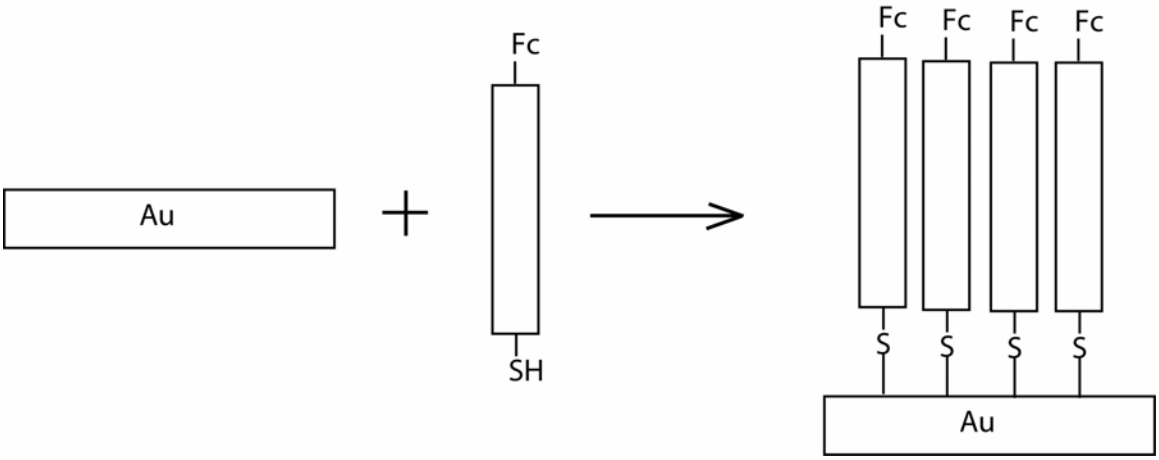

Scheme 1.2. Schematic representation of self assembly on gold surfaces.

The modified electrode is then attached to an electrochemical cell and cyclic voltammograms (CV) are recorded. In CV, potential of the gold electrode is scanned over a range and at certain potentials, the Fc moiety is oxidized, the electron travels through the spacer to the electrode and a current peak is obtained. When the direction of the scan is reversed, the oxidized Fc^+ takes up the lost electron back from the electrode giving another peak in the opposite direction (Figure 1.8).[51] CVs are recorded at different scan rates. Depending on the ET kinetics, scan rate can vary from 0.001 (for slow ET kinetics) to thousands of V/s (fast). If the rate of ET between the Fc and the gold electrode through the spacer is faster than the scan rate in CV, there will be no separation between the oxidation and the reduction peaks. When ET is slower than the scan rate, the moving electron lags behind the scan rate and those peaks becomes

separated. The CVs collected in these faster scan rates are used to extract the rate of ET through the spacer.[51]

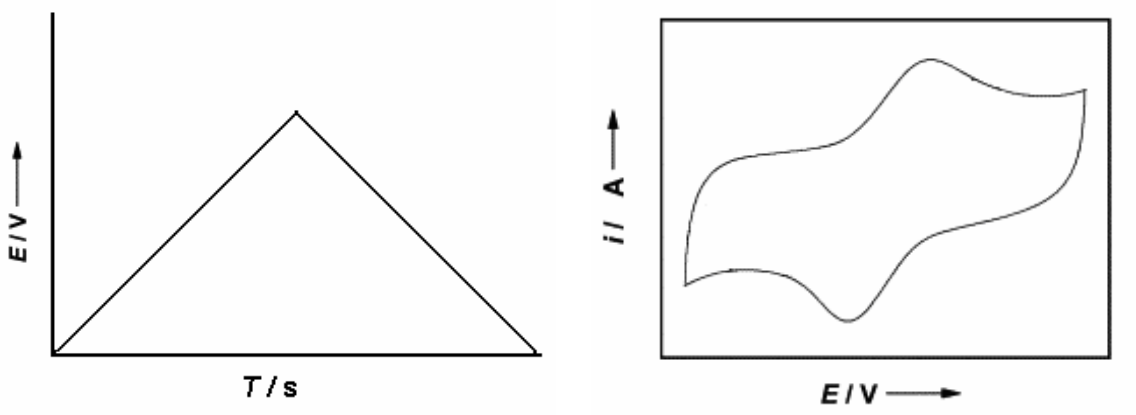

Figure 1.8. Change of potential with time in a CV experiment (left) and a typical CV showing peaks due to the redox activity of the Fc moiety (right).

The application of the Marcus theory (discussed in section 1.3) to extract k_{et} from the above electrochemical assembly is not straight-forward.[54] In this case, Butler-Volmer (B-V) formalism[55] is simple and at low driving force, gives results consistent with the Marcus model.[54,56] In the B-V formalism, the current and the rate for a reversible ET process are given by Equations 1.3-1.5:[55]

$$\mathrm{Ox} + \mathrm{e} \underset{k_{Ox}}{\overset{k_{Red}}{\rightleftharpoons}} \mathrm{Red}$$

$$k_{\mathrm{Red}} = k^o e^{-\alpha f(E-E^{o'})} \qquad \textbf{1.3}$$

$$k_{Ox} = k^o e^{(1-\alpha) f(E-E^{o'})} \qquad \textbf{1.4}$$

$$i = FAk^o[C_{Ox} e^{-\alpha f(E-E^{o'})} - C_{\mathrm{Red}} e^{(1-\alpha) f(E-E^{o'})} \qquad \textbf{1.5}$$

Where,

k^o = the standard rate constant,

α = the transfer coefficient,

C_{Oxd} = concentration of the oxidized species,

C_{Red} = concentration of the reduced species,

E = the potential,

$E^{o'}$ = the formal potential of the redox group,

i = the current,

F = the Faraday constant, and

A = the surface area of the working electrode.

After background subtraction, the redox peaks in CV can be used to extract ET rates using spreadsheet programs. The B-V formalism is a very popular method and using this, to date, a vast amount of work exists in the literature that reported ET rates through different spacers like alkyl,[57] peptide,[58] protein,[54] DNA,[59] etc..

1.5. Literature Review on Electron Transfer in α-Helices

A detailed survey of the literature indicates that the discussion on ET in the α-helix is controversial.

Inai *et al.*[60,61] excluded the possibility for α-helical peptides as charge mediators. The authors observed an irregular distance dependence of ET and concluded that the helical peptide backbone in between the D and A has no influence on ET, which otherwise would have shown a decrease in the ET rate with the increase of the distance.

Quite controversially, Batchelder *et al.* reported the helical backbone as an excellent conducting medium.[62] By investigating photo-induced ET from a donor (*N*,*N*-dimethylanilino, DMA) to an acceptor (2-naphthalenyl, Np) in two sets of helical peptides of increasing length (Figure 1.9), they observed weakly distance dependent intra-molecular ET and suggested that the electronic coupling between the D and A through the helical backbone is strong and is responsible for the weak decay of ET rate with the increase of the distance. They also investigated[18] the effect of the helix dipole moment on ET by switching the positions of the D and A in the same sequence. In the first set (Figure 1.9), the direction of ET is with the direction of the DM, whereas in the second set, it is opposite. ET was found to be favored when the direction of ET was against the DM (second set) and thereby, electrostatically favored (note that a charged-separated pair, $D^{\bullet+}A^{\bullet-}$ is produced after ET event in the neutral DA pair). Similar observations were reported when the same group investigated this phenomenon with different sets of α-helical peptides and different donors.[63]

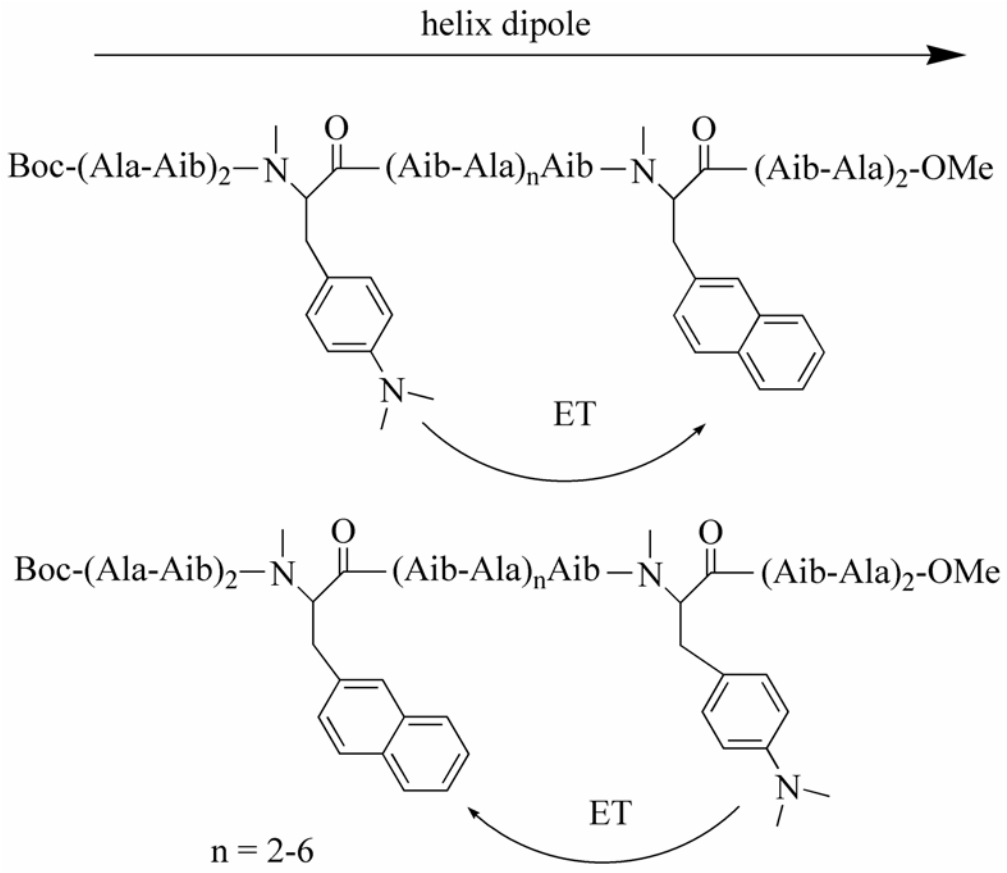

Figure 1.9. The helical peptides used by Batchelder *et al.* for studying photo-induced ET.[62] Figure redrawn from ref. 62.

The fact that α-helical peptides are good conductors was also supported by several other groups[19,64] and the mechanistic details of ET raised significant interest from both theoretical and experimental points of view. However, the discussion is still debated and involves several suggestions.

Zheng *et al.*[65] suggested the involvement of a tunneling mechanism in ET through the helical peptide. They also reported that the tunneling of electron follows the "distance model" of ET in proteins, i.e. ET is simply a function of the distance between the donor and the acceptor, and is not sensitive to the detailed structure (whether α-helical or β-sheet, etc) of the intervening peptide matrix.[5,6] The authors investigated ET

in a “metal-ion assembled parallel three-helix bundle” containing a ruthenium(II)-tris(bipyridyl) as the electron donor and ruthenium(III)pentammine as the acceptor (Figure 1.10), separated by ~15Å. The ET rate obtained for this system was compared to those in which specific amide groups (which were responsible for the intra-molecular H-boning network) in the peptide backbone were deleted with ester moieties (thereby, deleting specific intramolecular H-bonds). CD spectroscopy indicated that the deletion of the H-bonds did not produce any significant structural change and the separation between the D and A was assumed to be unchanged compared to that in the undeleted sequence. The experimentally determined ET rates for the “wild-type” and the H-bond deleted three-helix bundles were similar.

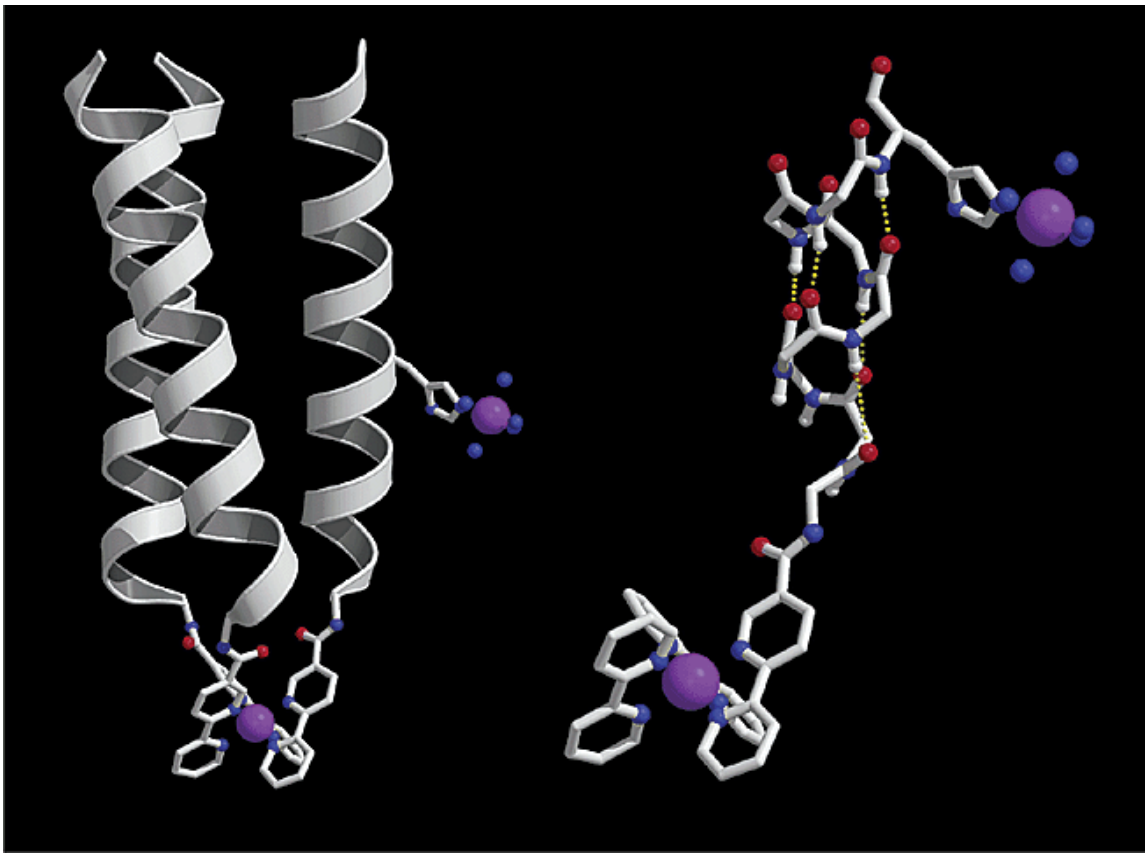

Figure 1.10. The "*parallel three-helix bundle*" containing $[Ru(bpy)_3]^{2+}$ as the electron donor and $[Ru(NH_3)_5(his)]^{3+}$ as the electron acceptor studied by Zheng *et al.* (left) and it's H-bond deleted analog (right). For clarity, only the helical backbone in which H-bond was deleted, is shown.[65] Figure reproduced with the permission from Zheng et al, *J. Phys. Chem. B.,* 2003, **107**, 7288. Copyright © 2003 American Chemical Society.

Sisido *et al.*[66] also suggested tunneling as the possible mechanism in the helix, but proposed that the intra-molecular H-bond pathways play a critical role in the tunneling process and ET is sensitive to the structure of the peptide spacer in between the donor and the acceptor, i.e. tunneling follows the "pathway model" of ET in proteins introduced by Beraton and Gray.[7,8] The authors synthesized a set of helical peptides having increasing length and containing a pyrenyl group as the donor and a nitrophenyl as the acceptor. The ET rate constants showed a complex distance dependence (Figure 1.11) and the authors pointed out that the H-bonds in between the D and A may provide

a shortcut for ET so that an electron tunnels through the H-bond pathway rather than taking the path via the entire helical loop. Sisido's observations agree with a vast body of work indicating the importance of H-bond in mediating ET in nature.[7,67-70]

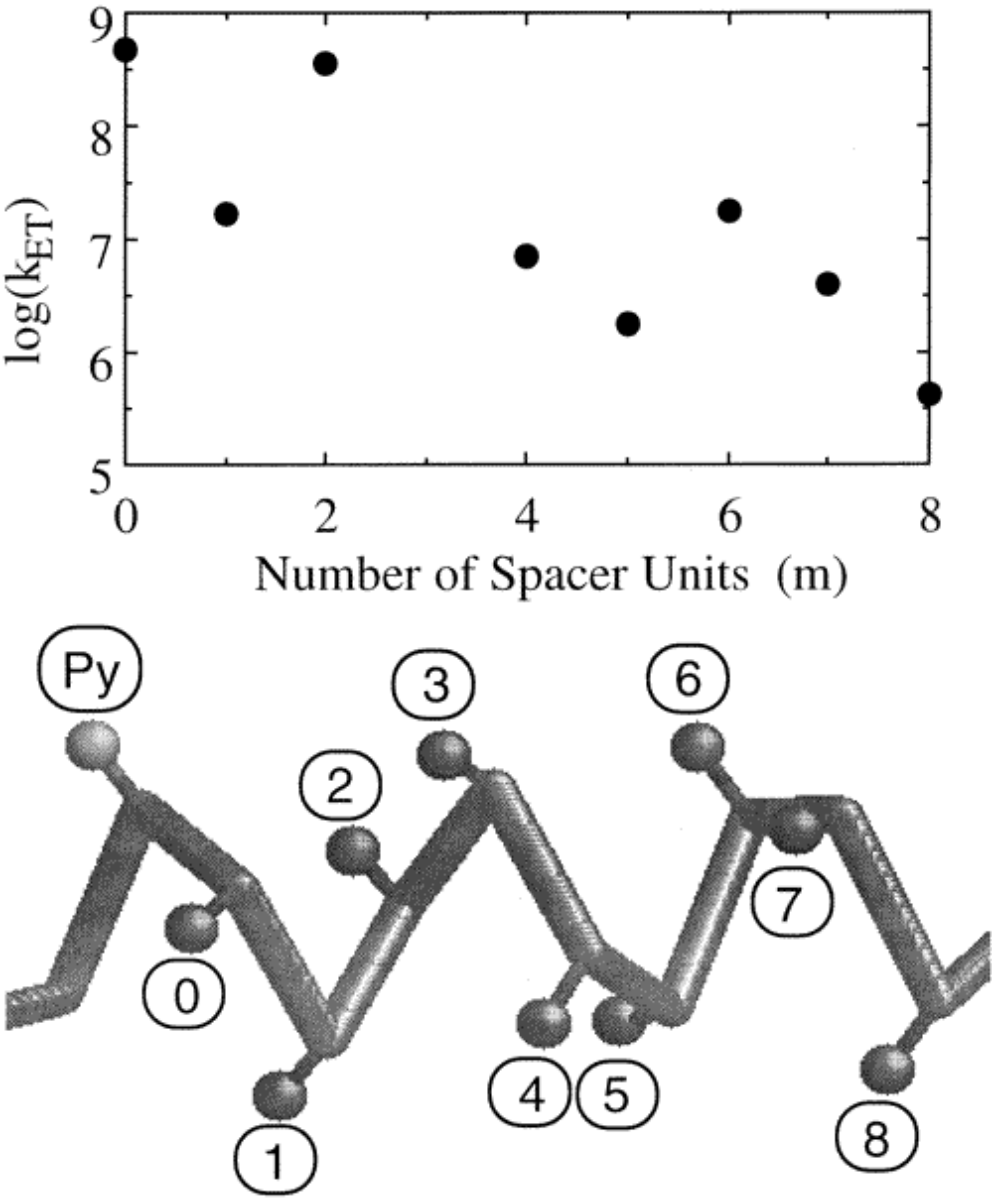

Figure 1.11. ET rate constants of the helical peptides studied by Sisido *et al.* plotted as a function of the spacer unit between the donor pyrenyl (Py) group and the acceptor nitrophenyl group. The molecular model shows the positions of the acceptor in the peptides.[66] Figure reproduced with the permission from Sisido *et al.*, *J. Phys. Chem. B.,* 2001, **105**, 10407. Copyright © 2001 American Chemical Society.

Morita *et al.*[19] suggested an alternative mechanism of ET in helical peptides. They electrochemically investigated ET through films of helical peptides formed on gold surface via the Au-S bond and having terminally attached redox-active ferrocene (Fc) (Figure 1.12). The ET rates were found to be faster than those calculated assuming tunneling through the peptide backbone and the authors suggested that the faster rates are due to a sequential hopping mechanism.[71-73] According to this model, it is proposed that when an electron has to travel a long distance, i.e. when the length of the bridge is large, tunneling is not favorable. Instead the electron is transferred first from the D to the nearby unoccupied molecular orbital (MO) of the bridge and then, it hops sequentially via the local MOs and finally reaches the A (Figure 1.13). Morita *et al.* suggested the amide groups as the most possible hopping sites. However in this study, the role of H-bond in the calculation of ET (assuming tunneling) was completely ignored.

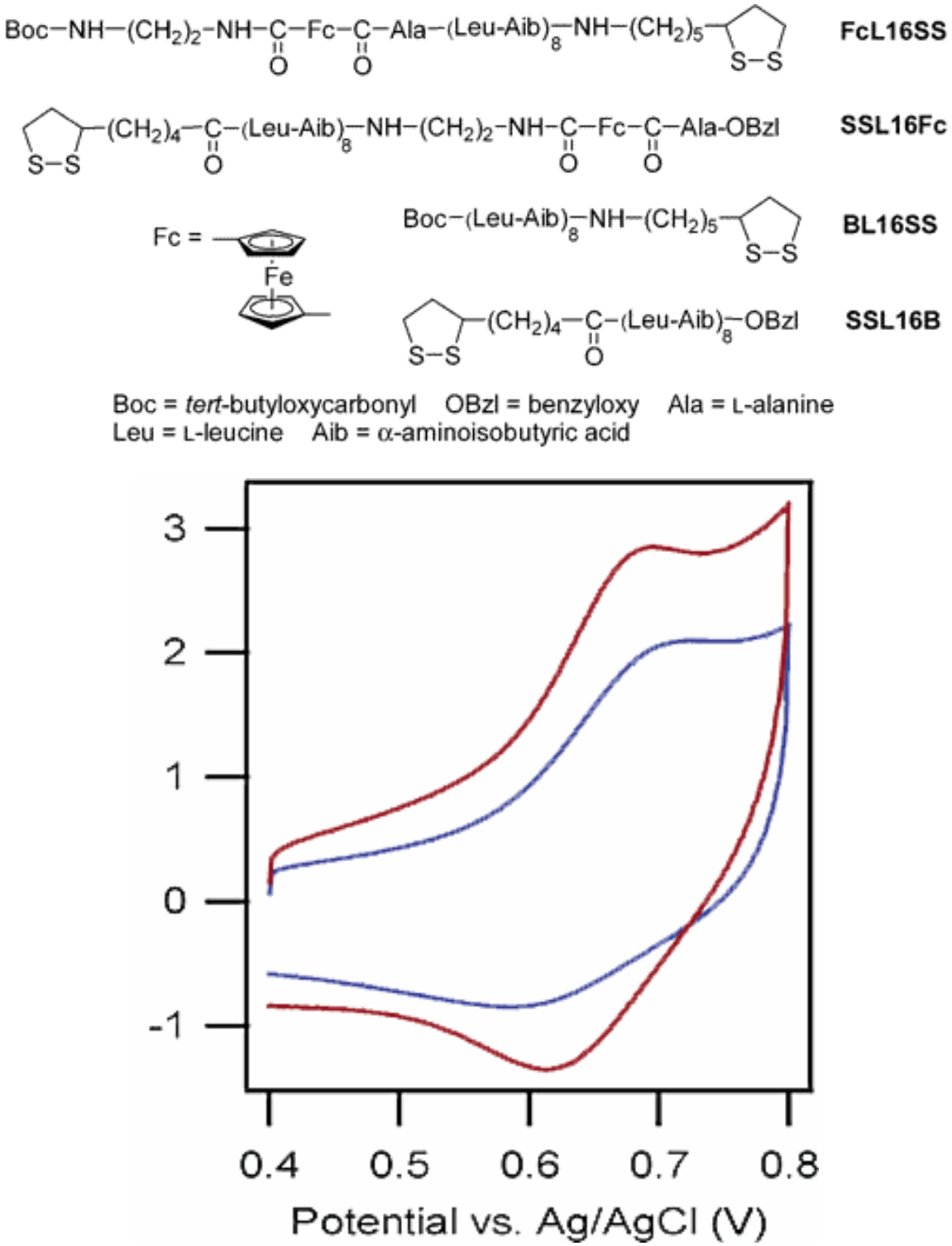

Figure 1.12. Molecular structures of the helical peptides investigated by Morita *et al.* (upper panel) and CVs of the peptide SAMs on gold electrodes: FcL16SS (red), SSL16Fc (blue) (lower panel).[19] Figures reproduced with the permission from Morita *et al.*, *J. Am. Chem. Soc.,* 2003, **125**, 8732. Copyright © 2003 American Chemical Society.

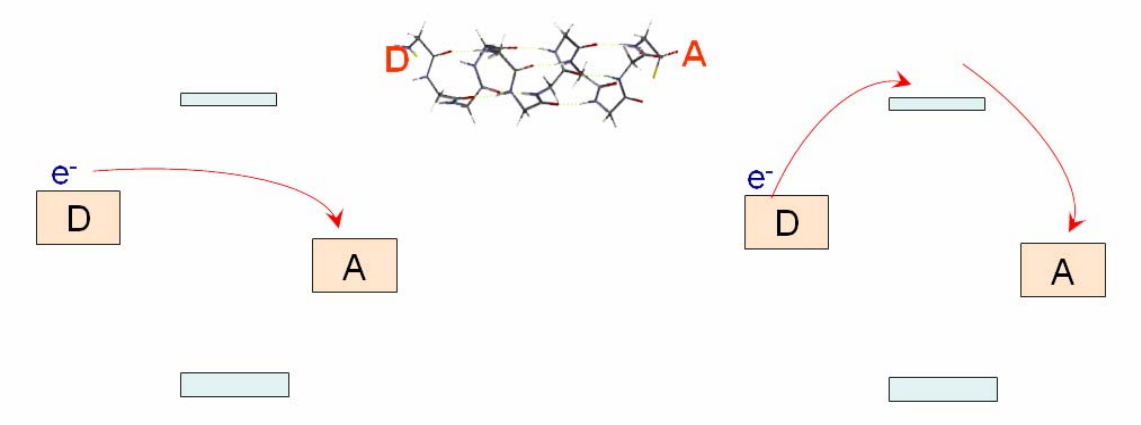

Figure 1.13. Representation of the tunneling (left) and hopping (right) mechanisms in a D-B-A system containg a helical peptide as the bridge (B).

Malak *et al.* investigated ET in a series of oligoprolines $[(bpy)_2Ru^{II}L\text{-}Pro_n\text{-}apyRu^{III})(NH_3)_5]^{5++}$ n= 0 to 9) (Figure 1.14).[74] The corresponding separation between the D and the A was 9-32 Å and a transition from a strong distance dependent ET regime to a weak one was observed (Figure 1.15). The shorter peptides (n = 0-4) showed an exponential decay of the rate constant (the decay constant, β = 1.4 $Å^{-1}$), consistent with the tunneling mechanism. But for the longer peptides, β was very low (0.18 $Å^{-1}$). The authors suggested that tunneling may be possible for shorter peptides, but for longer ones in which the separations between the D and the A are large, the mechanism of ET changes from tunneling to the more favorable sequential hopping.

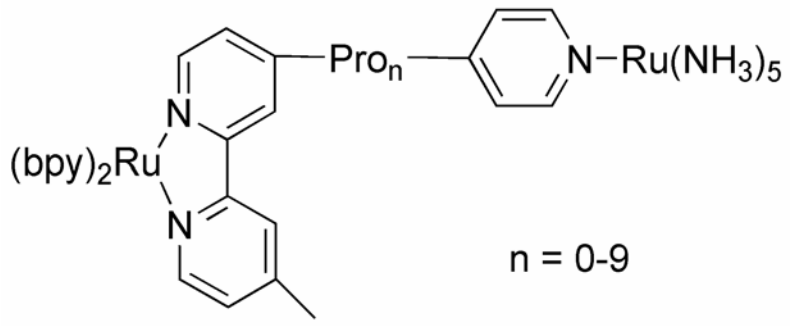

Figure 1.14. Molecular structures of the oligoprolines investigated by Malak *et al.*[74] Figure redrawn from ref. 74.

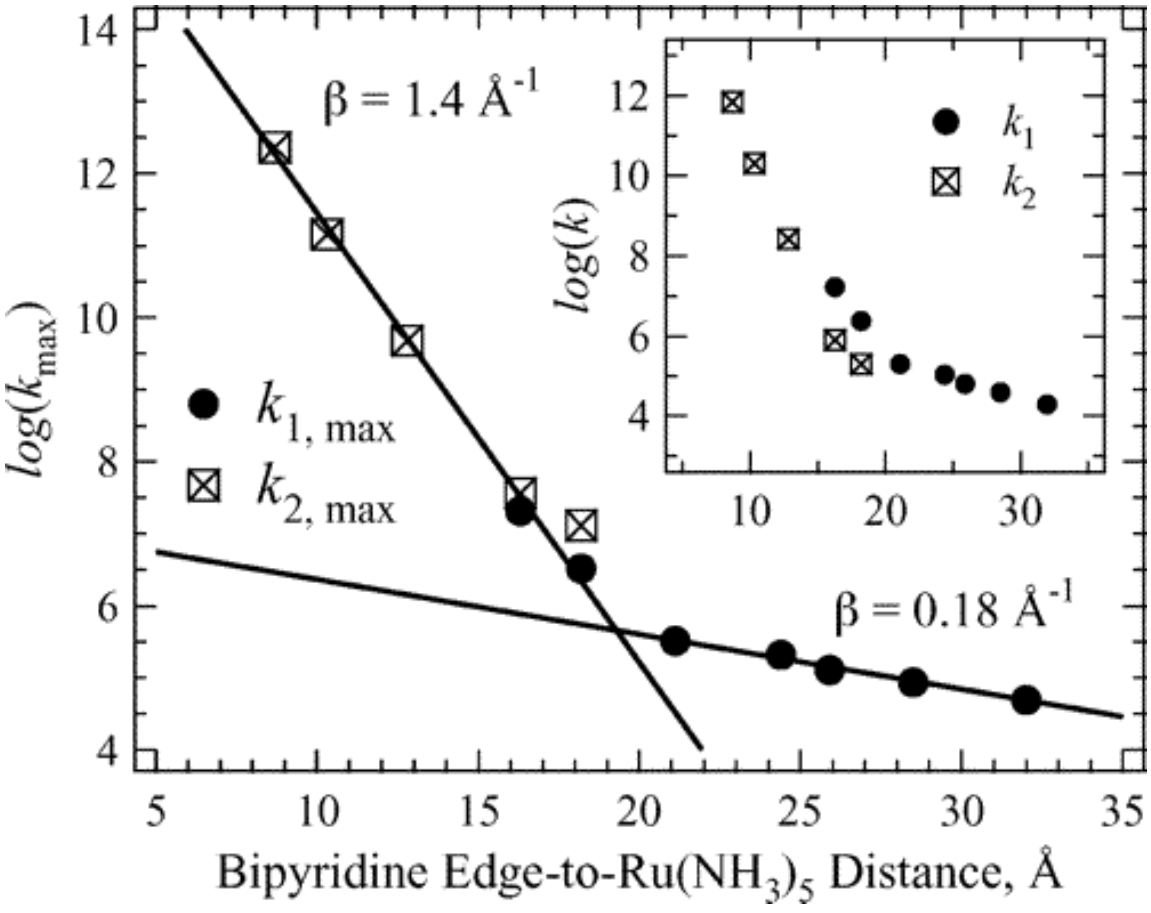

Figure 1.15. ET rates plotted as a function of the distance for the oligoprolines studied by Malak *et al.*[74] Figure reproduced with the permission from Malak *et al.*, *J. Am. Chem. Soc.,* 2004, **126**, 13888. Copyright © 2004 American Chemical Society.

In this regard, the work performed by Sek *et al.* is also worth mentioning. Sek investigated[75] ET through a series of oligoglycine (Fc-CO(Gly)$_n$NH-(CH$_2$)$_2$-SH (where Fc = ferrocene; Gly = glycine; n = 2-6). Like Malak *et al.*,[74] they also observed exponential decrease of ET for shorter peptides and a transition to a weaker regime with the increase of the peptide length. They supported the notion that this transition is related to the change in ET mechanism i.e. from tunneling to hopping. Watanabe *et al.*[76] calculated the energies of the HOMO and LUMO of the Fc and the amide. The energy of the amide LUMO was found to be too high to transfer an electron from the Fc and the authors suggested that the hopping process in the bridge possibly involves hole transfer via the local HOMOs (Figure 1.16).

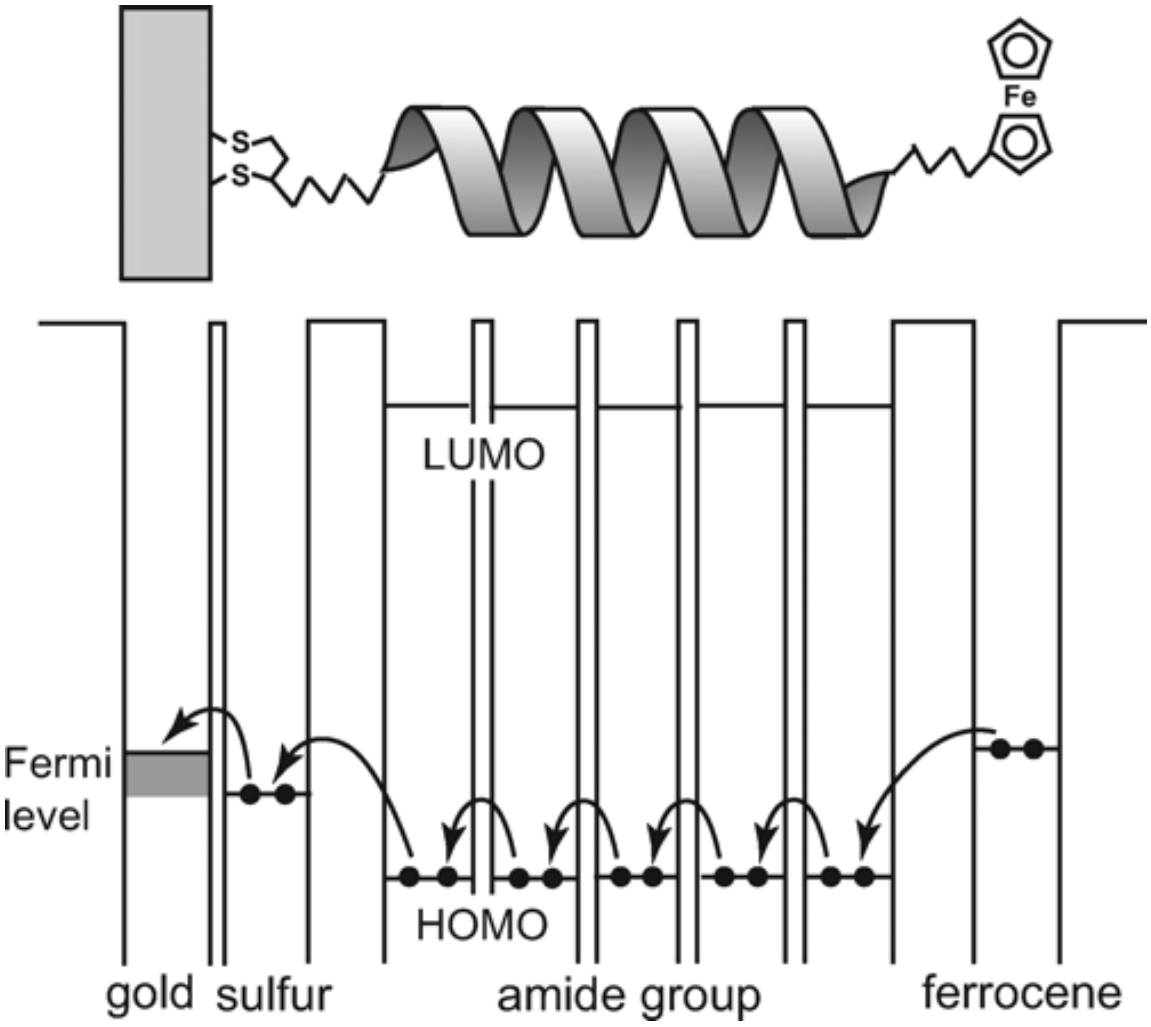

Figure 1.16. Illustration of the hole transfer in helical peptides.[76] Figure reproduced with the permission from Watanabe *et al. J. Phys. Chem. B.,* 2005, **109**, 14416. Copyright © 2005 American Chemical Society.

The transition from an exponential to a weakly distance dependent regime is the basis for the above authors[19,74-76] to suggest the hopping mechanism in ET through helical peptides. But unfortunately, these authors completely neglected the importance of tunneling through the intra-molecular H-bond. Polo *et al.*[64] pointed out that with the increase of the length of the helix by the addition of an extra AA, an extra intra-

molecular H-bond is formed and this H-bond can act as a bypass for the tunneling electron and is responsible for the weak distance dependence and higher rates of ET.

From the above discussion, we see conflicting reports about the conductivity of the α-helix: Inai *et al.* described it as an insulator,[60,61] whereas Batchelder *et al.* reported it as a conducting medium.[62] The mechanistic discussion of ET also includes several suggestions (tunneling following different models,[65,66] hopping of electrons[19] or holes[76]) and can be visualized from the following flow chart (Figure 1.17).

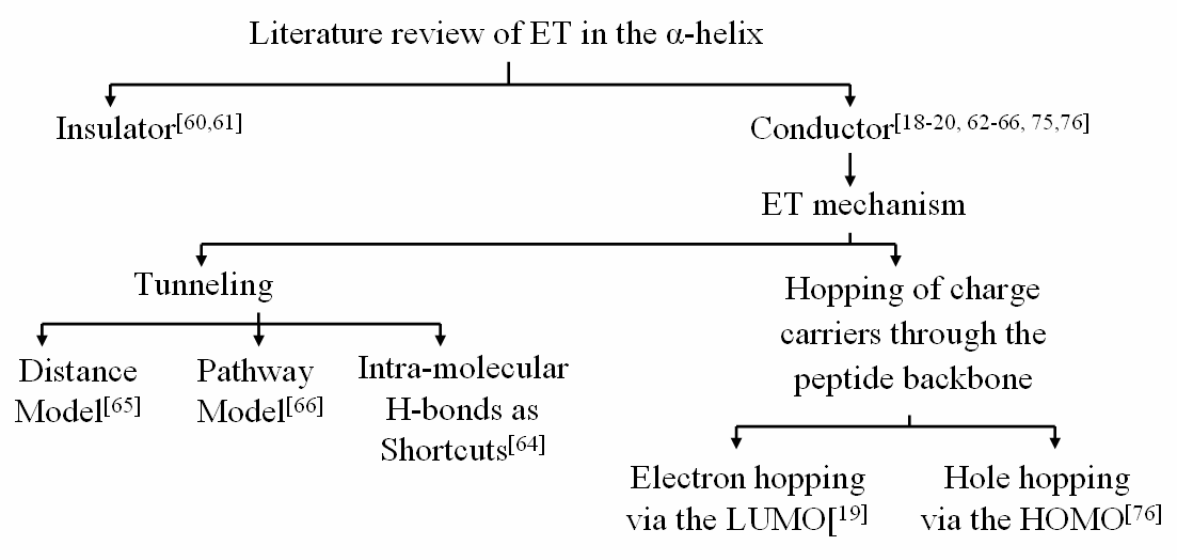

Figure 1.17. A flow chart reflecting the controversies that exist in the literature about the conductivity and ET mechanism of the α-helix.

1.6. Applications of α-Helical Peptides

1.6.1. Photocurrent Generation with Chromophore-functionalized Helical Peptides

There are several fascinating reports[77-80] in which the natural photo-system was mimicked by synthetic α-helices functionalized with light-harvesting chromophores. In these studies, films of helical peptides with chromophores are formed on the surface of gold electrodes. Upon excitation of the chromophore by a laser of suitable wavelength (the λ_{max} of the chromophore), a photocurrent is generated. The potential of the modified electrode can be varied to change the direction and the intensity of the generated photocurrent.

The first report[77] on photocurrent generation by peptide films was published by Morita *et al.* SAMs of helical peptides containing *N*-ethylcarbazolyl (ECz) group were prepared and after the excitation of the ECz group, photocurrent was produced. Later, Yanagisawa *et al.* reported[78] the increase of photocurrent intensity with the increase of the number of light-harvesting chromophores in the helical backbone. Yasutomi *et al.*[80] exploited the use of chromophores having λ_{max} at different wavelengths and the effect of the helix dipole moment on the photocurrent to prepare "molecular diodes". They synthesized two helical peptides having chromophores that absorb at different wavelengths (Figure 1.18). In one peptide the disulfide group was at the N-terminal side, whereas in the other it was at the C-terminal side of the peptide. A mixed film of the peptides was prepared on gold surface via the formation of the Au-S bond and upon excitation of the chromophore, generation of dipole-controlled photocurrent was demonstrated.

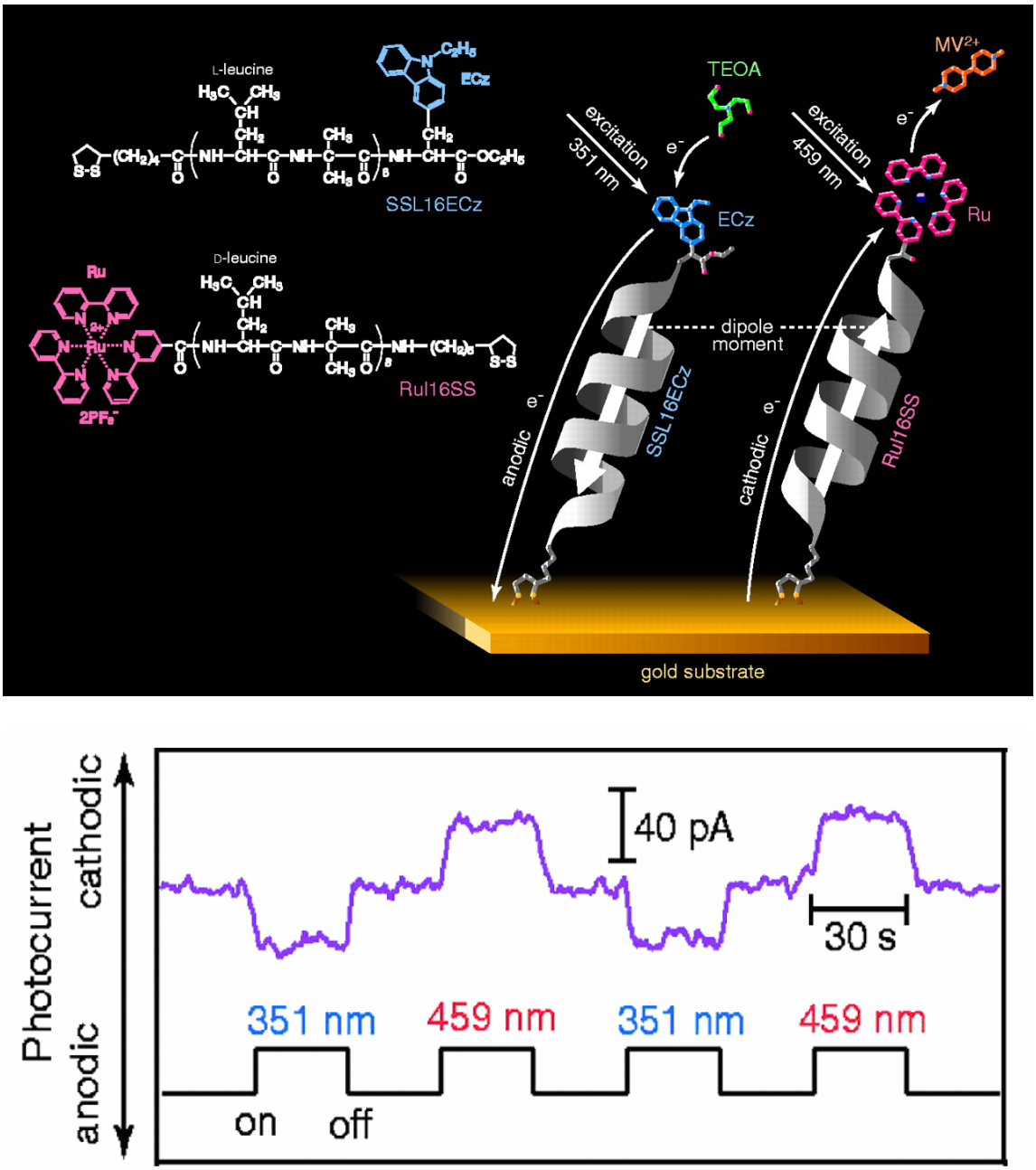

Figure 1.18. The upper panel shows the chemical structures of the chromophore-functionalized helical peptides studied by Morita *et al.* and illustrates the light-induced photocurrent generation by the molecular assembly formed on the surface of gold electrodes. The lower panel shows photocurrent signals from the "molecular diode" upon irradiation at different wavelengths. Figures reproduced with the permission from Yasutomi *et al. Science*, 2004, **304**, 1944. Copyright © 2004 by the American Association for the Advancement of Science.

1.6.2. Peptide-Protected Gold Nanoparticles

Peptide-protected nanoparticle is another active area of research receiving significant attention these days due to their potential relevance in biomedical applications. There are several reports[81-84] in which peptide/protein protected nanoparticles have been suggested for applications like targeted drug delivery, imaging, and molecular recognition. Especially, labelling of peptides or proteins of interest with gold nanoparticles offers the use of imaging techniques, such as electron microscopy, video-enhanced color differential interference contrast microscopy, and fluorescence for the elucidation of targeted drug delivery *in vitro*.[81,82] Fuente *et al.*[81] tracked the delivery of peptide-protected nanoparticles and studied "*the cell-particle interactions"*. Tkachenko *et al.*[82] took this approach one step further to study the feasibility of some biologically important peptide sequences to target the cell nucleus (Figure 1.19).

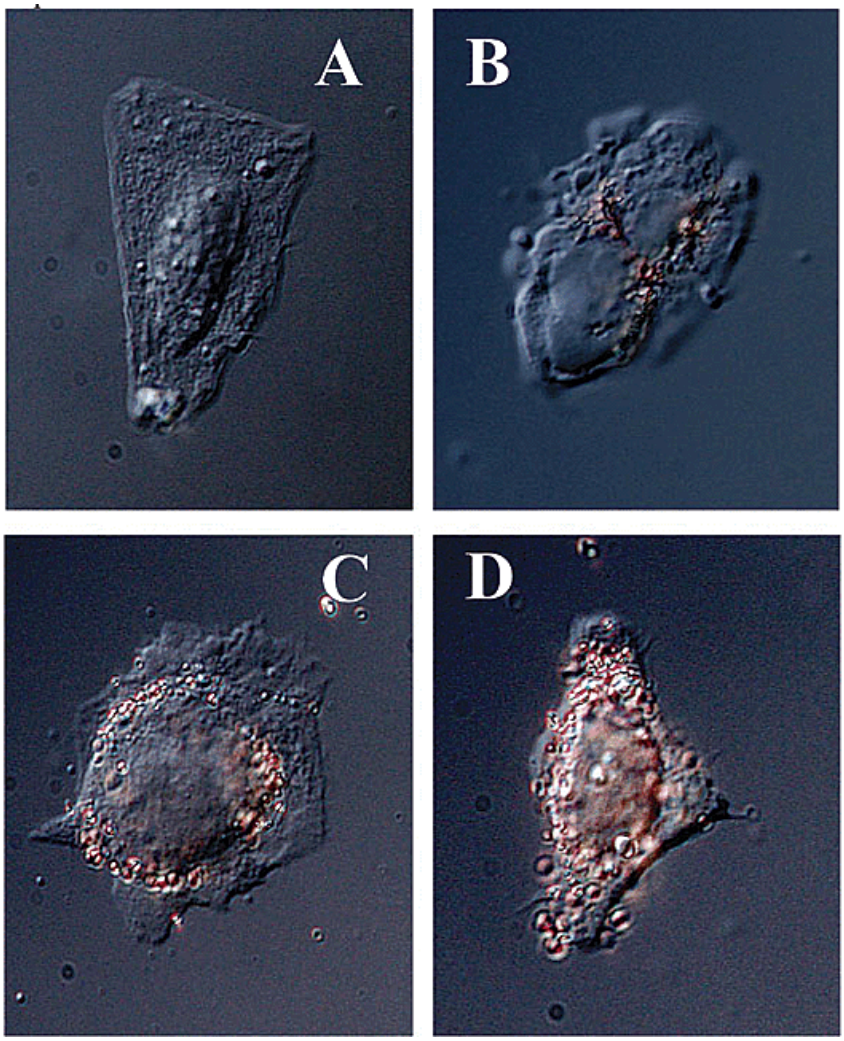

Figure 1.19. Images showing different degrees of incorporation of the peptide protected gold nanoparticles into the cell nucleus.[82] Figures reproduced with the permission from Tkachenko *et al.*, *J. Am. Chem. Soc.,* 2003, **125**, 4700. Copyright © 2003 American Chemical Society.

1.7. Research Objectives

As described in section 1.5, the published reports describing the ET in α-helical peptides, are highly controversial. Reports excluding the possibility for α-helical peptides as charge mediators were published,[60,61] although several groups claimed the helical backbone as an excellent ET medium.[62,63] At this point, the mechanistic interpretation of the experimental data is even more controversial. Despite the well-documented flexibility of the α-helical structure and its ability to undergo large amplitude motions,[85-87] none of the existing studies on ET in peptides has included the role of the dynamic properties in their mechanistic interpretations. The result is a range of often contradicting ET mechanisms that change widely between different peptide systems and different experimental conditions, making it exceedingly difficult to extract a coherent model for ET in helical peptides.

Similar confusion existed in the discussion[88-94] of ET in DNA, which is another semi-rigid molecule. However, recent work by Barton and Schuster demonstrated a non-static model, in which the dynamic properties of DNA are crucial for the correct mechanistic interpretation of experimental data.[95-97] Thus, we speculated that a similar type of behavior may be a factor in ET in α-helical peptides and decided to explore whether molecular dynamics (MD) plays a role in the ET in this particular structural motif. If MD is indeed relevant in ET in α-helical peptides, then neglecting this effect would ultimately lead to incorrect interpretations of the experimental observations and may explain the current confusion in this area.

In this thesis, I am addressing this issue directly and will present a novel strategy to clarify this concern, making use of a series of α-helical model peptides. In Chapter 2, results will be presented demonstrating that ET in the α-helix is indeed dependent on the

MD properties. Work presented in this thesis is the first to suggest the importance of MD. This, of course, raises related questions. How does MD modulate the ET in α-helical peptides? How does it relate to the existing ET theories for proteins? Chapter 3 will address these questions.

After exploring the mechanism of ET in α-helical peptides, I decided to explore the feasibility of this particular secondary structure for nano-scaled applications. Two extremely important areas have been investigated and the results are presented in this thesis:

(1) The first application is "photocurrent generation with chromophore-functionalized helical peptides". As described in section 1.6.1, the study of photocurrent generation by mimicking the natural photo-system with synthetic α-helices functionalized with light-harvesting chromophores is important for developing artificial solar energy converters, and exploring the possibility of using α-helical peptides as scaffolds for nano-scaled photovoltaic devices. We wanted to study the possibility of using our peptides for this purpose and the results of this study are described in Chapter 4.

(2) The second application investigated in this thesis is "peptide-protected gold nanoparticles". As described in section 1.6.2, peptide-protected nanoparticles are potentially important for biomedical application. One of the inherent problems in this regard is that peptides are highly flexible and can change their structure depending on the chemical environment. Since the function of peptides is related to their secondary structure, it is crucial to test the structural integrity of the peptides in any given chemical environment. We conducted a structural investigation of an α-helix on the surface of nanoparticles having different sizes and discovered significant structural changes of the

peptide secondary structure as a function of the radius of curvature of the nanoparticle surface. The results of this study are presented in Chapter 5.

1.8. References

[1] J. M. Berg, L. Stryer, J. L. Tymoczko, *Biochemistry* Freeman, New York, ed. 5, **2000**.
[2] R. A. Marcus, N. Sutin, *Biochim. biophys. Acta* **1985**, 811, 265-322.
[3] R. J. P. Williams, *J. Biol. Inorg. Chem*. **1997**, 2, 373-377.
[4] J. J. Hopfield, *Proc. Natl. Acad. Sci. U.S.A*. **1974**, 71, 3640-3644.
[5] C. C. Page, C. C.Moser, X. Chen, P. L. Dutton, *Nature* **1999**, 402, 47-52.
[6] C. C. Moser, J. M. Keske, K. Warncke, R. Farid, P. L. Dutton, *Nature* **1992**, 355, 796-802.
[7] D. N. Beratan, J. N. Betts, J. N. Onuchic, *Science* **1991**, 252, 1285-1288.
[8] D. N. Beratan, J. N. Onuchic, J. R. Winkler, H. B. Gray, *Science* **1992**, 258, 1740-1741.
[9] A. V. Finkelstein, O. Ptitsyn, *Protein Physics* Academic Press, New York, **2002**.
[10] N. Go, T. Noguti, T. Nishikawa, *Proc. Natl. Acad. Sci. U S A* **1983**, 80, 3696-3700.
[11] R. M. Daniel, R. V. Dunn, J. L. Finney, J. C. Smith, *Annu. Rev. Biophys. Biomol. Struct*. **2003**, 32, 69-92.
[12] P. Martel, H. Lin, *J. Biol. Phys.* **1989**, 17, 137144.
[13] P. Bernado, M. J. Blackledge, *J. Am. Chem. Soc.* **2004**, 126, 7760-7761.
[14] (a) V. I. Vullev, J. II Jones, *Res. Chem. Interm.* **2002**, 28, 795-781; (b) D. M. Lawson, C. E.M. Stevenson, C. R. Andrew, and R. R. Eady, *The EMBO Journal* **2000**, 19, 5661–5671.
[15] (a) M. J. I. Andrews, A. B. Tabor, *Tetrahedron* **1999**, 55, 11711-11743; (b) N. Sewald, H. D. Jakubke, Peptides: Chemistry and Biology, WILEY-VCH Verlag GmbH Weinheim, **2002.**
[16] L. G. Presta, G. D. Rose, *Science* **1988**, 240, 1632-1641.
[17] W. G. Hol, P. T. van Duijnen, H. J. Berendsen, *Nature* **1978**, 273, 443-446.
[18] M. A. Fox, E. Galoppini, *J. Am. Chem. Soc.* **1996**, 118, 2299-2300.
[19] T. Morita, S. Kimura, *J. Am. Chem. Soc.* **2003**, 125, 8732-8733.
[20] S. Sek, A. Tolak, A. Misicka, B. Palys, R. Bilewicz, *J. Phys. Chem. B.* **2005**, 109, 18433-18438.
[21] J. M. Scholtz, R. L. Baldwin, *Annu. Rev. Biophys. Biomol. Struct.* **1992**, 21, 95-118.
[22] B. H. Zimm, J. K. Bragg, *J. Chem. Phys.,* **1959**, 31, 526-535.
[23] L. Mayne, S. W. Englander, R. Qiu, J. Yang, Y. Gong, E. J. Spek, N. R. Kallenbach, *J. Am. Chem. Soc.* **1998**, 120, 10643-10645.
[24] D. Y. Jackson, D. S. King, J. Chmielewski, S. Singh, P. G. Schultz, *J. Am. Chem. Soc.* **1991**, 113, 9391-9392.
[25] E. Cabezas, A. C. Satterthwait, *J. Am. Chem. Soc.* **1999**, 121, 3862-3875.

[26] E. Schievano, S. Mammi, A. Bisello, M. Rosenblatt, M. Chorev, E. Peggion, *J. Pept. Sci.* **1999**, 5, 330-337.
[27] C. Bracken, J. Gulyas, J. W. Taylor, J. Baum, *J. Am. Chem. Soc.* **1994**, 116, 6431-6432.
[28] J. C. Phelan, N. J. Skelton, A. C. Braisted, R. S. McDowell, *J. Am. Chem. Soc.* **1997**, 119, 455-460.
[29] C. Yu, J. W. Taylor, *Bioorg. Med. Chem.* **1999**, 7, 161-175.
[30] C. Yu, J. W. Taylor, *Tetrahedron Lett.* **1996**, 37, 1731-1734.
[31] M. Zhang, B. Wu, J. Baum, J. W. Taylor, *J. Pept. Res.* **2000**, 55, 398-408.
[32] M. J. Kelso, R. L. Beyer, H. N. Hoang, A. S. Lakdawala, J. P. Snyder, W. V. Oliver, T. A. Robertson, T. G. Appleton, D. P. Fairlie, *J. Am. Chem. Soc.* **2004**, 126, 4828-4842.
[33] S. M. Butterfield, P. R. Patel, M. L. Waters, *J. Am. Chem. Soc.* **2002**, 124, 9751-9755.
[34] P. Y. Chou, G. D. Fasman, *J. Mol. Biol.* **1973**, 74, 263-281.
[35] C. P. Hill, D. H. Anderson, L. Wesson, W. F. DeGrado, D. Eisenberg, *Science* **1990**, 249, 543-546.
[36] H. A. Arfmann, R. Labitzke, K. G. Wagner, *Biopolymers* **1975**, 14, 1381-1393.
[37] J. S. Albert, A. D. Hamilton, *Biochemistry* **1995**, 34, 984-990.
[38] G. Hungerford, M. Martinez-Insua, D. J. S. Birch, B. D. Moore, *Angew. Chem., Int. Ed.* **1996**, 35, 326-329.
[39] C. Toniolo, M. Crisma, F. Formaggio, G. Valle, G. Cavicchioni, G. Precigoux, A. Aubry, J. Kamphuis, *Biopolymers* **1993**, 33, 1061-1072.
[40] C. Toniolo, A. Polese, F. Formaggio, M. Crisma, J. Kamphuis, *J. Am. Chem. Soc.* **1996**, 118, 2744-2745.
[41] C. Toniolo, E. Benedetti, *Macromolecules* **1991**, 24, 4004-4009.
[42] T. S. Yokum, T. J. Gauthier, R. P. Hammer, M. L. McLaughlin, *J. Am. Chem. Soc.* **1997**, 119, 1167-1168.
[43] G. Yoder, A. Polese, R. A. G. D. Silva, F. Formaggio, M. Crisma, Q. B. Broxterman, J. Kamphuis, C. Toniolo, T. A. Keiderling, *J. Am. Chem. Soc.* **1997**, 119, 10278-10285.
[44] G. L. Millhauser, *Biochemistry,* **1995**, 34, 3873-3877.
[45] C. Toniolo, E. Benedetti, *Trends Biochem. Sci.* **1991**, 16, 350-353.
[46] S. E. Huston, G. R. Marshall, *Biopolymers* **1994**, 34, 75-90.
[47] J. Tirado-Rives, D. S. Maxwell, W. L. Jorgensen, *J. Am. Chem. Soc.* **1993**, 115, 11590-11593.
[48] W. R. Fiori, S. M. Miick, G. L. Millhauser, *Biochemistry* **1993**, 32, 11957-11962.
[49] M. Sjödin, *PhD thesis* (Regulation of proton coupled electron transfer from amino acids in artificial model systems: a mechanistic study), Acta Universitatis Upsaliensis, Upsala **2004**.
[50] R. A. Malak, *PhD thesis* (Distance dependence of electron transfer across polyproline bridges: experimental evidence for the existence of two distinct mechanisms), the State University of New Jersey, New Brunswick, New Jersey, **2003**.
[51] C. E. D. Chidsey, Science, 1991, 251, 919-922
[52] (a) R. G. Nuzzo, D. L. Allara, *J. Am. Chem. Soc.* **1983**, 105, 4481-4483; (b) D. Bain, J. Evall, G. M. Whitesides, *J. Am. Chem. Soc.* **1989**, 111, 7155-7164.

[53] C. D. Bain, G. M. Whitesides, *J. Am. Chem. Soc.* **1988**, 110, 6560-6561.
[54] F. A. Armstrong, R. Camba, H. A. Heering, J. Hirst, L. J. Jeuken, A. K. Jones, C. Leger, J. P. McEvoy, *Faraday Discuss.* **2000**, 116, 191-203.
[55] A. J. Bard, L. R. Faulkner, *Electrochemical Method: Fundamentals, Applications*, 2nd ed.; John Wiley: New York, **2001**.
[56] L. Tender, M. T. Carter, R. W. Murray, *Anal. Chem.* **1994**, 66, 3173-3181.
[57] J. F. Smalley, S. W. Feldberg, C. E. D. Chidsey, M. R. Linford, M. D. Newton, Y.-P. Liu, *J. Phys. Chem.* **1995**, 99, 13141-13149.
[58] I. Bediako-Amoa, T. C. Sutherland, C.-Z. Li, R. Silerova,, H.-B. Kraatz, *J. Phys. Chem. B* **2004**, 108, 704-714.
[59] Y.-T. Long, C.-Z. Li, T. C. Sutherland, M. Chahma, J. S. Lee, H.-B. Kraatz, *J. Am. Chem. Soc.* **2003**, 125, 8724-8725.
[60] Y. Inai, M. Sisido, Y. Imanishi, *J. Phys. Chem.* **1991**, 95, 3847-3851.
[61] Y. Inai, M. Sisido, Y. Imanishi, *J. Phys. Chem.* **1990**, 94, 6237-6243.
[62] T. L. Batchelder, R. J. III Fox, M. S. Meier, M. A. Fox, *J. Org. Chem.* **1996**, 61, 4206-4209.
[63] M. A. Fox, E. Galoppini, *J. Am. Chem. Soc.* **1997**, 119, 5277-5285.
[64] F. Polo, S. Antonello, F. Formaggio, C. Toniolo, F. Maran, *J. Am. Chem. Soc.* **2005**, 127, 492-493.
[65] Y. Zheng, M. A. Case, J. F. Wishart, G. L. McLendon, *J. Phys. Chem. B.* **2003**, 107, 7288-7293.
[66] M. Sisido, S. Hoshino, H. Kusano, M. Kuragaki, M. Makino, H. Sasaki, T. A. Smith, K. P. Ghiggino, *J. Phys. Chem. B.* **2001**, 105, 10407-10415.
[67] R. Langen, J. L. Colon, D. R. Casimiro, T. B. Karpishin, J. R. Winkler, H. B. Gray, *J. Biol. Inorg. Chem.* **1996**, 1, 221-225.
[68] H. B. Gray, J. R. Winkler, *J. Electroanal. Chem.* **1997**, 438, 43-47.
[69] H. B. Gray, J. R. Winkler, *Annu. Rev. Biochem.* **1996**, 65, 537-561.
[70] S. S. Isied, M. Y. Ogawa, J. F. Wishart, *Chem. Rev.* **1992**, 92, 381-394.
[71] E. G. Petrov, Ye. V. Shevchenko, V. I. Teslenko, V. May, *J. Chem. Phys.* **2001**, 115, 7107-7122.
[72] E. G. Petrov, Ye. V. Shevchenko, V. May, *Chem. Phys.* **2003**, 288, 269-279.
[73] M. Bixon, J. Jortner, *J. Chem. Phys.* **1997**, 107, 5154-5170.
[74] R. A. Malak, Z. Gao, J. F. Wishart, S. S. Isied, *J. Am. Chem. Soc.* **2004**, 126, 13888-13889.
[75] S. Sek, A. Sepiol, A. Tolak, A. Misicka, R. Bilewicz, *J. Phys. Chem. B.* **2004**, 108, 8102-8105.
[76] J. Watanabe, T. Morita, S. Kimura, *J. Phys. Chem. B.* **2005**, 109, 14416-14425.
[77] T. Morita, S. Kimura, S. Kobayashi, Y. Imanishi, *J. Am. Chem. Soc.* **2000**, 122, 2850-2859.
[78] K. Yanagisawa, T. Morita, S. Kimura, *J. Am. Chem. Soc.* **2004**, 126, 12780-12781.
[79] S. Yasutomi, T. Morita, S. Kimura, *J. Am. Chem. Soc.* **2005**, 127, 14564-14565.
[80] S. Yasutomi, T. Morita, Y. Imanishi, S. Kimura, *Science* **2004**, 304, 1944-1947.
[81] J. M. de la Fuente, C. C. Berry, M. O. Riehle, A. S. G. Curtis, *Langmuir* **2006**, 22, 3286-3293.
[82] A. G. Tkachenko, H. Xie, D. Coleman, W. Glomm, J. Ryan, M. F.,erson, S. Franzen, D. L. Feldheim, *J. Am. Chem. Soc.* **2003**, 125, 4700-4701.
[83] E. Katz, I. Willner, *Angew. Chem., Int. Ed.* **2004**, 43, 6042-6108.

[84] R. Levy, N. T. K. Thanh, R. C. Doty, I. Hussain, R. J. Nichols, D. J. Schiffrin, M. Brust, D. G. Fernig, *J. Am. Chem. Soc.* **2004**, 126, 10076-10084.
[85] S.-Y. Sheu, E. W. Schlag, D.-Y. Yang, H. L. Selzle, *J. Phys. Chem. A.* **2001**, 105, 6353-6361.
[86] G. V. Papamokos, I. N. Demetropoulos, *J. Phys. Chem. A.* **2004**, 108, 8160-8169.
[87] A. Idiris, M. T. Alam, A. Ikai, *Protein Eng.* **2000**, 13, 763-770.
[88] E. M. Boon, J. K. Barton, *Curr. Opin. Struct. Biol.* **2002**, 12, 320-329.
[89] B. Giese, *Curr. Opin. Chem. Biol.* **2002**, 6, 612-618.
[90] G. B. Schuster, *Acc. Chem. Res.* **2000**, 33, 253-260.
[91] M. Bixon, J. Jortner, *J. Am. Chem. Soc.* **2001**, 123, 12556-12567.
[92] M. Bixon, B. Giese, S. Wessely, T. Langenbacher, M. E. Michel-Beyerle, J. Jortner, *Proc. Natl. Acad. Sci. U.S.A.* **1999**, 96, 11713-11716.
[93] P. T. Henderson, D. Jones, G. Hampikian, Y. Z. Kan, G. B. Schuster, *Proc. Natl. Acad. Sci. U.S.A.* **1999**, 96, 8353-8358.
[94] R. N. Barnett, C. L. Cleveland, A. Joy, U. Landman, G. B. Schuster, *Science* **2001**, 294, 567-571.
[95] M. A. O'Neill, J. K. Barton, *J. Am. Chem. Soc.* **2004**, 126, 13234-13235.
[96] M. A. O'Neill, J. K. Barton, *J. Am. Chem. Soc.* **2004**, 126, 11471-11483.
[97] R. N. Barnett, C. L. Cleveland, A. Joy, U. Landman, G. B. Schuster, *Science* **2001**, 294, 567-571.

Chapter 2

Electron Transfer across α-Helical Peptides: Potential Influence of Molecular Dynamics

2.1. Connecting Text

As described in chapter one, the discussion of ET in the α-helix is highly controversial, and in spite of the well-known dynamic properties of this particular motif and the effect of dynamics on ET in similar systems like DNA, none of the existing literature has addressed the role of this important factor on ET in the α-helix. Chapter 2 deals with this issue. Results of an in-depth surface electrochemical study are presented for a series of leucine-rich α-helical peptides. For the first time, the role of molecular dynamics on the ET properties of peptide films is reported. This chapter forms the foundation for the later chapters that deal with this issue in more depth.

 This paper is co-authored by H.-B. Kraatz. I am the major contributor to this work in terms of the experimental study and writing. The final manuscript is the result of valuable suggestions and thorough revision from Prof. Kraatz. The manuscript will be used *verbatim* in my thesis.

2.2. Introduction

Intramolecular electron transfer (ET) across proteins using synthetic α-helical model peptides has currently received significant attention. Understanding the mechanistic details of ET is important for elucidating ET in biological processes, such as photosynthesis,[1-3] and the knowledge might be useful for the emerging field of molecular electronics.

Recently, theoretical studies have predicted that ET along a polypeptide chain involves essential large amplitude chain motions.[4] Computational vibration analysis also confirmed several types of vibrations in α-helical peptides: C–C and C–N torsions, and bond angle bending, which produce collective motions, such as global bending, stretching, and cylindrical deformation.[5] Experimental evidence for spring mechanics of α-helical polypeptides has already been reported.[6] The collective motions could play a very important role in ET through α-helical peptide. In fact, similar types of global motions were theoretically studied for DNA[7-10] and dynamic effect on ET through DNA has been invoked.[11,12] Torsional motions primarily affect the electronic coupling between adjacent electronic sites[13] and for DNA, a model was suggested whereby ET is gated by base motions, with only certain well-coupled arrangements of the DNA bases being active toward ET. Although the electronic coupling between the donor and acceptor through the intramolecular H-bonding network in α-helical peptides is assumed to be very high,[14-18] ET can be similarly anticipated to be controlled, or "gated", by the molecular dynamics.

To investigate the hypothesis, we synthesized one redox-active α-helical peptide: Fc-KTAL_{18}NPC-NH_2 (**Fc18L**), and two redox-inactive peptides: Ac-KTAL_{18}NPC-NH_2 (**Ac18L**) and Ac-CTAL_{18}NPK-NH_2 (**18LAc**). Both **Fc18L** and **Ac18L** possess the thiol-

functionalized Cys residue at the C-terminal, whereas, peptide **18LAc** has it at the N-terminal (Figure 2.1).

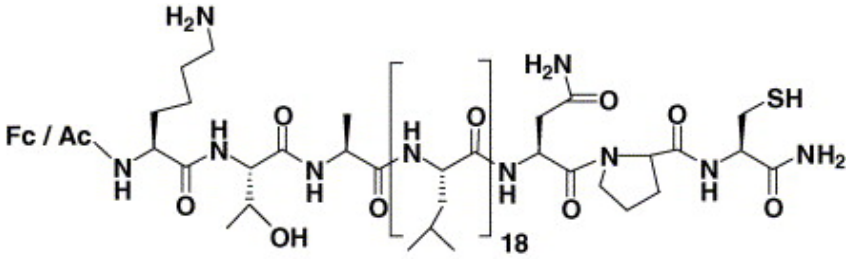

Fc18L and **Ac18L**

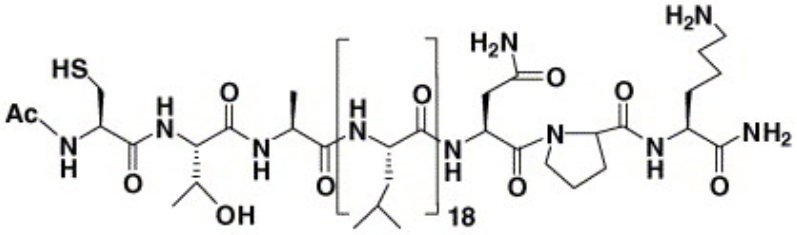

18LAc

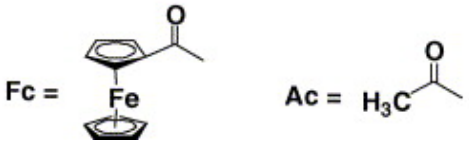

Figure 2.1. Molecular structures of the peptides **Fc18L, Ac18L** and **18LAc**.

Two types of self-assembled films having **Fc18L** diluted in a matrix of Ac-peptides were prepared: **SAM1** consists of **Fc18L** and **Ac18L** (5:95), and **SAM2** consists of **Fc18L**, **Ac18L** and **18LAc** (5:45:50). In **SAM1**, the dipole moments of the peptides are aligned parallel, whereas in **SAM2**, they are aligned antiparallel (Figure 2.2). Since packing in helical peptide SAMs is known to be influenced significantly by the relative orientation of the peptide macrodipole,[19,20] **SAM1** and **SAM2** allowed us to

evaluate the influence of the packing on ET through the redox-active **Fc18L**. Here we describe the results of our study showing that there are significant differences in the ET kinetics of **Fc18L** in **SAM1** and **SAM2**.

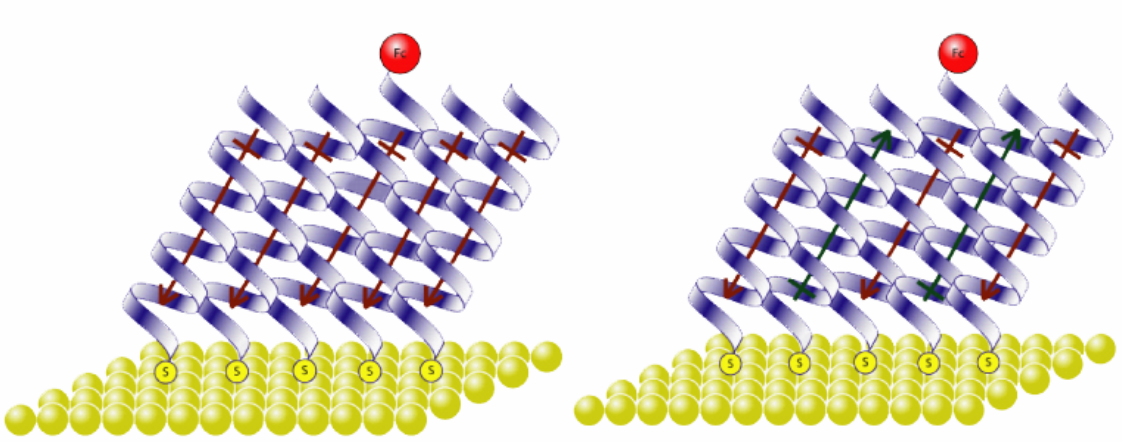

Figure 2.2. Schematic diagram of: **SAM1** (left) and **SAM2** (right), showing the direction of the dipole moments of the α-helical peptides on gold surface.

2.3. Experimental

2.3.1. Peptide Synthesis and Characterization

Fmoc-protected l-α-amino acids, hydroxybenzotriazole (HOBt), (1H-benzotriazol-1-yloxy)tris(dimethylamino)-phosphonium hexafluorophosphate (BOP) and PAL resin were purchased from Advanced ChemTech (Louisville, KY). All other reagents and solvents were obtained from Sigma–Aldrich Canada Ltd. and used as received. Peptides were synthesized following the Fmoc-based strategy with PAL resin at 0.1 mmol scale. N^{α}-Fmoc was removed with a solution of 1% Triton X-100 and 1% DBU in piperidine-DMF (1:3 v/v). Coupling was carried out for 2 h with AA/BOP/HOBt/DIEA (3:3:3:6 equivalents with respect to the resin) in 1% Triton X-100 and 2 M ethylene carbonate in DCM-DMF (3:4 v/v). Twenty percent acetic anhydride in

DMF was used (30 min) for acetylation. Crude peptides were precipitated with ice-cold ether, washed with 1 ml MeCN (5 times) and purified using Merk silica gel 60 F254 aluminum plates. The solvent system used was $CHCl_3$/MeOH/CH_3COOH (85/12/3 v/v/v).

18LAc: IR (cm^{-1} KBr disk): 3300 Amide A; 1658 Amide I; 1542 Amide II. ESI-MS: calculated for $C_{135}H_{245}N_{27}O_{27}S$ = 2709.8 [M]; found: 1356.5 $[M + 2H]^{2+}$, 1303.9 $[M - (CH_3CONH)–(CONH_2)]^{2+}$, 1052.7 $[M - (L_2NPC)]^{2+}$, 991.7 $[M - (L_3NPC)]^{2+}$, 935.2 $[M - (L_4NPC)]^{2+}$, 878.6 $[M - (L_5NPC)]^{2+}$, 822.1 $[M - (L_6NPC)]^{2+}$, 765.5 $[M - (L_7NPC)]^{2+}$, 709.0 $[M - (L_8NPC)]^{2+}$.

Ac18L: IR (cm^{-1} KBr disk): 3301 Amide A; 1657 Amide I; 1542 Amide II. ESI-MS: calculated for $C_{135}H_{245}N_{27}O_{27}S$ = 2709.8 [M]; found: 911.6 $[M + Na + 2H]^{3+}$, 904.3 $[M + 3H]^{3+}$, 979.7 $[M - (CH_3CO)–(L_{12}NPC)]^{+}$, 866.6 $[M - (CH_3CO)–(L_{13}NPC)]^{+}$.

Fc18L: IR (cm^{-1} KBr disk): 3301 Amide A; 1658 Amide I; 1541 Amide II. ESI-MS: calculated for $C_{144}H_{251}N_{27}O_{27}FeS$ = 2879.8 [M]; found: 903.4 $[M - (CONHCysCONH_2) + 3H]^{3+}$, 923.1 $[M - (L_6NPC)]^{2+}$, 866.1 $[M - (L_7NPC)]^{2+}$, 809.5 $[M - (L_8NPC)]^{2+}$, 753.0 $[M - (L_9NPC)]^{2+}$, 332.1 $[NPC]^{2+}$.

2.3.2. Solution and Surface Characterization Methods

Circular dichroism (CD) spectra were recorded with an Applied Photophysics π^*-180 instrument interfaced to an Acorn PC. Fourier transform-reflection absorption infrared (FT-RAIR) spectra were recorded in a Bio-Rad FTS-40 system interfaced to a PC. Ellipticity was reported as the mean residue ellipticity (θ, in deg cm^2/dmol) and calculated as, $\theta = \theta_{obs}(MRW/10\ lc)$, where θ_{obs} is the ellipticity measured in millidegrees, MRW is the mean residue molecular weight of the polypeptide molecular

weight divided by the number of amino acid residues), c is the concentration of the sample in milligrams/milliliter, and l is the optical path length of the cell in centimeters. Wavelength scans were performed in a 0.1 mm CD cell. The helix content, $f_h = -(\theta_{222} + 2340)/30{,}300$, was calculated from the observed mean residue ellipticity θ_{222} for a particular peptide.[21] The helix contents of all the peptides were above 90% (Table 2.1).

2.3.3. Electrochemistry

Details of the preparation of microelectrodes are published elsewhere.[22] The gold electrodes were immersed in 0.1 mM solutions of the peptides in TFE and self assembly was allowed for 5 days. Electrochemical measurements were carried out on a CHI 660B potentiostat. The supporting electrolyte was 2.0 M $NaClO_4$, and the working, counter and reference electrodes were gold microelectrode (diameter of 50 μm), Pt wire, and Ag/AgCl/3.0 M KCl (BAS), respectively. All data were analyzed with OriginLab 7.0 software.

2.4. Results and Discussion

The ferrocenoylated and acetylated leucine-rich hydrophobic peptides **Fc18L**, **Ac18L** and **18LAc** were synthesized by solid phase synthesis on PAL resin using the Fmoc-based protocol. Their α-helical conformation was confirmed by circular dichroism (CD) spectroscopy in trifluoroethanol (TFE), known to stabilize the α-helicity.[23] All three peptides showed minima at 222 and 208 nm (Figure 2.3), characteristic of the α-helical structure.[24-26]

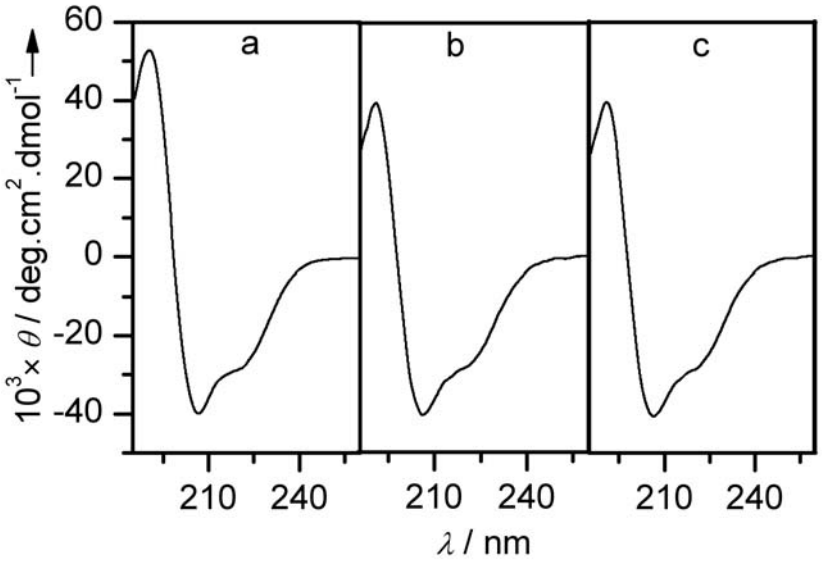

Figure 2.3. CD spectra of **18LAc** (a), **Ac18L** (b) and **Fc18L** (c) in trifluoroethanol at a concentration of 100 μM at 22 ± 1 °C.

We prepared two types of peptide films. **SAM1** was prepared by depositing a solution of **Fc18L** and**Ac18L** (5:95) onto gold surfaces. Once linked to the gold surface via the cystein thiolate, both **Fc18L** and **Ac18L** have their dipole moments oriented in the same direction. The positive end of the peptide dipole is on the film surface, while the negative end of the dipole is at the gold surface. **SAM2** was formed from a solution of **Fc18L**, **Ac18L** and **18LAc** (5:45:50). In this film, the redox-active peptide **Fc18L** is embedded in a matrix of **Ac18L** and **18LAc**. Most noteworthy is that dipole of peptide **18LAc** is the opposite compared to the other diluent **Ac18L**. The difference in peptide orientation and dipole alignment in the two films is shown in Figure 2.2.

To gain insight into the conformation of the peptides on gold surfaces, RAIRS was used. The Amide I band for both films **SAM1** and **SAM2** was observed around 1669 cm^{-1} (Figure 2.4) and is in agreement with that reported previously for bacteriorhodopsin[27] and some other synthetic α-helical peptides on surface.[19,28] The

tilt angles of **SAM1** and **SAM2** (26° and 22°, respectively) on the gold surface were obtained from the ratio of the Amide I and the Amide II following the procedure described before.[19,20] The lower tilt angle of **SAM2** is consistent with the more compact packing of the peptides due to the antiparallel arrangement of intermolecular macrodipoles.[19,20] Since all three peptides have the same number of the hydrophobic Leu residues, the van der Waals interactions among the neighboring peptides should be similar in both **SAM1** and **SAM2**, it can be assumed that differences in the compactness is due to the different alignment of the peptide dipoles and that this results in a tighter packing in **SAM2** compared to **SAM1**. The estimated dipole moment for all three oligopeptides, assuming 3.46 D per amino acid residue,[29] is 83.04 D (3.46 × 24). MMFF calculations (using SPARTAN '04 Mechanics Program, Irvine, CA) indicated the dipole moments of the optimized **Fc18L**, **Ac18L** and **18LAc** to be 87.12, 92.77 and 87.10 D, respectively, whereas in the case of an alkanthiol of comparable length ($C_{31}SH$), the dipole moment is only 2.2 D. The higher calculated values are reasonable because theoretical considerations indicated an increase in the residual dipole moment by polarization due to H-bonds in the α-helix, yielding values of up to 5 D.[29] Direct evidence for helix–helix–macrodipole interaction and consequent enhanced molecular packing (on gold surfaces) has been specifically reported.[19,20] Antiparallel helix–macrodipole interactions are of sufficient strength to allow the discrimination of N- and C-termini of helical peptide guests in solution by forming complexes with surface supported host peptides.[20,30] The capability for complex formation was lost when the host peptide was not helical and consequently, had no net dipole moment. On the basis of helix–macrodipole interactions, single- and double-layered helix polypeptide assemblies can be spontaneously produced on gold substrates, which are readily

controlled by the polypeptide conformation.[31] Furthermore, the interaction plays an important role in the higher order structures and functions of proteins.[32,33]

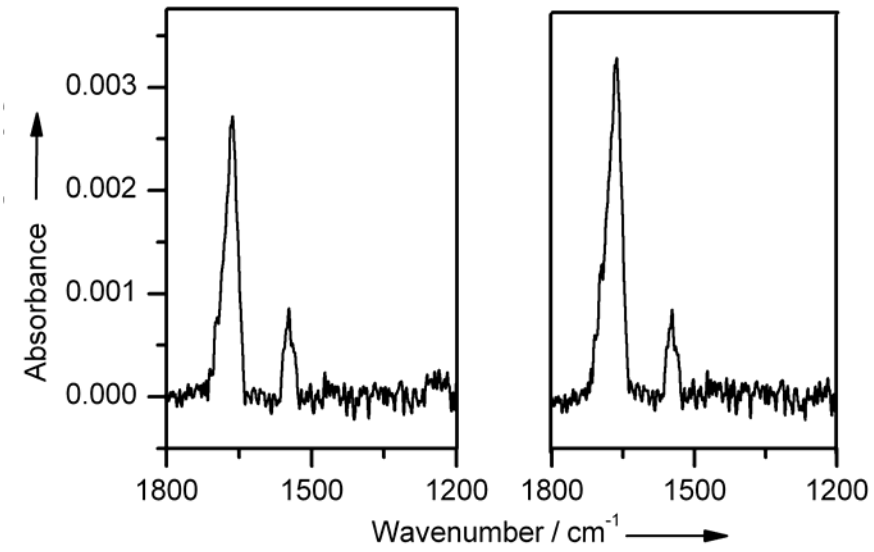

Figure 2.4. FT-RAIRS of **SAM1** (left) and **SAM2** (right).

Cyclic voltammetry (CV) was employed to investigate the electrochemical properties of the films and ET kinetics of the redox-labeled peptide **Fc18L** in **SAM1** and **SAM2**. The corresponding rationale is that tighter packing of the peptides in **SAM2** would result in a more restricted molecular dynamics compared to **SAM1**. We kept the concentration of the redox-labeled peptides at 5% in order to minimize interactions amongst neighboring redox centers during the electrochemical measurements. Both films exhibited reversible redox reaction of the ferrocene moiety, as the ratios of the anodic to the cathodic peak were near unity. The formal potentials ($E°$) were 450 ± 15 and 400 ± 10 mV for **SAM1** and **SAM2**, respectively. The values of E_{fwhm} was higher (~170 mV in **SAM1** and ~210 mV in **SAM2**) compared to the ideal (90 mV) which is attributed to the slow ET process across the peptide.[34] Also the capacitive current is

lower in **SAM2** (Figure 2.5) indicating more compact packing[19,20] Standard ET rate constants ($k_{et}°$) were evaluated from CV using the Butler–Volmer methodology[35] and **SAM2** exhibited a much slower rate [1.2(3) × 10^{-3} s^{-1}] than **SAM1** [1.5(5) × 10^{-2} s^{-1}].

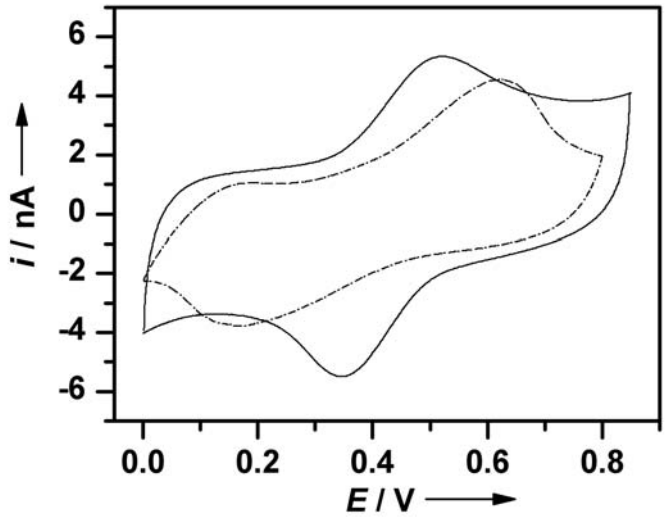

Fig. 2.5. Cyclic voltammograms of **SAM1** (—) and **SAM2** (– · – · –) in 2.0 M $NaClO_4$ (scan rate = 4 mV/s) at 22 °C.

Table 2.1. Summary of structural parameters for the helical peptides and films (**SAM1** and **SAM2**)

Parameters	**18LAc**	**Ac18L**	**Fc18L**	**SAM1**	**SAM2**
Dipole moment/*D*	87.10	92.77	87.12	–	–
Helix contents (f_h)/%	99	97	99	–	–
Tilt angle θ/°	–	–	–	22	26
$k_{et}°/s^{-1}$	–	–	–	1.5(5) × 10^{-2}	1.2(3) × 10^{-3}

The interfacial properties of both **SAM1** and **SAM2** were evaluated by electrochemical impedance spectroscopy (EIS) and the data agreed qualitatively with the observations from RAIRS and CV. Figure 2.6 shows the Nyquist plots of **SAM 1** and

SAM 2, measured at their formal potentials. The data were fit to a modified Randles circuit (Figure 2.6) and the parameters are listed in Table 2.2. Similar type of circuit was previously used to describe films of DNA[36,37] and 4-hydroxy-4-mercaptobiphenyl.[38] The presence of a constant-phase element (CPE), which acts as a nonlinear capacitor accounts for the inhomogeneity on the electrode surface.[39] CPE (i.e., film capacitance) is lower in **SAM2** indicating higher film thickness and/or more compact film.[36] The corresponding frequency power (n) is higher compared to that in **SAM1**, which specifies that **SAM2** is also more ordered.[40] The diameter of the semicircle in a Nyquist plot is a measure of the charge transfer resistance (R_{CT})[36] and R_{CT} is considerably (order of magnitude) higher for **SAM2** than for **SAM1**. R_{CT} is inversely proportional to ET rate[41,42] and thereby indicates a slower ET rate for **SAM2**. R_X is the interfacial resistance through the SAM. Although the correct nature of R_X is unknown, it has been suggested to be a consequence of reorientation of dipoles in the SAM structure.[38] Both R_X and R_{CT} for **SAM2** were significantly higher compared to **SAM1**.

To date, the mechanistic discussion of ET through α-helical peptides is highly controversial. A "hopping mechanism" through the amide groups[43,44] was suggested but evidence in favor of ET by "tunneling" through the intramolecular hydrogen-bonding network has also been reported.[14,15] The lower ET rate of **Fc18L** in **SAM2** cannot be explained by simple "hopping" or "tunneling". Due to the stabilization among the helix dipoles, the structure of the peptide **Fc18L** should be more ordered in **SAM2**, compared

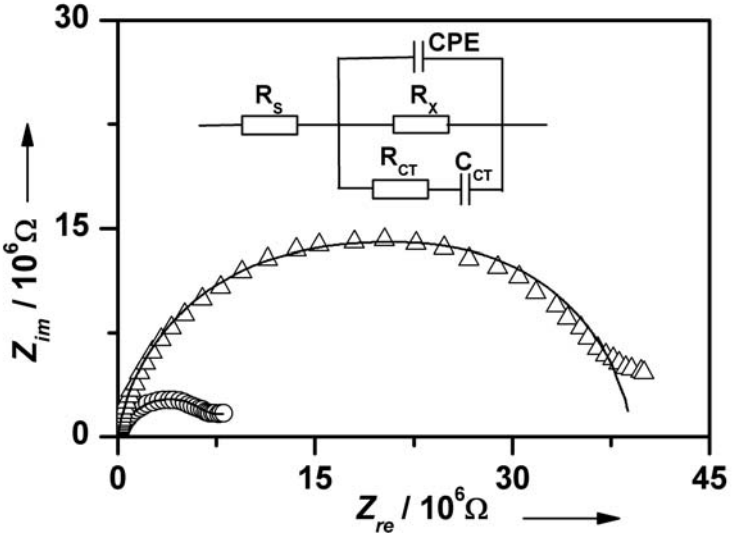

Figure 2.6. Nyquist plots (Z_{im} vs. Z_{re}) for the Faradaic impedance measurements in 2.0 M $NaClO_4$. Points represent experimental data for **SAM1** (▫) and **SAM2** (△), respectively. The data were fit (solid line) to the equivalent circuit that includes a solution resistor R_S, a constant-phase element (CPE), the interfacial resistor R_X, the charge transfer resistor R_{CT} and a capacitor C_{CT} (using ZsimpWin software, Princeton Applied Research).

Table 2.2. Equivalent circuit element values for **SAM1** and **SAM2.**

Element	**SAM1**	**SAM2**
R_s / Ω	7.53×10^2	6.39×10^2
R_X / Ω	9.67×10^6	3.91×10^7
CPE / S-s$^{1/2}$	2.53×10^{-9}	1.20×10^{-9}
n	7.79×10^{-1}	9.01×10^{-1}
R_{CT} / Ω	3.79×10^7	1.30×10^8
C_{CT} / F	3.34×10^{-9}	4.34×10^{-10}

to in **SAM1**[19,20] and ET should increase in **SAM 2** if one of those mechanisms would be the major ET pathway. Furthermore, the $E°$ of **SAM2** is lower than that of **SAM1** by ~50 mV (~5 kJ mol^{-1}), indicating that ET is thermodynamically more favorable for **SAM2**, although we observe a slower ET kinetics. We speculate that the slower ET kinetics through **Fc18L** in **SAM2** is a consequence of the restricted molecular dynamics of **Fc18L** due to tighter intermolecular interaction among the antiparallel helical

macrodipoles. This would point to a conformationally gated ET mechanism. This type of mechanism has been shown to be important in ET through DNA.[11,12] CVs were recorded for both **SAM1** and **SAM2** at lower temperature and ET was found to decrease (increase in peak separation[35]) with lowering the temperature (Figure 2.7), which demonstrates the effect of decreased molecular dynamics on ET across the peptide.

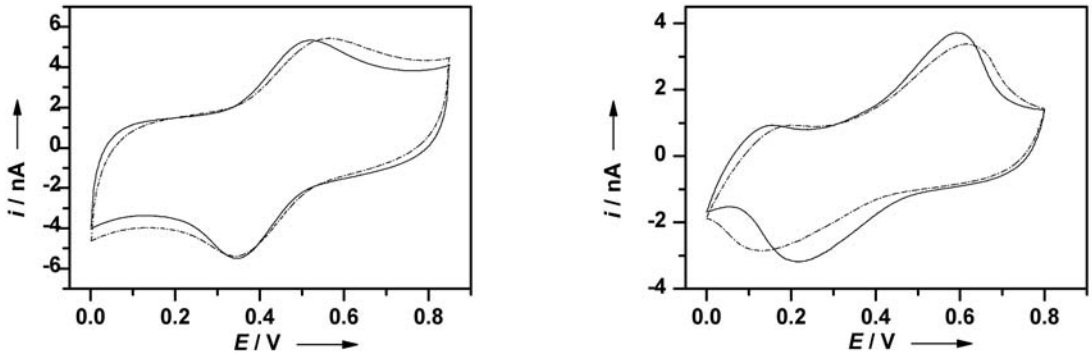

Figure 2.7. Cyclic voltammograms in 2.0 M $NaClO_4$ at 22 ºC (—) and 0 ºC (– · – ·): (left) **SAM1** (scan rate = 4 mV/s) and (right) **SAM2** (scan rate = 3 mV/s).

In conclusion, it is proposed that ET in α-helical peptides occurs through certain well-coupled ET active conformers and that the ET process is limited by the frequency of forming the conformers from which ET can take place. At present, we are working on time-resolved IR and Raman studies, which would allow us to gain more insight into the conformational properties of the peptide films.

2.5. Acknowledgments

This work was funded by the Natural Science and Engineering Research Council of Canada. H.-B.K. is the Canada Research Chair in Biomaterials.

2.6. References

[1] A.B. Hope, *Biochim. Biophys. Acta* **2000**, 1456, 5-26.
[2] G.W. Canters, C. Dennison, *Biochimie* **1995**, 77, 506-515.
[3] J.R. Winkler, H.B. Gray, *J. Biol. Inorg. Chem.* **1997**, 2, 399-404.
[4] S.-Y. Sheu, E. W. Schlag, D.-Y. Yang, H. L. Selzle, *J. Phys. Chem. A.* **2001**, 105, 6353-6361.
[5] G. V. Papamokos, I. N. Demetropoulos, *J. Phys. Chem. A.* **2004**, 108, 8160-8169.
[6] A. Idiris, M. T. Alam, A. Ikai, *Protein Eng.* **2000**, 13, 763-770.
[7] T. H. Duong, K. J. Zakrzewska, *Comput. Chem.* **1997**, 18, 796-811.
[8] L. Donghai, A. Matsumoto, G. Nobuhiro, *J. Chem. Phys.* **1997**, 107, 3684-3690.
[9] A. Matsumoto, N. Go, *J. Chem. Phys.* **1999**, 110, 11070-11075.
[10] S. Cocco, R. Monasson, *J. Chem. Phys.,* **2000**, 110, 11070-.
[11] M. A. O'Neill, J. K. Barton, *J. Am. Chem. Soc.* **2004**, 126, 13234-13235.
[12] M. A. O'Neill, J. K. Barton, *J. Am. Chem. Soc.* **2004**, 126, 11471-11483.
[13] W. B. Davis, M. A. Ratner, M. R. Wasielewski, *J. Am. Chem. Soc.* **2001**, 123, 7877-7886.
[14] F. Polo, S. Antonello, F. Formaggio, C. Toniolo, F. Maran, *J. Am. Chem. Soc.* **2005**, 127, 492-493.
[15] S. Antonello, F. Formaggio, A. Moretto, C. Toniolo, F. Maran, *J. Am. Chem. Soc.* **2003**, 125, 2874-2875.
[16] S. I. Stephan, Y. O. Michael, F. W. James, *Chem. Rev.* **1992**, 92, 381-394.
[17] T. Morita, S. Kimura, S. Kobayashi, Y. Imanishi, *J. Am. Chem. Soc.* **2000**, 122, 2850-2859.
[18] H. B. Gray, J. R. Winkler, *J. Electroanal. Chem.* **1997**, 438, 43-47.
[19] S. Yasutomi, Y. Imanishi, S. Kimura, *Science* **2004**, 304, 1944-1947.
[20] M. Niwa, M. Morikawa, N. Higashi, *Angew. Chem. Int. Ed.* **2000**, 39, 960-963.
[21] Y. -H. Chen, J. T. Yang, H. M. Martinez, *Biochemistry* **1972**, 11, 4120-4131.
[22] I. Bediako-Amoa, T. C. Sutherland, C.-Z. Li, R. Silerova, H.-B. Kraatz, *J. Phys. Chem. B.* **2004**, 108, 704-714.
[23] T. Kiyota, S. Lee, S. Sugihara, *Biochemistry* **1996**, 35, 13196-13204.
[24] K. Kitagawa, T. Morita, S. Kimura, *J. Phys. Chem. B.* **2004**, 108, 15090-15095.
[25] G. Holzwarth, P. Doty, *J. Am. Chem. Soc.* **1965**, 87, 218-228.
[26] Y. H. Chen, J. T. Yang, H. M. Martinez, *Biochemistry* **1972**, 11, 4120-4131.
[27] M. Sonoyama, S. Mitaku, *J. Phys. Chem. B* **2004**, 108, 19496-19500.
[28] K. Fujita, N. Bunjes, K. Nakajima, M. Hara, H. Sasabe, W. Knoll, *Langmuir* **1998**, 14, 6167-6172.
[29] A. Wada, *Adv. Biophys.* **1976**, 9, 1-63.
[30] M. Niwa, M. Morikawa, N. Higashi, *Langmuir* **1999**, 15, 5088-5092.
[31] M. Niwa, T. Murata, M. Kitamatsu, T. Matsumoto, N. Higashi, *J. Mater. Chem.* **1999**, 9, 343-344.
[32] A. Chakrabartty, A. J. Doig, R. L. Baldwin, *Proc. Natl. Acad. Sci.* **1993**, 90, 11332-11336.
[33] K. M. Armstrong, R. L. Baldwin, *Proc. Natl. Acad. Sci.* **1993**, 90, 11337-11340.
[34] R. Murray, *Electroanal. Chem.* **1984**, 13, 191-368.
[35] A. J. Bard, L. R. Faulkner, *Electrochemical Method: Fundamentals and Applications*, 2nd ed.; John Wiley: New York, **2001**.

[36] Y.T. Long, C. Z. Li, T. C. Sutherland, H. B. Kraatz, J. S. Lee, *Biophy. J.* **2003**, 84, 3218-3225.
[37] Y.T. Long, C. Z. Li, T. C. Sutherland, H. B. Kraatz, J. S. Lee, *Anal. Chem.* **2004**, 76, 4059-4065.
[38] R. P. Janek, W. R. Fawcett, A. Ulman, *Langmuir* **1998**, 14, 3011-3018.
[39] M. Dijksma, B. A. Boukamp, B. Kamp, W. P. van Bennekom, *Langmuir* **2002**, 18, 3105-3112.
[40] W. R. Fawcett, Z. Kovacova, A. J. Motheo, C. A. Foss, *J. Electroanal. Chem.* **1992**, 326, 91-103.
[41] H. O. Finklea, M. S. Ravenscroft, D. A. Snider, *Langmuir* **1993**, 9, 223-227.
[42] V. Pardo-Yissar, E. Katz, O. Lioubashevski, I. Willner, *Langmuir* **2001**, 17, 1110-1118.
[43] T. Morita, S. Kimura, *J. Am. Chem. Soc.* **2003**, 125, 8732-8733.
[44] R. A. Malak, Z. Gao, J. F. Wishart, S. S. Isied, *J. Am. Chem. Soc.* **2004**, 126, 13888-13889.

Chapter 3

Study of Electron Transfer in α-Helical Peptides: Implication of a Dynamically Controlled Bridge-mediated Tunneling Mechanism

3.1. Connecting Text

In the previous chapter, it was suggested that ET in a peptide film made up of α-helical peptides is controlled by the dynamic properties of the molecules and the film. In this chapter, I will expand on the connection between the dynamic properties of α-helical peptides and the electron transfer process, and will present an in-depth discussion of the mechanistic details.

This manuscript is co-authored by H.-B. Kraatz. My contributions to this work are the experimental study and writing. The manuscript has gone through revisions by Prof. Kraatz.

3.2. Introduction

The α-helix is a frequently observed secondary structure in proteins.[1] Specifically, the photosynthetic reaction center is rich in helical content[2] and electron transfer (ET) studies of synthetic α-helical model peptides may help to elucidate the mechanism of complex biological ET processes. There are several interesting reports[3,4] in which the natural photo-system was mimicked by synthetic α-helices functionalized with light-harvesting chromophores, making such studies relevant to the development of artificial solar energy converters, and exploiting α-helices as part of nano-scaled photovoltaic devices. At present, the mechanistic discussion of the long range ET from a donor (D) to an acceptor (A) through the helix is, however, highly controversial and involves ET by

a) tunneling through the peptide matrix[5] following the "distance model" which considers proteins as a "generic organic matrix". ET depends simply on the D-A distance;[6]

b) tunneling according to the "pathway model",[7] and involves the peptide backbone and the intra-molecular H-bonding network, which offer the highest coupled ET paths;[8]

c) tunneling *via* intra-molecular H-bond "shortcuts";[9]

d) hopping of electrons[10] or holes[11] through the peptide backbone akin to what has been reported for DNA;[12]

e) a conformationally gated mechanism[13] although its exact nature remains unexplored.

In this work, we report a detailed ET study of a set of Leu-based α-helical peptides of increasing lengths. The peptides possess a cysteine residue at the C-terminal and the redox-active ferrocene (Fc) at the N-terminal: Fc-KTAL_nNPC-NH_2, where n = 10 (**Fc10L**), 14 (**Fc14L**) and 18 (**Fc18L**). For the preparation of redox-diluted films,

suitable for electrochemical studies,[14] acetylated peptides having an *N*-terminal acyl group rather than a Fc group, were also prepared (Figure 3.1). We used Leu since it has a high helix-forming propensity.[15] The resulting hydrophobic peptides should have a high probability of forming well-packed and ordered films due to van der Waals interactions and inter-digitations of the hydrophobic side chains of Leu residues.[16] In addition, solvent penetration into the resulting hydrophobic film is reduced, avoiding complications due to any solvent-mediated long range ET.[17,18]

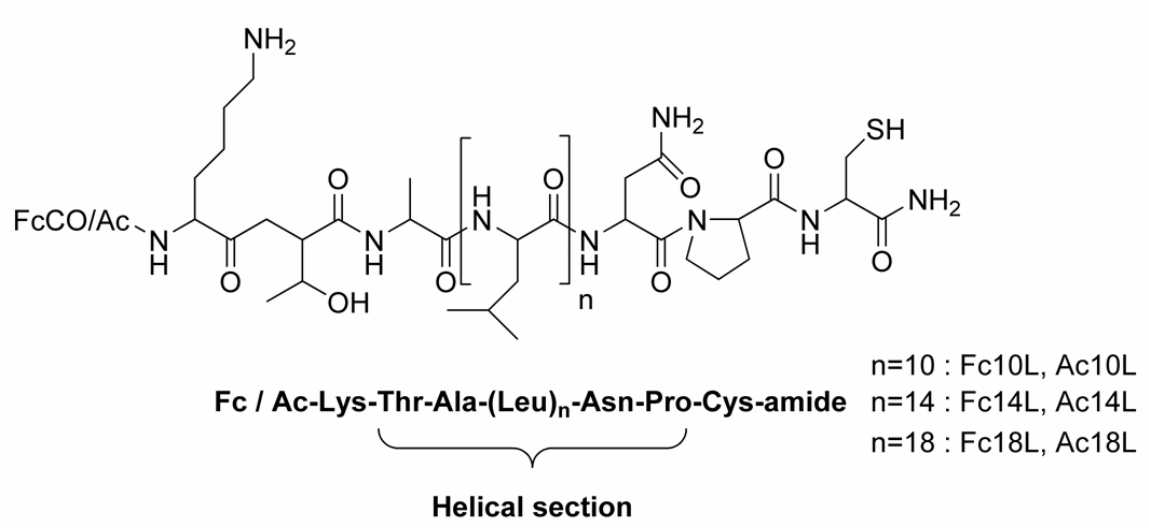

Figure 3.1. Chemical structures of the ferrocenoyl/acetyl-peptides.

3.3. Experimental

3.3.1. Materials

Fluorenylmethyloxycarbonyl (Fmoc)-protected L-α-amino acids, 1-hydroxybenzotriazole (HOBt) were purchased from SynPep (Dublin, CA). 5-(4-Fmocaminomethyl-3, 5-dimethoxyphenoxy)valericacid-MBHA (PAL) resin, (1H-benzotriazol-1-yloxy)tris-(dimethylamino)phosphoniumhexafluorophosphate (BOP) were from Advanced ChemTech (Louisville, KY). All other reagents and solvents including N-methyl-2-

pyrrolidinone (NMP), 1,8-diazabicyclo[5.4.0]undec-7-ene (DBU) and diisopropylethyl-amine (DIPEA) were obtained from Sigma-Aldrich Canada Ltd. and used as received.

3.3.2. Peptide Synthesis

The polypeptides were synthesized using a semi-automated synthesizer (Argonaut Technologies Quest 210) following the Fmoc-solid phase peptide synthesis (SPPS) methodology with PAL resin as the solid support. This type of resin is acid labile and results in a peptide amide as the final product.[19] The following acid labile side-chain protecting groups were used: O-t-Butyl (Thr), N^{α}-tert-butyloxycarbonyl (Lys), trityl (Cys, Asn), so that after completion of the synthesis, the peptides could be simultaneously deprotected and cleaved by trifluoroacetic acid (TFA). Initially, the Fmoc-protected resin was swelled for 2 hours in DMF followed by removal of the Fmoc group with 20% piperidine in DMF (1 × 5 ml, 1 × 15 ml). N^{α}-Fmoc and side-chain protected amino acids were added stepwise in the C → N direction (see Scheme 3.1). After completion of the chain assembly, the peptidyl resins were washed thoroughly with DMF and DCM, and dried by purging N_2 through the system. Cleavage of the peptide from the solid support and simultaneous side chain deprotection were achieved by treatment with TFA:phenol:triethylsilane (95:2.5:2.5) for 2 hours at room temperature. Filtrates from the cleavage mixture were collected, concentrated by flowing N_2 and treated with cold ether to precipitate the crude product. Purification was performed using Merk silica gel 60 F_{254} aluminum preparatory plates using the solvent system $CHCl_3$/MeOH/CH_3COOH (85/12/3 v/v/v).

Scheme 3.1. Peptide synthesis protocol.

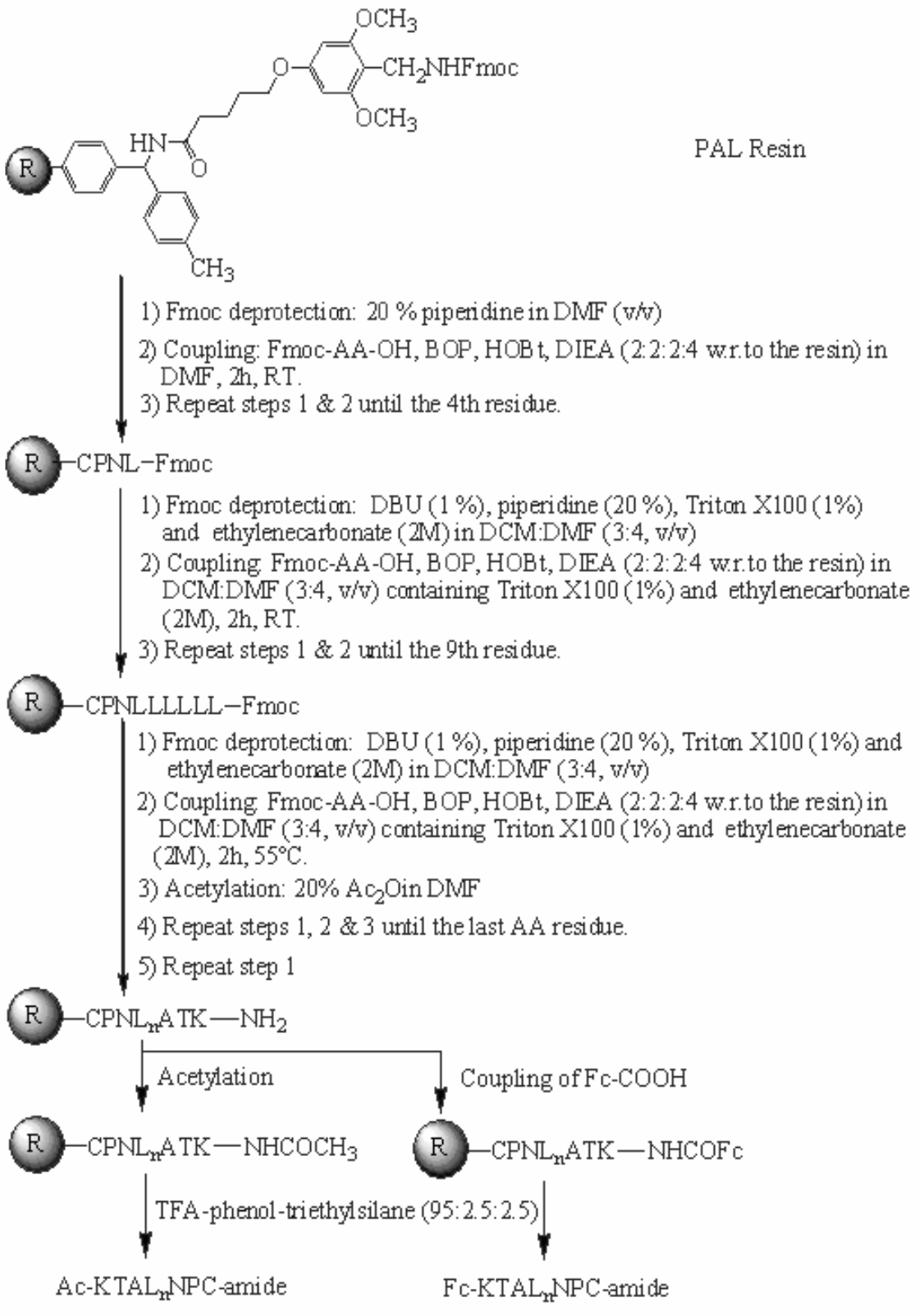

Fc10L R_f = 0.45. ESI-MS: calculated for $C_{96}H_{164}N_{19}O_{19}FeS$ = 1976.1 $[M+H]^+$; found 988.6 $[M+2H]^{2+}$.

Fc14L R_f = 0.41. ESI-MS: calculated for $C_{120}H_{208}N_{23}O_{23}FeS$ = 2428.5 $[M+H]^+$; found 1214.8 $[M+2H]^{2+}$ 810.2 $[M+3H]^{3+}$.

Fc18L R_f = 0.38. ESI-MS: calculated for $C_{144}H_{252}N_{27}O_{27}FeS$ = 2880.8 $[M+H]^+$; found: 903.4 $[M-(CONHCysCONH_2)+3H]^{3+}$, 923.1 $[M-(L_6NPC)]^{2+}$, 866.1 $[M-(L_7NPC)]^{2+}$, 809.5 $[M-(L_8NPC)]^{2+}$, 753.0 $[M-(L_9NPC)]^{2+}$, 332.1 $[NPC]^{2+}$.

Ac10L R_f = 0.45. ESI-MS: calculated for $C_{87}H_{158}N_{19}O_{19}S$ = 1805.2 $[M+H]^+$; found: 903.1 $[M+2H]^{2+}$.

Ac14L R_f = 0.41. ESI-MS: calculated for $C_{111}H_{202}N_{23}O_{23}S$ = 2258.5 $[M+H]^+$; found 1129.7 $[M+2H]^{2+}$, 1078.7 $[M-(CH_3CONH)-(CONH_2) + 2H]^{2+}$.

Ac18L R_f = 0.38. ESI-MS: calculated for $C_{135}H_{246}N_{27}O_{27}S$ = 2710.8 $[M+H]^+$; found: 911.6 $[M+Na+2H]^{3+}$, 904.3 $[M+3H]^{3+}$, 979.7 $[M-(CH_3CO)-(L_{12}NPC)]^+$, 866.6 $[M-(CH_3CO)-(L_{13}NPC)]^+$.

3.3.3. Circular Dichroism (CD) Spectroscopy

CD spectra were taken with an Applied Photophysics π*-180 instrument interfaced to an Acorn PC at 22 ± 1ºC. The spectropolarimeter was calibrated daily with an aqueous solution of recrystallized ammonium camphorsulfonate-10-d. Ellipticity was reported as the mean residue ellipticity (θ, in deg·cm^2·dmol^{-1}) and calculated as, $\theta = \theta_{obs}(MRW/10lc)$, where θ_{obs} is the ellipticity measured in millidegrees, MRW is the mean residue molecular weight of the polypeptide molecular weight divided by the number of amino acid residues), c is the concentration of the sample in mg/ml, and l is

the optical path length of the cell in centimeters. Wavelength scans were performed in a 0.1 mm CD cell.

3.3.4. Fourier Transform Infrared (FT-IR) Spectroscopy

A Bio-Rad FTS-40 system was used to record the FT-IR (KBr) spectra at a resolution of 0.5 cm^{-1}.

3.3.5. Preparation and Characterization of Ac-Peptide Films on Gold Substrates

Au on Si (100) (Platypus Technologies, Inc) wafers were incubated in 0.1 mM Ac-peptides in trifluoroethanolic solution for 5 days, washed with TFE, dried under a stream of N_2 and characterized by X-ray photoelectron spectroscopy (XPS), Fourier transform-reflection absorption infrared spectroscopy (FT-RAIRS) and atomic force microscopy (AFM). The XPS spectra were recorded in an Axis-165 X-ray photoelectron spectrometer (Kratos Analytical). AFM images were obtained with a U-SPM system (Quesant Instrument Corporation) using non-contact mode. Before taking the image, the probe was checked using a 100 nm width calibration grating. A Bio-Rad FTS-40 system was used to collect FT-RAIR spectra.

3.3.6. Electrochemistry

Gold microelectrodes (diameter of 50 μm) were immersed in 0.1 mM solutions of the Fc and Ac-peptides (5:95, respectively) in TFE and self assembly was allowed for 5 days, washed with TFE and dried under a stream of N_2. Electrochemical measurements were carried out on a CHI 660B potentiostat. The supporting electrolyte was 2.0 M $NaClO_4$, and the working, counter and reference electrodes were peptide-modified gold

microelectrodes, Pt wire, and Ag/AgCl/3.0 M KCl (BAS), respectively. All data were analyzed with OriginLab 7.0 software.

3.3.7. Current-Voltage (*I-V*) Measurements

For *I-V* data collection, scanning tunneling microscopic (STM) images were taken using a U-SPM system (Quesant Instrument Corporation) at room temperature. A Pt-Ir tip (mechanically cut) was used and constant current mode was employed (bias voltage -1.5 V and current 10 pA). Then the built-in scanning tunneling spectroscopic (STS) module was engaged to collect *I-V* data at different points in the images. The data presented in this work is an average of 100 data points and fitted in MS Office Excel and OriginLab 7.0 softwares.

3.3.8. Computation

The optimized structures, the lengths and the cross-sections of the peptides were obtained using SPARTAN '04 Mechanics Program (Irvine, CA). Molecular mechanics force field (MMFF) calculations were employed. For calculating the molecular orbital energies of a intra-molecularly H-bonded α-helical peptide, a short peptide Ac-Gly_5-amide was generated in SPARTAN '04, exported to Gaussian 03[20] (Gaussian Inc., Pittsburgh, PA) and restricted Hartree-Fock (HF) level calculation of the molecular orbital energies was performed. The basis set was 6-31+G(d, p).

3.4. Results and Discussion

3.4.1. Characterization of the Peptides

Before preparing films on gold surfaces, the secondary structure of all peptides prepared here was studied in solution. We first investigated the circular dichroism (CD) spectra of the peptides in trifluoroethanol (TFE). All the peptides showed an intense maximum at ~190-191 nm and minima at ~206-207 and 220-222 nm (Figure 3.2), which are generally accepted as the characteristics of the helical structure.[21] CD has been proposed for distinguishing between 3_{10}- and α-helix structures by using the ratio of CD bands at 222 nm and 207/208 nm (for the ideal 3_{10}-helical peptide the ratio is 0.4, whereas for ideal α-helical, it is ~1)[22] and the observed ratios (0.55-0.74) can arise from equilibrium mixtures of 3_{10}- and α-helices (Table 3.1). The ratio and the molar ellipticity per residue for the 18 Leu containing peptides are higher than those for the shorter peptides which may indicate that the relative stability of the two conformations can be altered by changing the length of the peptide, and longer peptides favor the population of the α-helical conformation over 3_{10}.[23]

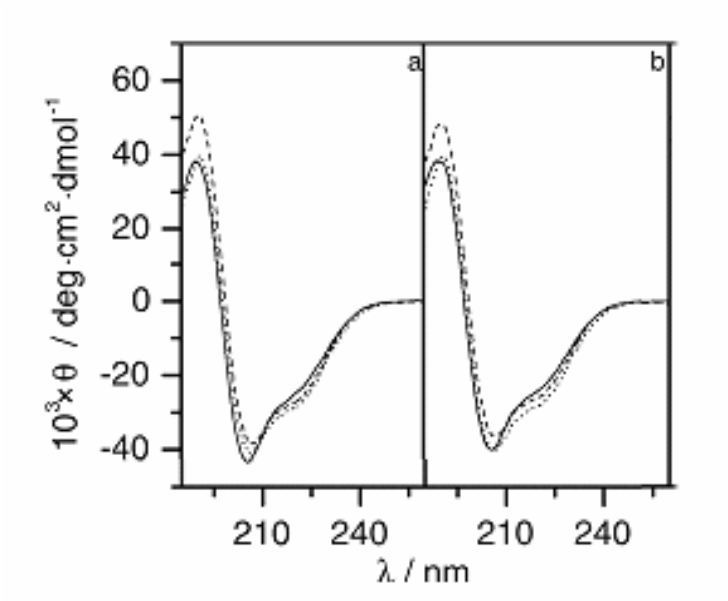

Figure 3.2. CD spectra ferrocenylated and acylated peptides. (a) **Fc10L** (——), **Fc14L** (— —) and **Fc18L** (···); (b) **Ac10L** (——), **Ac14L** (— —) and **Ac18L** (···) in trifluoroethanol at 22 ± 1ºC.

Table 3.1. CD data (in TFE) for the peptides studied. λ in nm.

Peptide	max / nm	min / nm	ratio of minima
Fc10L	190	206, 222	0.55
Fc14L	190	207, 221	0.70
Fc18L	191	206, 220	0.74
Ac10L	190	206, 221	0.58
Ac14L	190	207, 221	0.70
Ac18L	191	206, 221	0.70

The FT-IR spectra of all peptides in KBr also confirmed the helical structure of the peptides. The Amide I (C=O stretch) and II (coupled CN stretch and NH bending) bands for the peptides in KBr appear at 1660-1657 cm^{-1} and 1542-1538 cm^{-1}, respectively, which indicate that the peptides are α-helical in the solid state.[24] Amide A (the stretching vibration band of the H-bonded NH groups in the backbone in helical peptides[25]) occurs with a maximum at 3310-3300 cm^{-1} (Figure 3.3) and with the increase in the peptide length, the band shifts to lower frequency (Table 3.2) indicating stronger intra-molecular H-bonding and more compact structure in longer peptides.

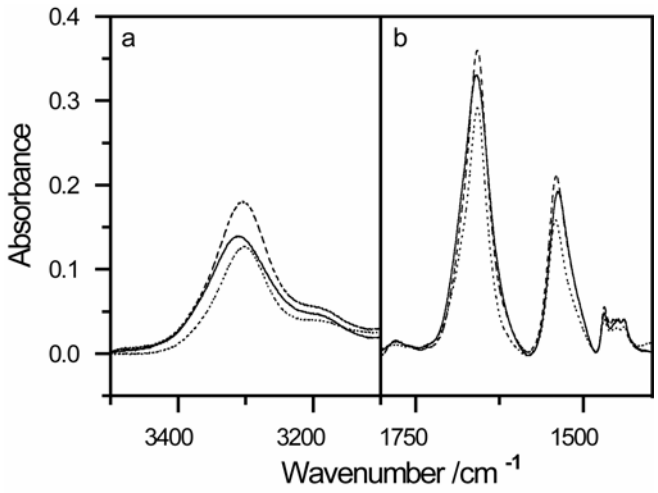

Figure 3.3. IR spectra of **Fc10L** (——), **Fc14L** (— —) and **Fc18L** (···): (a) Amide A and (b) Amide I and II regions.

Table 3.2. IR data for the Amide A, I and II regions for the peptides studied.

Peptides	Amide A / cm^{-1}	Amide I / cm^{-1}	Amide II / cm^{-1}
Fc10L	3310	1659	1538
Fc14L	3304	1658	1540
Fc18L	3301	1658	1541
Ac10L	3307	1659	1538
Ac14L	3304	1658	1540
Ac18L	3301	1657	1542

The redox properties of the Fc-peptides were investigated by cyclic voltammetry (CV) in TFE containing 50 mM TBAP as the supporting electrolyte. As expected, the Fc-peptides showed redox activity and the halfwave potential $E_{1/2}$ was found to increase with increasing length of the peptides, presumably due to more hydrophobic environments[26] in the longer peptides during the redox processes near the electrode surface (450, 485 and 530 mV vs. Ag/AgCl, for **Fc10L**, **Fc14L** and **Fc18L**, respectively. Experimental uncertainty is within ±15 mV).

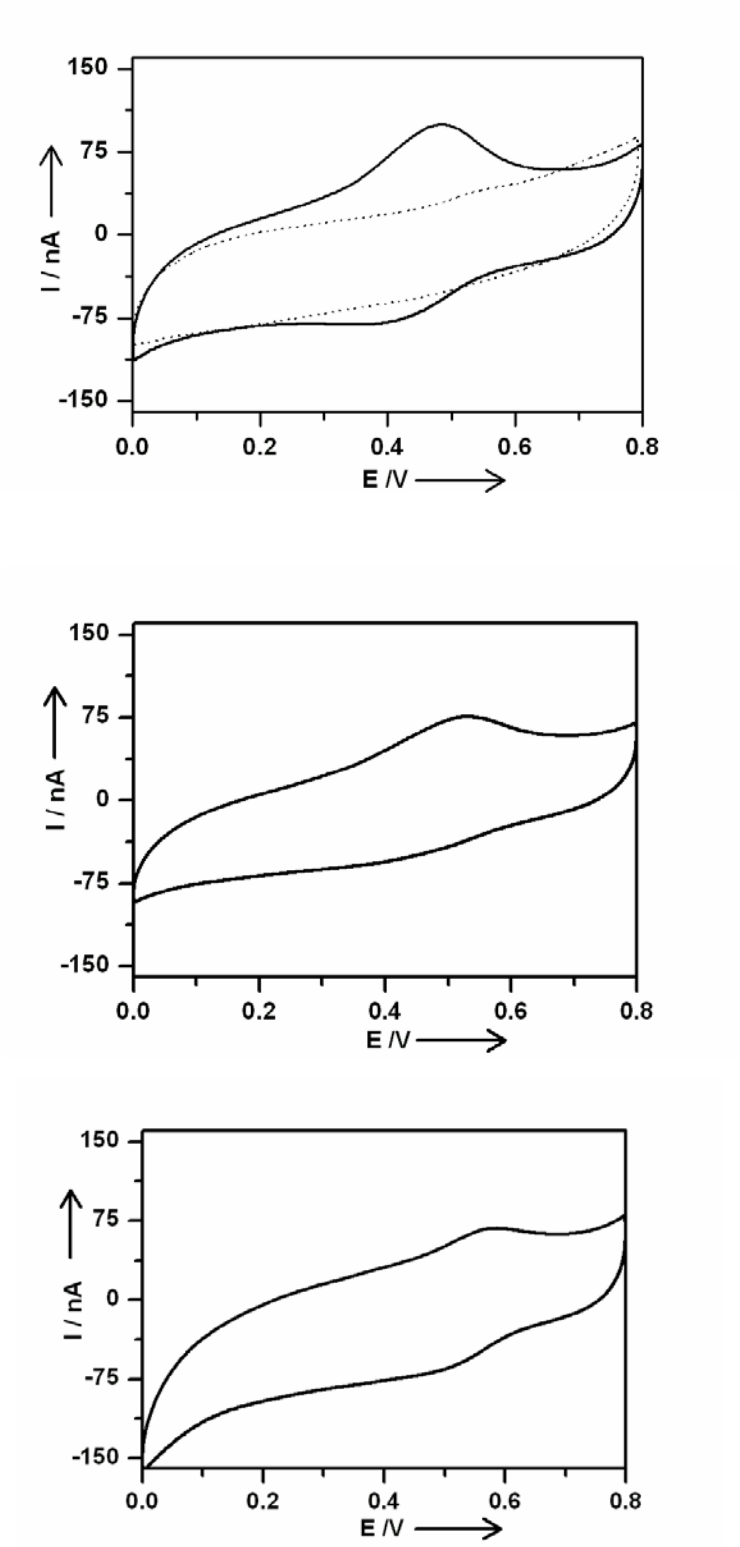

Figure 3.4. Cyclic voltammograms of **Fc10L** (solid) and **Ac10L** (dash) (upper panel), **Fc14L** (middle panel) and **Fc18L** (lower panel) (1.6 mm glassy carbon electrode, 0.1 mM Fc-peptide in TFE containing 50 mM TBAP, scan rate 5 mV/s, Ag/AgCl reference electrode).

3.4.2. Characterization of the Peptide Films

Thin films were prepared on gold substrates by self-assembly from 0.1 mM solutions of Ac-peptides in TFE. The X-ray photoelectron spectroscopy (XPS) of the films showed two S_{2p} signals for all three systems at 162 and 163 eV in a 2:1 ratio indicating the cystein-thiolate bound to Au.[27] The XPS spectra also showed other elements like C and N supporting the presence of the peptides on gold surfaces (Figure 3.5).

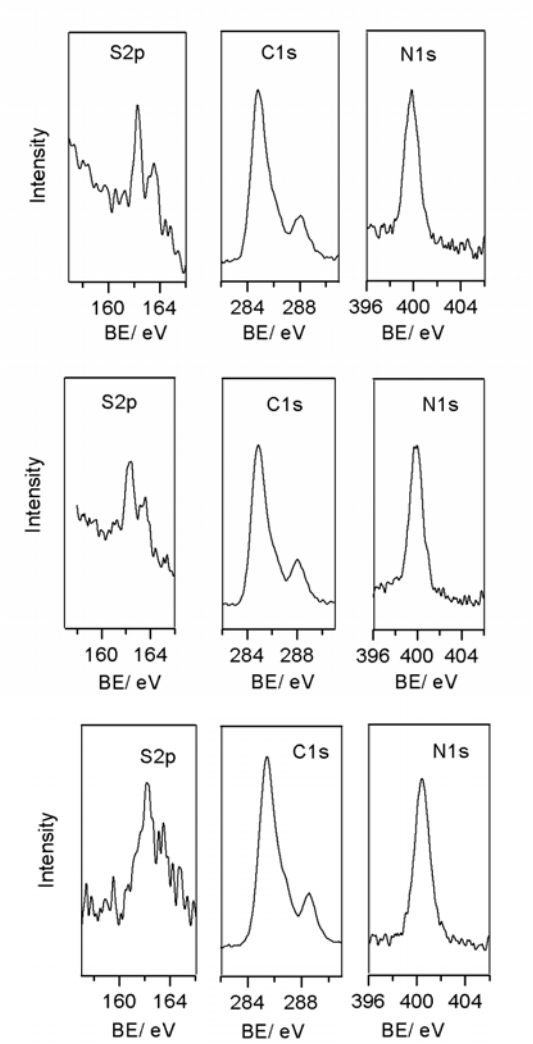

Figure 3.5. XPS of the three Ac-peptide films on gold substrates: **Ac10L** (upper panel), **Ac14L** (middle panel) and **Ac18L** (lower panel).

To gain information about molecular conformation and orientation of the peptides on the gold surface, FT-RAIRS were carried out for the Ac-peptides. The Amide I band for all peptides films was observed at around 1672-1680 cm^{-1} (Figure 3.6) and is in agreement with those reported previously for other synthetic α-helical peptides on gold surfaces.[3,28] For films, this absorption appears at a higher frequency compared to peptides in KBr due to the so-called "optical effect".[29,30] The tilt angles (with respect to the surface normal) of the peptides on the gold surface were calculated from the ratio of the amide I and the amide II bands in the FT-RAIR spectra following Equation 3.1,[31] and are close to 35°.

$$\frac{I_1}{I_2} = C\frac{2\left[\frac{1}{2}(3\cos^2\gamma - 1)\right]\left[\frac{1}{2}(3\cos^2\theta_1 - 1)\right] + 1}{2\left[\frac{1}{2}(3\cos^2\gamma - 1)\right]\left[\frac{1}{2}(3\cos^2\theta_2 - 1)\right] + 1} \qquad 3.1$$

where, I_1 and I_2 are the observed absorbances of amide I and amide II respectively, C (= 1.5) is the scaling constant, γ is the tilt angle of the helical axis, and θ_1 (= 39°) and θ_2 (= 75°) represent the angles between the helix axis and the transition moments of amide I and amide II vibrations, respectively.[32]

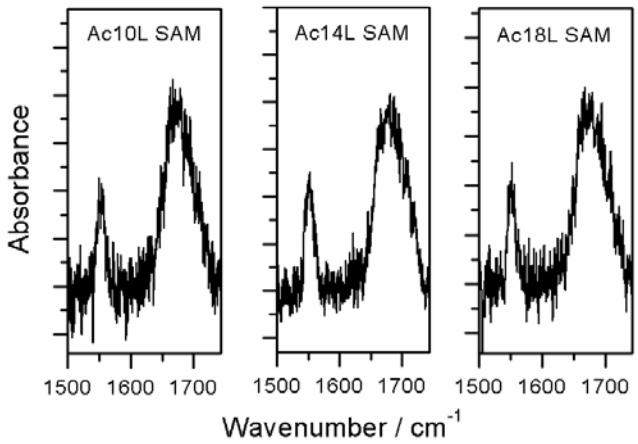

Figure 3.6. FT-RAIR spectra of the Ac-peptide films on gold surfaces showing the Amide I and II region.

Next, it was important to evaluate the properties of the films in more detail. For this purpose, it was decided to evaluate the films by CV and study their blocking behaviour towards ferro/ferricyanide anions in aqueous medium. The voltammogram of the gold surface before and after film deposition is shown in Figure 3.7. All peptides form well-packed and almost defect-free films on gold surfaces, since the peptide modified electrodes showed negligible ferricyanide/ferrocyanide redox activity compared to a bare gold electrode (Figure 3.7).

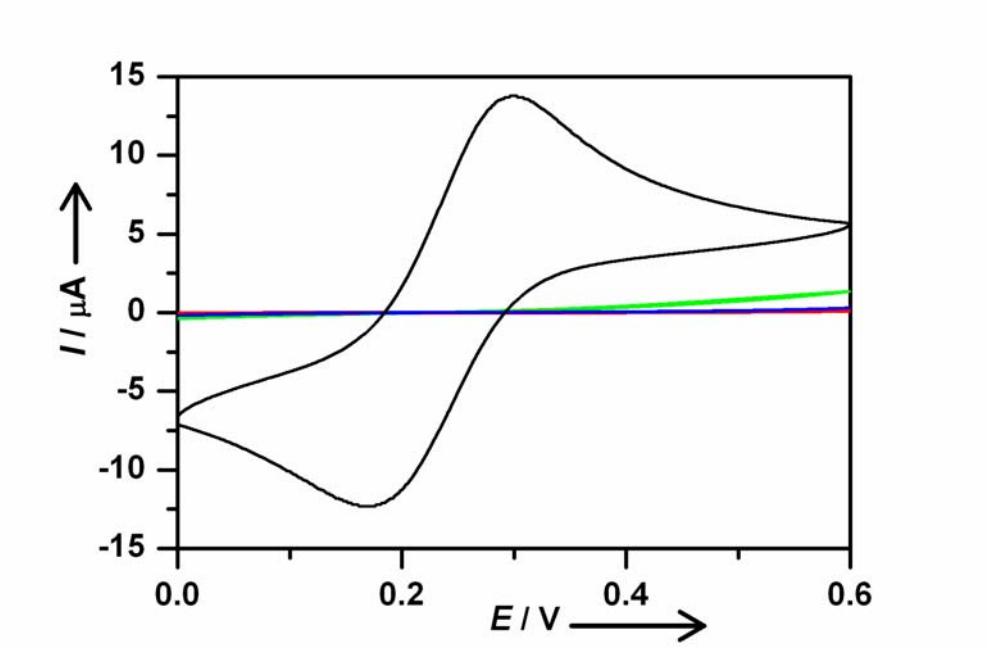

Figure 3.7. Cyclic voltammograms of bare (black), **Ac10L** (green), **Ac14L** (blue) and **Ac18L** (red) modified gold electrodes (1.6 mm) in 2.0 M $NaClO_4$ aqueous solution containing 4 mM ferricyanide/ferrocyanide (scan rate 0.1 V/s and Ag/AgCl is the reference electrode).

Atomic force microscopy (AFM) studies of the Ac-peptide films were also carried out, which indicate that the peptides are well-ordered in the films and the cross-sections in the images compare well with those of the optimized peptide structures (Figure 3.8, Table 3.3).

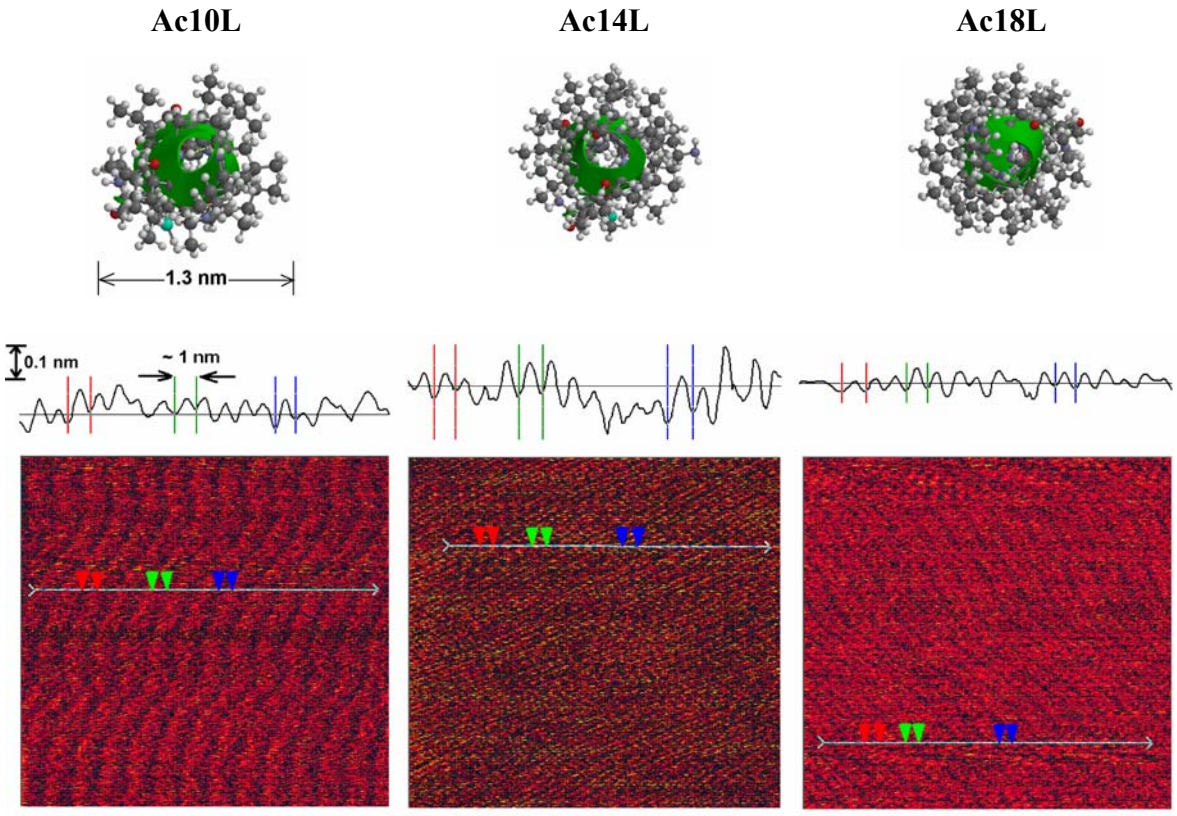

Figure 3.8. Cross-section of molecular mechanics force field (MMFF) optimized Ac-peptides using SPARTAN '04 Mechanics Program (Irvine, CA) (upper panel) and AFM images (raw data) of the Ac-peptide films on gold surfaces (non-contact mode, 25×25 nm^2) (lower panel). The middle panel shows the corresponding cross-sectional analysis of the images.

Table 3.3. AFM cross-sectional data for the Ac-peptides.

Peptides	Diameter from MMFF optimized structure (Å)	Diameter from AFM (Å)
Ac10L	13.0	9.4±0.5
Ac14L	13.5	9.5±0.5
Ac18L	13.5	9.5±0.6

3.4.3. ET Studies

For ET studies, mixed films were prepared on gold microelectrodes from TFE solutions of each Fc-peptide and the corresponding Ac-peptide (5:95).

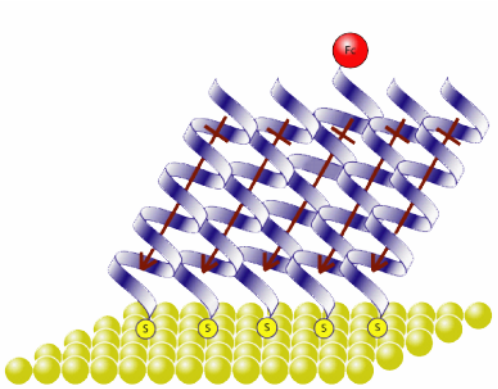

Figure 3.9. Schematic diagram of the mixed film showing the direction of the dipole moments of the α-helical peptides on the surface of a gold electrode.

CVs of the peptide-modified electrodes were recorded in 2 M $NaClO_4$ aqueous solutions (Figure 3.9). The formal potentials $E^{0\prime}$ were similar (~ 450 ± 15 mV) for all the peptide films suggesting a comparable environment around the redox active Fc moiety. The standard ET rate constants (k_{et}^{o}) were calculated from the CVs following the Butler-Volmer methodology[33] and a gradual decrease of the ET rates with the increase of the peptide length was revealed, which is consistent with the electrochemical impedance spectroscopic (EIS) measurements. Figure 3.10 shows the Nyquist plots of the films, measured at their formal potentials. The data were fit to a modified Randles circuit and the parameters are listed in Table 3.4. A simpler circuit was used rather than that mentioned in reference 13 which is more reliable due to less fitting parameters. Q_{DL} which represents the capacitance of a non ideal film,[34] decreases with the increase of the length of the peptide. This may indicate higher film thickness and/or more compact film.[35] The diameter of the semicircle in a Nyquist plot is a measure of the charge

transfer resistance (R_{CT}).[35] R_{CT} is higher for longer peptide films and points to lower ET rates.

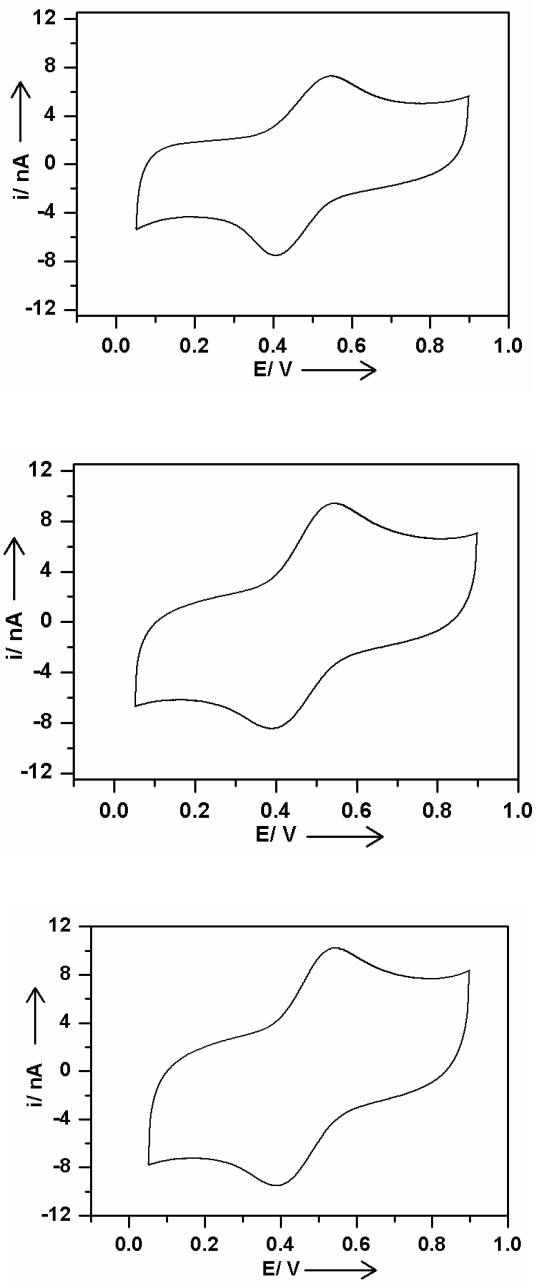

Figure 3.10. CVs of the **Fc10L/Ac10L** 5:95 (upper panel), **Fc14L/Ac14L** 5:95 (middle panel) and **Fc18L/Ac18L** 5:95 (lower panel) films on 50 μm gold working electrodes (scan rate 0.02 Vs^{-1}, 2M $NaClO_4$ aqueous solution, Pt as the counter electrode, potential versus Ag/AgCl reference electrode).

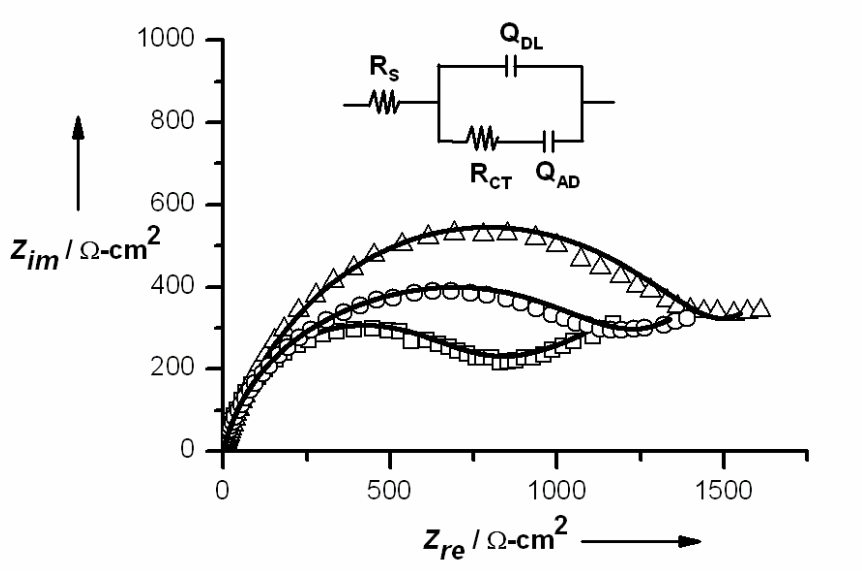

Figure 3.11. Nyquist plots (Z_{im} vs. Z_{re}) for the Faradaic impedance measurements in 2.0 M $NaClO_4$. Points represent experimental data for **Fc10L/Ac10L** (∀), **Fc14L/Ac14L** (–), **Fc18L/Ac18L** (8) films. The data were fit (solid line, ZsimpWin software, Princeton Applied Research) to the equivalent circuit that includes a solution resistor R_S, film capacitor Q_{DL}, charge transfer resistor R_{CT} and a pseudocapacitor Q_{AD} due to the redox process at the surface.

Table 3.4. Equivalent circuit element values for the helical peptides films

Element	**Fc10L/Ac10L**	**Fc14L/Ac14L**	**Fc18L/Ac18L**
R_s / Ω	2.82 x10^3	1.15 x10^3	7.58 x10^2
Q_{DL} / S-s$^{1/2}$	7.06 x10^{-10}	6.59 x10^{-9}	2.53 x10^{-9}
n	0.873	0.887	0.780
R_{CT} / Ω	2.96 x10^6	4.45 x10^6	7.67 x10^6
Q_{AD} / S-s$^{1/2}$	1.73 x10^{-7}	4.31 x10^{-7}	2.07 x10^{-7}
n	0.303	0.525	0.692

Figure 3.11 shows a compilation of the ET rates from this work obtained from electrochemical studies of films prepared from the series of Fc/Ac peptides together with those of other Fc-peptides studied on gold surfaces,[10,36,37] as a function of the peptide spacer length (d). Two distinct ET regimes are clearly evident. For the shorter peptides (< 20Å), which are presumably not capable of forming a secondary structure, k_{et}^o decreases exponentially with increasing distance between the Fc probe and the electrode

surface (the decay constant, β = 1 Å^{-1}), reflecting an exponential decrease of the quantum mechanical electronic coupling matrix element $|H_{DA}|$ between the D and A, which suggests that ET occurs by through-bond tunneling.[38] But, for longer peptides that adopt a helical secondary structure, k_{et}^{o} does not decrease exponentially and it shows a distinct pattern of very weak distance dependence. Similar observations were reported elsewhere from photo-physical ET studies[39] of oligoprolines in solution and rationalized as a transition from tunneling to the hopping mechanism following several theoretical predictions.[40,41] Hopping has been suggested to be unlikely to occur in ET over short distances due to the energetic barrier to transfer an electron onto the lowest unoccupied molecular orbital (LUMO) of the peptide bridge, but is probable when the distance is large.[39-41]

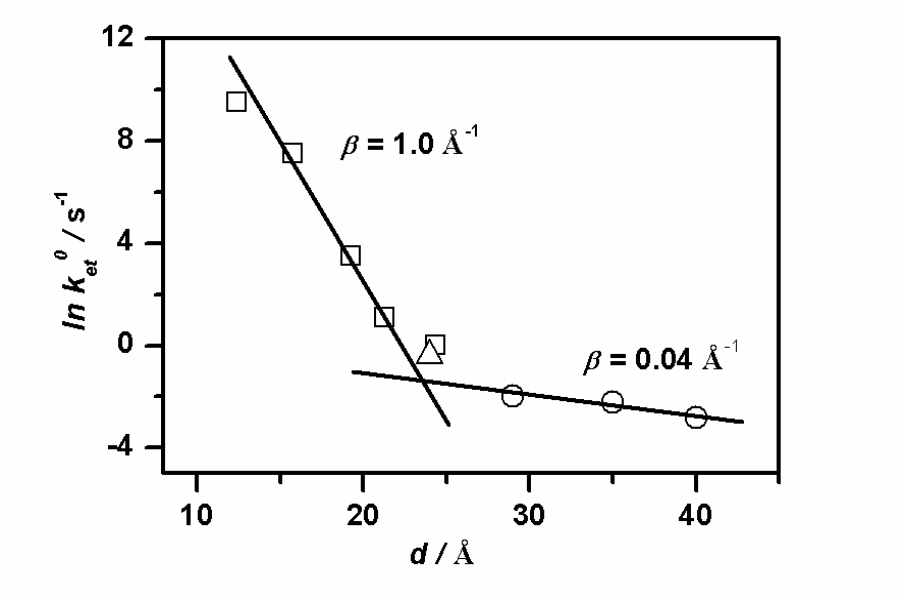

Figure 3.12. ET rate constant vs. the distance between the D and A, for several Fc-labeled peptides: (□),[10] (Δ),[37] and the peptides from the series of Fc-Leu peptides **Fc10L**, **Fc14L**, and **Fc18L** (○); the distances were obtained from molecular mechanics force field (MMFF) optimized structures (SPARTAN '04 Mechanics Program, Irvine, CA. See the ESI for the structures).

For hopping, the electron has to populate the LUMO (reduction) of the bridge first and then transfer to the acceptor.[41] In case of our acylated Leu-rich peptides, the CVs did not show any Faradic response due to a reduction or oxidation of the peptide (see upper panel of Figure 3.4). In addition, STS investigations of a film of peptide **Ac18L** (Figure 3.12) clearly shows an exponential increase of the current with the bias voltage, which is similar to the behavior observed for alkanethiol[42] and other films[43] that exhibit ET by electron tunneling. Furthermore, *ab initio* calculations of a helical pentaglycine which serves as a model (Ac-Gly_5-amide, see ESI) indicated that the HOMO-LUMO gap is ~ 5 eV, which appears not to agree with the barrier height (~2 eV) obtained from fitting the experimental data (Figure 3.12) with the Simmons model:[44,45]

$$I = \frac{Ce}{4\pi^2 \hbar d^2}\left\{\left(\phi - \frac{eV}{2}\right)\exp\left[-\frac{2(2m)^{1/2}}{\hbar}\alpha\left(\phi - \frac{eV}{2}\right)^{1/2} d\right] - \left(\phi - \frac{eV}{2}\right)\exp\left[-\frac{2(2m)^{1/2}}{\hbar}\alpha\left(\phi - \frac{eV}{2}\right)^{1/2} d\right]\right\} \qquad 3.2$$

where, I is the tunneling current, C is a proportionality constant, e is the charge of an electron, $\hbar$ is Plank's constant divided by 2Π, d is the distance, Φ is the tunneling barrier height, α is an adjustable parameter and V is the bias voltage.

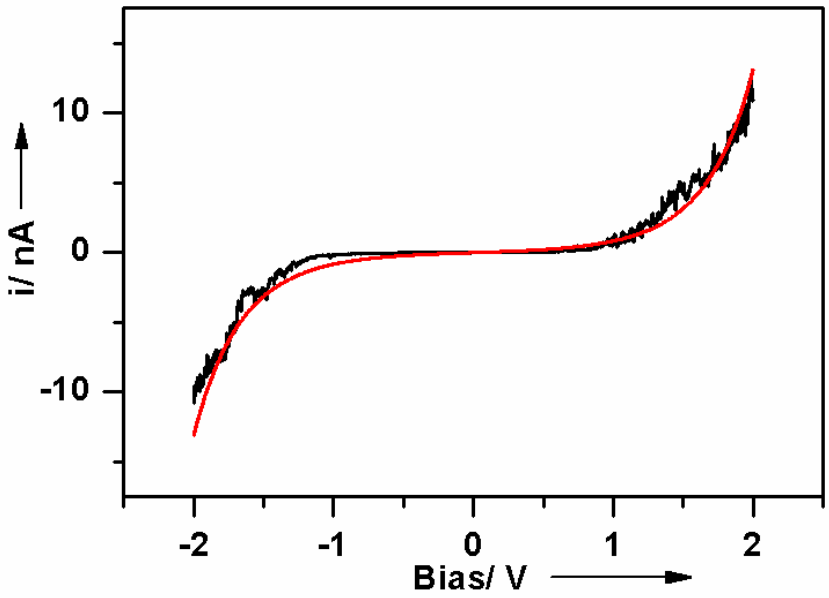

Figure 3.13. *I-V* response of the **Ac18L** film; the black and red curves represent experimental and calculated data, respectively.

In oligoprolines, no exponential decrease of k_{et}^{o} is observed once the polyproline II helical structure is fully formed.[46a] A similar behaviour is apparent for helical peptides (see Figure 3.11). Once a stable α-helical conformation is reached there appears to be a change in the ET rate from a strongly distance dependent regime in the case of short peptides to a weakly one for fully formed α-helical structure. So the transition in ET rates is related to the structural change, and considering the redox-inactive behavior of the peptide backbone and the *I-V* nature, it can be proposed that the mechanism of ET in the helix is tunneling which is in line with the large body of work reported on the involvement of the tunneling mechanism of ET in proteins.[6,7] Recently, we showed[13] that ET in α-helical peptide films is governed by the dynamics of the peptide: the more limited the dynamics, the slower the ET rate. So it is possible that a dynamically controlled tunneling mechanism is operative in the α-helix. In terms of the nature of the

dynamics, we point out that short synthetic peptide helices are known to exist as equilibrium mixtures of α and 3_{10} helices because of their low energetic barrier.[46b] CD studies of the peptides studied here also indicate the presence of this equilibrium and a comparable population of both conformers in trifluoroethanolic solutions. The time-scale (τ) for this equilibrium in solution is in the ns scale,[47] but recent studies of a 12 residue helical peptide showed a increase of τ by orders of magnitude when the peptide is present in a thin film (about 50 s).[48] This time-scale correlates well with our ET rates. Since, FT-IR studies specify that the equilibrium shifts exclusively to the α-helical conformation in solid state, and the 3_{10}-helix is known to be more conductive than the α-helix (because of increased number, $i \rightarrow i+3$ versus $i \rightarrow i+4$ respectively, and shorter, thereby stronger intra-molecular H-bonds),[46b] it can be suggested that the 3_{10} conformation may be a potential candidate for the ET active conformer, and the rate of formation of this particular conformation controls the overall ET rate on surface.

3.5. Acknowledgments

This work was funded by the Natural Sciences and Engineering Research Council of Canada. H.-B.K. is the Canada Research Chair in Biomaterials.

3.6. References

[1] L. G. Presta, G. D. Rose, *Science* **1988**, 240, 1632-1641.
[2] V. I. Vullev, J. Jones II, *Res. Chem. Interm.* **2002**, 28, 795-781.
[3] S. Yasutomi, T. Morita, Y. Imanishi, S. Kimura, *Science* **2004**, 304, 1944-1947.
[4] H. K. Rau, N. DeJonge, W. Haehnel, *Proc. Natl. Acad. Sci., U.S.A*. **1998**, 95, 11526-11531.
[5] Y. Zheng, M. A. Case, J. F. Wishart, G. L. McLendon, *J. Phys. Chem. B.* **2003**, 107, 7288-7293.
[6] C. C. Page, C. C.Moser, X. Chen, P. L. Dutton, *Nature* **1999**, 402, 47-52.
[7] D. N. Beratan, J. N. Betts, J. N. Onuchic, *Science* **1991**, 252, 1285-1288.

[8] M. Sisido, S. Hoshino, H. Kusano, M. Kuragaki, M. Makino, H. Sasaki, T. A. Smith, K. P. Ghiggino, *J. Phys. Chem. B.* **2001**, 105, 10407-10415.
[9] F. Polo, S. Antonello, F. Formaggio, C. Toniolo, F. Maran, *J. Am. Chem. Soc.* **2005**, 127, 492-493.
[10] T. Morita, S. Kimura, *J. Am. Chem. Soc.* **2003**, 125, 8732-8733.
[11] J. Watanabe, T. Morita, S. Kimura, *J. Phys. Chem. B.* **2005**, 109, 14416-14425
[12] B. Giese, J. Amaudrut, A.-K. Köhler, M. Spormann, S. Wessely, *Nature* **2001**, 412, 318-320.
[13] H. S. Mandal, H.–B. Kraatz, *Chem. Phys.* **2006**, 326, 246-251.
[14] Lateral interactions between electroactive groups may influence the ET kinetics (A. P. Brown, F. C. Anson, *Anal. Chem.* **1977**, 49, 1589-1595; S. Sek, B. Palys, R. Bilewicz, *J. Phys. Chem. B* **2002**, 106, 5907-5914
[15] P. Y. Chou, G. D. Fasman, *J. Mol. Biol.* **1973**, 74, 263-281.
[16] C. P. Hill, D. H. Anderson, L. Wesson, W. F. DeGrado, D. Eisenberg, *Science* **1990**, 249, 543-546.
[17] J. Lin, I. A. Balabin, D. N. Beratan *Science* **2005**, 310, 1311-1313.
[18] I. M. C. van Amsterdam, M. Ubbink, O. Einsle, A. Messerschmidt, A. Merli, D. Cavazzini, G. L. Rossis, G. W. Canters, *Nature* **2002**, 9, 48-52.
[19] F. Albericio, N. Kneib-Cordonier, S. Biancalana, L. Gera, R. I. Masada, D. Hudson, G. Barany, *J. Org. Chem.* **1990**, 55, 3730-3743.
[20] Gaussian 03, Revision B.05, M. J. Frisch, G. W. Trucks, H. B. Schlegel, G. E. Scuseria, M. A. Robb, J. R. Cheeseman, J. A. Montgomery, Jr., T. Vreven, K. N. Kudin, J. C. Burant, J. M. Millam, S. S. Iyengar, J. Tomasi, V. Barone, B. Mennucci, M. Cossi, G. Scalmani, N. Rega, G. A. Petersson, H. Nakatsuji, M. Hada, M. Ehara, K. Toyota, R. Fukuda, J. Hasegawa, M. Ishida, T. Nakajima, Y. Honda, O. Kitao, H. Nakai, M. Klene, X. Li, J. E. Knox, H. P. Hratchian, J. B. Cross, C. Adamo, J. Jaramillo, R. Gomperts, R. E. Stratmann, O. Yazyev, A. J. Austin, R. Cammi, C. Pomelli, J. W. Ochterski, P. Y. Ayala, K. Morokuma, G. A. Voth, P. Salvador, J. J. Dannenberg, V. G. Zakrzewski, S. Dapprich, A. D. Daniels, M. C. Strain, O. Farkas, D. K. Malick, A. D. Rabuck, K. Raghavachari, J. B. Foresman, J. V. Ortiz, Q. Cui, A. G. Baboul, S. Clifford, J. Cioslowski, B. B. Stefanov, G. Liu, A. Liashenko, P. Piskorz, I. Komaromi, R. L. Martin, D. J. Fox, T. Keith, M. A. Al-Laham, C. Y. Peng, A. Nanayakkara, M. Challacombe, P. M. W. Gill, B. Johnson, W. Chen, M. W. Wong, C. Gonzalez, and J. A. Pople, Gaussian Inc., Pittsburgh PA, **2003**.
[21] P. Wallimann, R. J. Kennedy, D. S. Kemp, *Angew. Chem. Int. Ed.* **1999**, 38, 1290-1292.
[22] C. Toniolo, A. Polese, F. Formaggio, M. Crisma, J. Kamphuis, *J. Am. Chem. Soc.* **1996**, 118*,* 2744-2745
[23] W. R. Fiori, S. M. Miick, G. L. Millhauser, *Biochemistry* **1993**, 32, 11957-11962.
[24] D. F. Kennedy, M. Crisma, C. Toniolo, D. Chapman *Biochemistry* **1991**, 30*,* 6541-6548.
[25] G. M. Bonora, C. Mapelli, C. Toniolo, R. R. Wilkening, E. S. Stevens, *Int. J. Biol. Macromol.* **1984**, 6, 179-188.
[26] H. J. Hwang, J. R. Carey, E. T. Brower, A. J. Gengenbach, J. A. Abramite, Y. Lu, *J. Am. Chem. Soc.* **2005**, 127, 15356-15357.
[27] P. E. Laibinis, G. M. Whitesides, *J. Am. Chem. Soc.* **1992**, 114, 1990-1995.

[28] K. Fujita, N. Bunjes, K. Nakajima, M. Hara, H. Sasabe, W. Knoll, *Langmuir* **1998**, 14, 6167-6172.
[29] D. L. Allara, A. Baca, C. A. Pryde, *Macromolecules* **1978**, 11, 1215-1220.
[30] Y. Miura, S. Kimura, Y. Imanishi, J. Umemura, *Langmuir* **1999**, 15, 1155-1160;
[31] Y. Miura, S. Kimura, Y. Imanishi, J. Umemura, *Langmuir* **1998**, *14*, 6935-6940.
[32] M. Tsuboi, *J. Polym. Sci.* **1962**, 59, 139-153.
[33] A. J. Bard, L. R. Faulkner, *Electrochemical Method: Fundamentals, Applications*, 2nd ed.; John Wiley: New York, **2001**.
[34] M. Dijksma, B. A. Boukamp, B. Kamp, W. P. van Bennekom, *Langmuir* **2002**, 18, 3105-3112.
[35] Y.T. Long, C. Z. Li, T. C. Sutherland, H. B. Kraatz, J. S. Lee, *Biophy. J.* **2003**, 84, 3218-3225.
[36] S. Sek, A. Tolak, A. Misicka, B. Palys, R. Bilewicz, *J. Phys. Chem. B.* **2005**, 109, 18433-18438.
[37] ET rates were estimated from Figure 3B, S. Sek, A. Sepiol, A. Tolak, A. Misicka, R. Bilewicz, *J. Phys. Chem. B.* **2004**, 108, 8102-8105.
[38] H. O. Finklea, D. D. Hanshew, *J. Am. Chem. Soc.* **1992**, 114, 3173-3181.
[39] R. A. Malak, Z. Gao, J. F. Wishart, S. S. Isied, *J. Am. Chem. Soc.* **2004**, 126, 13888-13889.
[40] E. G. Petrov, Ye. V. Shevchenko, V. I. Teslenko, V. May, *J. Chem. Phys.* **2001**, 115, 7107-7122.
[41] M. Bixon, J. Jortner, *J. Chem. Phys.* **1997**, 107, 5154-5170.
[42] X. D. Cui, X. Zarate, J. Tomfohr, O. F. Sankey, A. Primak, A. L. Moore, T. A. Moore, D. Gust, G. Harris, S. M. Lindsay, *Namotechnogoly* **2002**, 13, 5-14.
[43] D. Xu, G. D. Watt, J. N. Harb, R. C. Davis, *Nano. Lett.* **2005**, 5, 571-577.
[44] J. G. Simmons, *J. Appl. Phys.* **1963**, 34, 1793-1803.
[45] K. Kitagawa, T. Morita, S. Kimura, *J. Phys. Chem. B.* **2005**, 109, 13906-13911.
[46] (a) M. Y. Ogawa, J. F. Wishart, Z. Young, J. R. Miller, S. S. Isied, *J. Phys. Chem.* 1993, **97**, 11456-11463; (b) G. Hungerford, M. Martinez-Insua, D. J. S. Birch, B. D. Moore, *Angew. Chem., Int. Ed.* **1996**, 35, 326-329.
[47] S. E. Huston, G. R. Marshall, *Biopolymers* **1994**, 34, 75-90.
[48] K. Kitagawa, T. Morita, S. Kimura, *Angew. Chem., Int. Ed.* **2005**, 44, 6330-6333.

3.7. Supporting Information

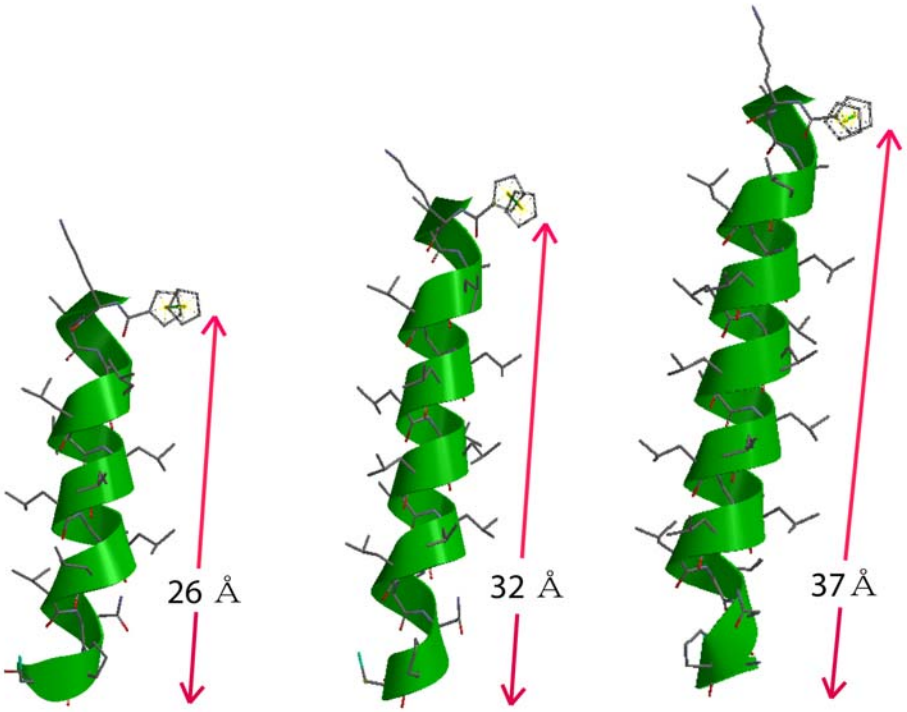

Figure S3.1. MMFF optimized structures of **Fc10L**, **Fc14L** and **Fc18L** (SPARTAN '04 Mechanics Program, Irvine, CA).

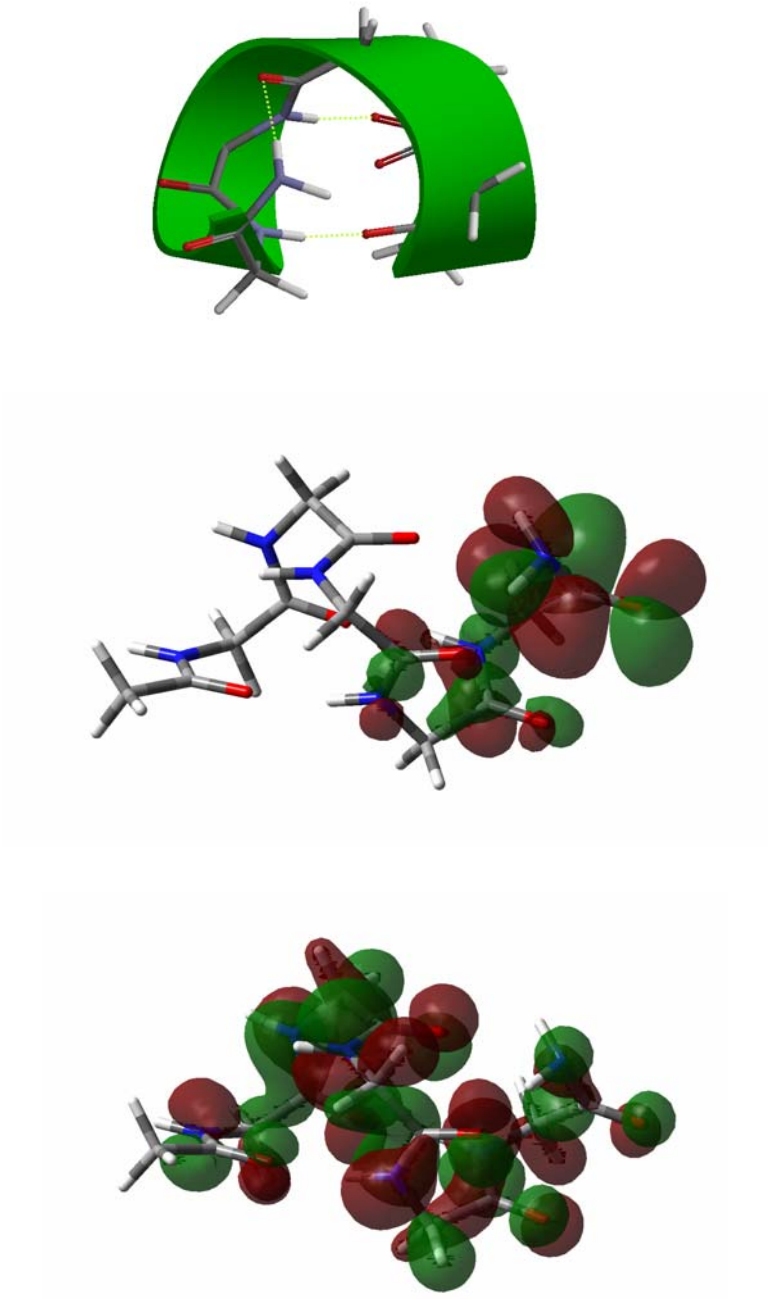

Figure S3.2. Ideal α-helical structure of Ac-Gly_5-amide used for calculating the HOMO-LUMO gap in an intra-molecularly H-bonded peptide structure (upper panel), LUMO (middle panel) and HOMO (lower panel).

Chapter 4

Investigation of Laser induced Photocurrent Generation Experiments

4.1. Connecting Text

Following the discoveries described in chapters 2 and 3, ET in peptide films is suggested to be governed by the dynamic properties of peptides. My mechanistic analysis of the experimental data suggests that ET by tunneling can account for the observed ET kinetics in the peptide films. These results are in direct conflict with published literature and thus made it necessary to re-visit photo-driven ET in α-helical peptides. This chapter describes the investigations into photo-driven ET and investigates the generation of photocurrents by films of α-helices. This chapter is one of two that report the potential application of peptide-modified gold surfaces. In this study, it is discovered that a serious experimental artifact can give rise to the photocurrent reported in the literature.

 This paper is co-authored by Ian J. Burgess and H.-B. Kraatz. I did the experimental study and wrote the first draft. The co-authors suggested some of the experiments, revised, rewrote and reformatted the manuscript. The manuscript will be used *verbatim* in my thesis.

4.2. Introduction

In recent years, photocurrent generation by molecular assemblies has received significant interest because of its potential in understanding the natural photo-systems,[1] which is crucial for developing artificial solar energy converters, and exploring the possibility of using molecules as scaffolds for nano-scaled photovoltaic devices. There are several reports in which natural photo-systems are mimicked by synthetic α-helices functionalized with light-harvesting chromophores.[2] Kimura and co-workers reported a molecular photodiode system composed of chromophore-modified helical peptides on gold surfaces and photocurrent generation by the chromophores upon laser excitation was described.[2a] The influence of dipole-moment was also probed with two peptide systems, making use of two chromophores (*N*-ethylcarbazoyl, laser excitation λ= 351 nm; tris(2,2′-bipyridine)ruthenium(II) complex, laser excitation λ= 459 nm) showing a dependence of the generated photocurrent on the orientation of the peptide. In another work,[2b] the same group reported reversible switching of the photocurrent direction by changing the pH of the solution using a naphthyl-labeled peptide (laser excitation λ= 280 nm).

These results are indeed exciting and they stimulated us to further investigate the feasibility of photocurrent generation in peptide films. In this paper, we report the results of our photo-electrochemical studies of peptide films having opposite dipole orientations on the gold surface. Surprisingly, we observed "photocurrent generation" and "pH switching" in the absence of a chromophore and even by the irradiation of a bare gold electrode with laser light. As a result of our study, we suggest that an important consequence of laser irradiation has been overlooked and that at least in some cases the

so-called photocurrent phenomenon is probably a result of the interfacial potential drop induced by laser heating.

4.3. Results and Discussion

Before outlining the results obtained on peptide-modified gold surfaces, we carried out a number of control experiments with unmodified polycrystalline gold electrodes. Figure 4.1 shows the experimental current signals for a polycrystalline gold electrode at different potentials (*vs*. Ag/AgCl) under 20 s laser (473 nm) irradiation (the supporting electrolyte is 0.1 M Na_2SO_4 aqueous solution). The directions of the current signals at different potentials are similar to those of the current transients produced by pulsed laser irradiation reported previously by Compton *et al*.[3] The current signal changes its direction from cathodic to anodic on changing the potential of the working electrode from negative to positive.

The illumination of the electrode with a laser pulse has been reported[3,4] to cause a sudden heating of the electrode surface according to the following expression:

$$\Delta T = \frac{I(1-R)}{\sqrt{\pi k c d}}\left(1+\sqrt{\frac{k_s c_s d_s}{k c d}}\right)^{-1}\sqrt{t_0}$$

where I is the intensity of the light, R the reflectivity of the surface, k, c, d, and k_s, c_s, d_s are the heat conductivity, specific heat, and density of the metal and solution, respectively and t_0 is the duration of the laser pulse. The heat instantaneously increases the temperature of the interfacial region[5–7] and a detailed analysis of the resulting electrochemical response (either the current transients in potentiostatic mode,[3] or the

potential transients in coulostatic mode[4,6,8–10]) showed that the transients mainly reflect the response of the double-layer to the increase of the temperature. The thermo-diffusion

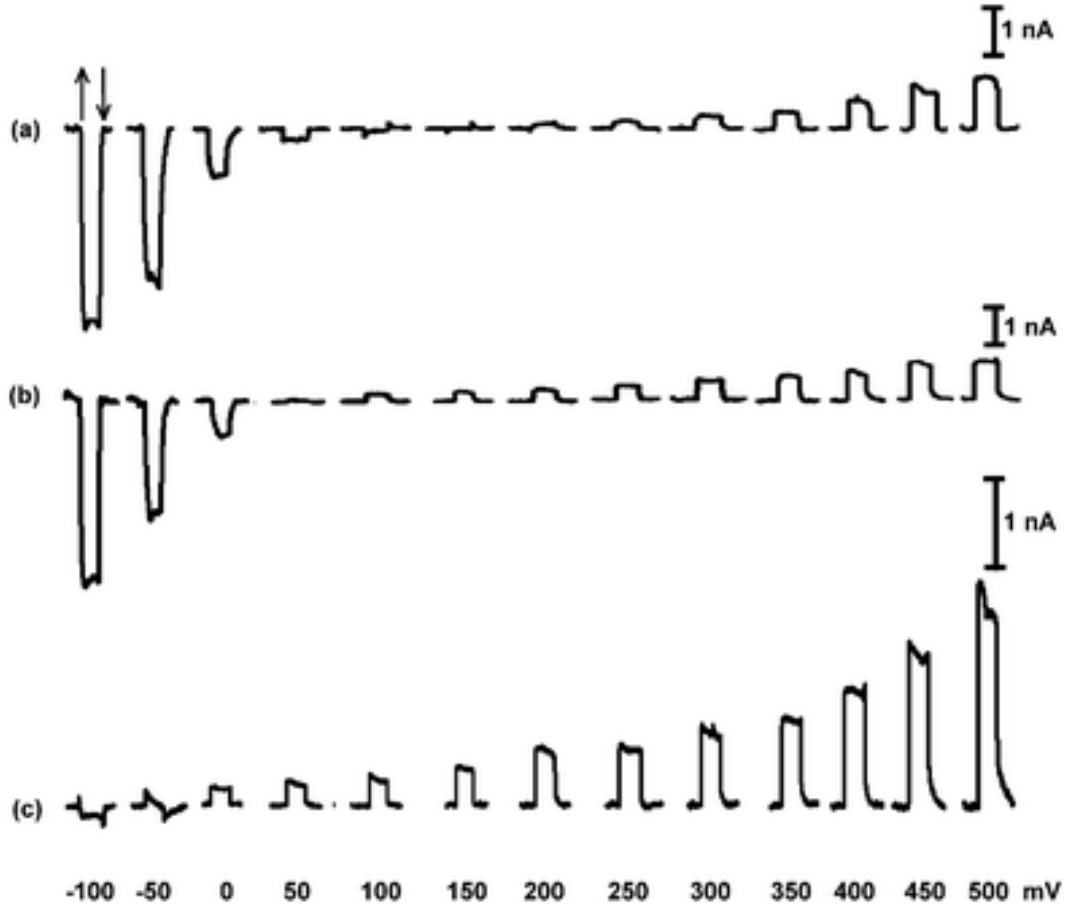

Figure 4.1. Current responses from a bare gold electrode at different applied potentials (mV *vs*. Ag/AgCl) in 0.1 M Na_2SO_4 aqueous solution: (a) pH = 3, (b) pH = 7, (c) pH = 10. Up and down arrows denote light on and off, respectively. Irradiation time = 20 s.

potential between the hot solution (in contact with the working electrode) and the cold solution (in contact with the reference electrode) has been reported to be very small.[4,7,10] The temperature coefficient of the metal/solution potential drop can be split into three contributions:[9,11]

$$\left(\frac{\partial \phi^{M-S}}{\partial T}\right)_{\sigma,m} = \frac{1}{e}\left(\frac{\partial \Phi}{\partial T}\right)_{\sigma} + \left(\frac{\partial \phi^{2}}{\partial T}\right)_{\sigma,m} + \left(\frac{\partial \phi^{w}}{\partial T}\right)_{\sigma,m}$$

Where ϕ is the work function at the given charge σ, ϕ^2 is the potential drop at the diffuse layer, and ϕ^w is the contribution to the potential drop due to solvent structuring. It has been shown[9–13] that the temperature coefficient of the work function and the contributions due to the thermal coefficient of the potential drop through the diffuse layer (estimated from the Gouy–Chapman theory) are negligible, and the potential transients are mainly because of the temperature coefficient of the potential drop across the electrochemical double layer due to the increased disorder (caused by the increase of the temperature) of the oriented solvent molecules in the interphase. The change in sign of the transients is explained as a change in sign of the dipolar contribution to the potential drop in the interphase.[9,10] The negative transients at lower potentials are due to the decrease of the positive contribution from the layer of water dipoles, and the positive transients at higher potentials reflect a decrease in the absolute value of the negative contribution to the potential drop.[9,10] When the electrode is irradiated continuously (as in our experiments) instead of a pulse, a gradual contribution to the potential drop is expected due to the constant temperature rise, resulting in a current response.[14]

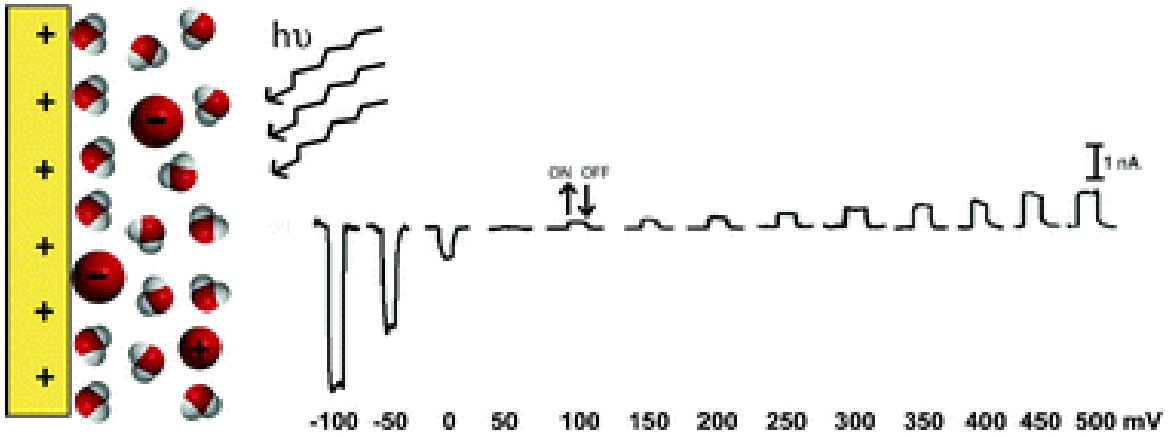

Figure 4.2. Schematic representation of the production of the so-called photo-current from a bare gold electrode.

The potential at which the current response is zero (the transition potential) has been identified as the potential of maximum entropy (pme) of formation of the double layer,[5,8] and is located in the vicinity of the potential of zero charge (pzc) of the working electrode.[8–12,15] The pzc of a gold electrode can vary over a wide range (for example, from –180 to +250 mV *vs*. Ag/AgCl for Na_2SO_4 aqueous solution)[16] depending on the crystallographic orientation of the electrode's surface. In addition, significant discrepancy exists among values determined by different methods.[17] In order to further determine if the transition potential is truly related to the pzc, we recorded current signals in solutions of different pH. The pzc of gold is known to shift negatively upon increasing the pH of the electrolyte solutions due to the increasing surface concentration and higher electrosorption of OH^-.[14,17b] Figure 4.1 shows that the transition potential shifts negatively with the increase of the solution pH. In another set of experiments, the transition potential in 0.1 M NaF aqueous solution was also found to shift negatively when 0.1 M NaCl was added to the solution (Figure S4.1), which is consistent with the greater electrosorption of Cl^- on the gold surface.[17b]

Similar types of laser-induced current signals were obtained for two helical peptide self-assembled monolayers (SAMs) (on polycrystalline gold electrode surfaces) having different dipole directions on the surface and no chromophore. The peptide **Ac18L** (Ac-KTAL_{18}NPC-NH_2) possesses the thiol-functionalized Cys residue at the C-terminal, whereas, peptide **18LAc** (Ac-CTAL_{18}NPK-NH_2) has the Cys residue at the N-terminal side of the molecule (Figure 4.2), so that when immobilized on the gold surface *via* the thiol linker, the positive end of the helix dipole is on the surface in **Ac18L** SAM and the negative end in **18LAc** SAM. Note that in both cases the amine functionalized Lys residue is facing the solution side.

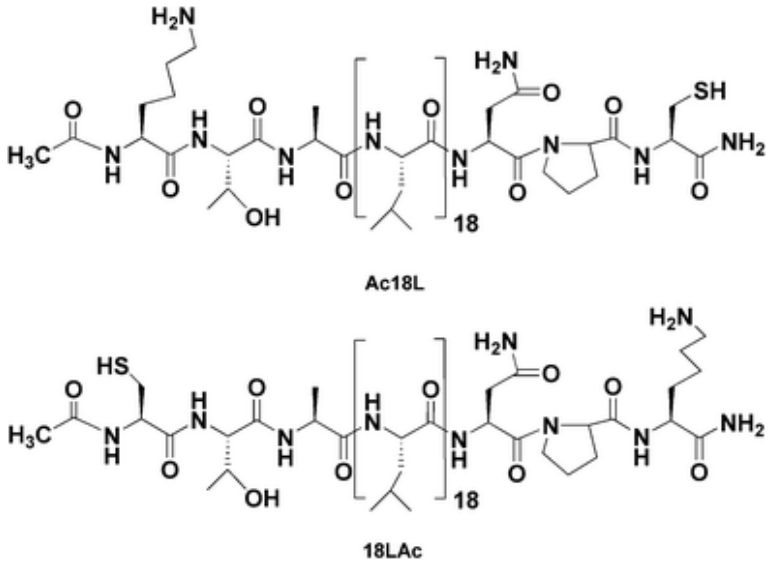

Figure 4.3. Molecular structures of the peptides **Ac18L** and **18LAc**.

A preliminary account of the syntheses and characterization of the peptides has already been published elsewhere.[18] Both peptides form well packed films on gold from trifluoroethanolic solutions (see ESI). At all pHs, the transition potentials of **Ac18L** SAM are higher than those of **18LAc** SAM, which can be explained by the nature of the helix dipole on the surface which is positive for **Ac18L** SAM and negative for **18LAc** SAM. Also for both SAMs, the transition potential shifts to the positive with the decrease of the pH of the solution due to the protonation of the amine group of the terminal Lys residue (Figure 4.3).

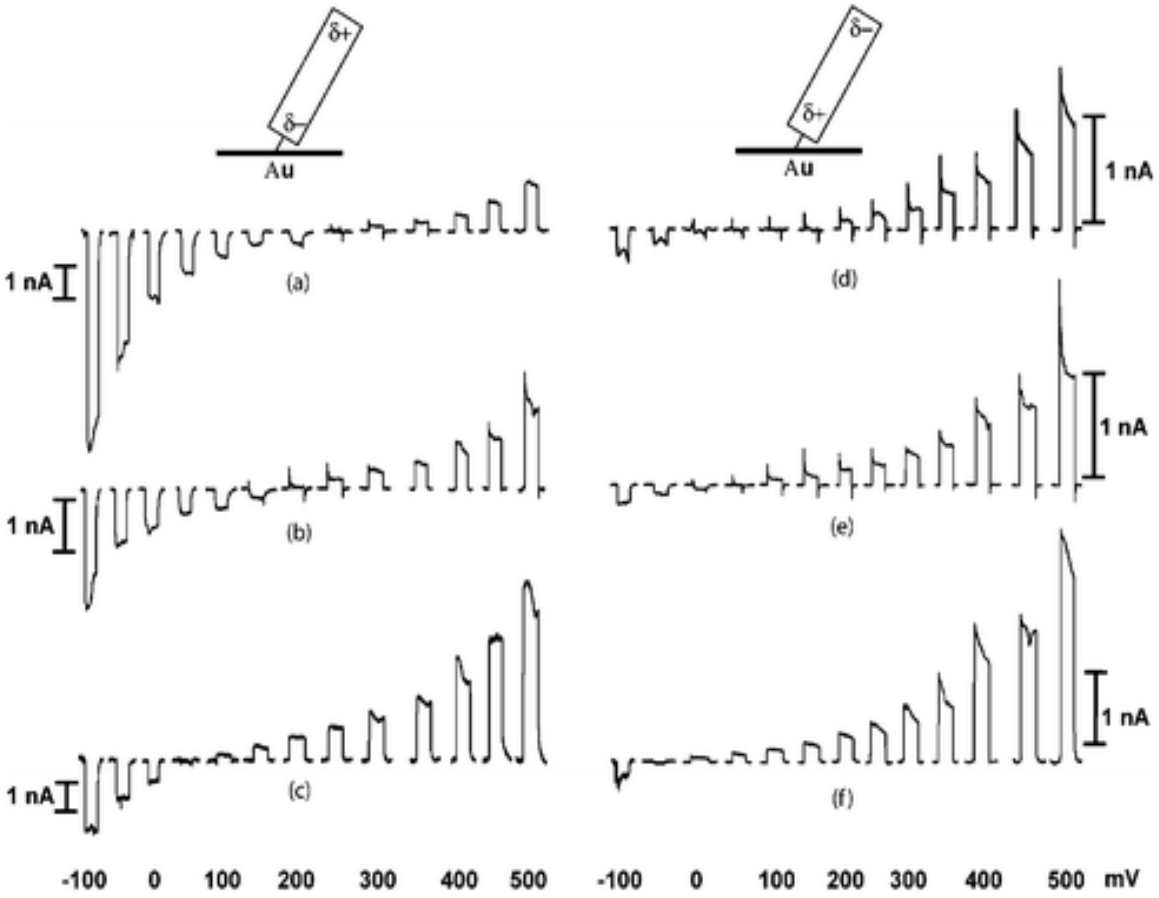

Figure 4.4. Current responses from peptide modified gold electrodes at different applied potentials in 0.1 M Na_2SO_4 aqueous solution: **Ac18L**, pH = 3 (a), 7 (b) and 10 (c); **18LAc**, pH = 3 (d), 7 (e) and 10 (f). Schematic diagrams of the orientation of the helix dipole moment on gold surface are also included.

At this point some features of the current signals at different potentials can be discussed. The intensity of the current signal is zero only near the pzc of the working electrode and for a particular type of electrode the position of the pzc is dependent on the pH, concentration and the nature of the supporting electrolyte of the solution,[17a,b] and also on the nature of the molecules in the SAM.[19] If the pzc is not at 0 V (*vs.* Ag/AgCl), laser irradiation produces a steady current signal at this potential (at which laser-irradiated photocurrent generation experiments are usually performed[2]) and depending on the position of the pzc, the direction of the current signal can be cathodic

(Figure 4.1a) or anodic (Figure 4.1c). Note that upon changing the pH of the solution from acidic to basic, the current signal (at 0 V) from bare gold switches from the cathodic to the anodic direction. In photocurrent generation experiments, action spectra of photocurrents at various wavelengths are sometimes reported[2] and compared to the absorption spectra of the chromophores. The similarity between the two types of spectra is claimed to be the proof for the generation of photocurrent from the chromophore. But our observation of similar photocurrents from bare gold and non-chromophore containing peptide modified electrodes, lead us to conclude that the phenomenon is probably correlated to the increase of temperature due to UV-absorption of the chromophores.[20] UV absorption is the highest at the λ_{max} of a particular chromophore and the associated increment in temperature is also highest at that particular wavelength giving the most intense current signal. In addition, the binding energy of a singlet exciton, *i.e.* the energy needed to split an exciton to coulumbically unbound charges, is no less than 0.5 eV.[21] So the commencement of photoconductivity right at the onset of optical absorption has been suggested not to be unambiguous proof for photocurrent generation from a chromophore.[22] Furthermore, the photoemission threshold for gold is around 200 nm (the work function of gold is around 5 eV)[23] and we do not think that photoemission from the gold electrode is occurring due to the laser (473 nm). To date, photocurrent generation has been reported for various systems and, since the current signal from bare and non-chromophore containing modified electrodes is similar to the so-called photocurrent response, at least some reports about photocurrent generation should be revisited.

We thank the Natural Science and Engineering Research Council of Canada for funding. H.-B. K. is the Canada Research Chair in Biomaterials.

4.4. Notes and References

[1] C. C. Page, C. C. Moser, X. X. Chen, P. L. Dutton, *Nature* **1999**, 402, 47-52.

[2] (*a*) S. Yasutomi, T. Morita, Y. Imanishi, S. Kimura, *Science* **2004**, 304, 1944-1947; (*b*) K. Yanagisawa, T. Morita, S. Kimura, *J. Am. Chem. Soc.* **2004**, 126, 12780-12781; (*c*) S. Yasutomi, T. Morita, S. Kimura, *J. Am. Chem. Soc.* **2005**, 127, 14564-14-565; (*d*) T. Morita, S. Kimura, S. Kobayashi, Y. Imanishi, *J. Am. Chem. Soc.* **2000**, 122, 2850-2859.

[3] V. Climent, B. A. Coles, R. G. Compton, *J. Phys. Chem. B* **2001**, 105, 10669-10673.

[4] V. A. Benderskii, S. D. Babenko, A. G. Krivenko, *J. Electroanal. Chem. Interfacial Electrochem.* **1978**, 86, 223-225.

[5] V. A. Benderskii, G. I. Velichko, *J. Electroanal. Chem. Interfacial Electrochem.* **1982**, 140, 1-22.

[6] V. A. Benderskii, G. I. Velichko, I. Kreitus, *J. Electroanal. Chem. Interfacial Electrochem.* **1984**, 181, 1-20.

[7] J. F. Smalley, C. V. Krishnan, M. Goldman, S. W. Feldberg, I. Ruzic, *J. Electroanal. Chem. Interfacial Electrochem.* **1988**, 248, 255-282.

[8] V. Climent, B. A. Coles, R. G. Compton, *J. Phys. Chem. B* **2002**, 106, 5258- 5265.

[9] V. Climent, B. A. Coles, R. G. Compton, *J. Phys. Chem. B* **2002**, 106, 5988-5647.

[10] V. Climent, B. A. Coles, R. G. Compton, J. M. Feliu, *J. Electroanal. Chem.* **2004**, 561, 157-165.

[11] R. Guidelli, G. Aloisi, E. Leiva, W. Schmickler, *J. Phys. Chem.* **1988**, 92, 6671-6675.

[12] F. Silva, M. J. Sottomayor, A. Martins, *J. Chem. Soc., Faraday Trans.* **1996**, 92, 3693-3699.

[13] G. Aloisi, R. Guidelli, *J. Electroanal. Chem. Interfacial Electrochem.* **1989**, 260, 259-267.

[14] A. J. Bard, L. R. Faulkner, *Electrochemical Methods, Fundamentals and Applications*, John Wiley & Sons, Inc., New York, **1980**.

[15] (*a*) J. A. Harrison, J. E. B. Randles, D. J. Schiffrin, *J. Electroanal. Chem. Interfacial Electrochem.* **1973**, 48, 359-381; (*b*) G. J. Hills, S. Hsieh, *J. Electroanal. Chem. Interfacial Electrochem.* **1975**, 58, 289-298; (*c*) Trends in Interfacial Electrochemistry, *NATO ASI Ser., Ser. C*, ed. A. F. Silva, Reidel, Boston, **1986**, 179, 49-54; (*d*) A. Hamelin, L. Stoicoviciu, F. Silva, *J. Electroanal. Chem. Interfacial Electrochem.* **1987**, 229, 107-124; (*e*) F. Silva, M. J. Sottomayor, A. Hamelin, *J. Electroanal. Chem. Interfacial Electrochem.* **1990**, 294, 239-251.

[16] (*a*) B. S. Krasikov, *Zh. Prikl. Khim. (S.-Peterberg)* **1964**, 37, 2420; (*b*) K. I. Norninski, E. M. Lazarova, *Elektrokhimiya* **1975**, 11, 1103; (*c*) A. Hamelin, M. Sotto, G. C. R. Valette, *C. R. Acad. Sci., Ser. C* **1969**, 268, 213.

[17] (*a*) J. Chen, L. Nie, S. Yao, *J. Electroanal. Chem.* **1996**, 414, 53-59; (*b*) D. D. Bode, T. N. Andersen, H. Eyring, *J. Phys. Chem.* **1967**, 71, 792-797; (*c*) O. J. Murphy, J. S. Wainright, *J. Electrochem. Soc.* **1988**, 135, 138-143; (*d*) J. O'M. Bockris, S. D. Argade, E. Gileadi, *Electrochim. Acta* **1969**, 14, 1259-1283; (*e*) S. H. Kim, *J. Phys. Chem.* **1973**, 77, 2787-2789.

[18] H. S. Mandal, H.-B. Kraatz, *Chem. Phys.* **2006**, 326, 246-251.

[19] Y. Iwami, D. Hobara, M. Yamamoto, T. Kakiuchi, *J. Electroanal. Chem.* **2004**, 564, 77-83.
[20] (*a*) R. Ono, T. Kamimura, S. Fukumoto, Y. K. Yap, M. Yoshimura, Y. Mori, T. Sasaki, K. Yoshida, *J. Cryst. Growth* **2002**, 237–239, 645-648; (*b*) E. K. Kim, C. G. Willson, *Microelectron. Eng.* **2006**, 83, 213-217; (*c*) A. J. Holder, J. A. Morrill, D. A. White, J. D. Eick, C. C. Chappelow, *THEOCHEM* **2000**, 507, 63-73; (*d*) C. Chappelow, C. S. Pinzino, M. D. Power, A. J. Holder, J. A. Morrill, L. Jeang, J. D. Eick, *J. Appl. Polym. Sci.* **2002**, 86, 314-326; (*e*) C. Decker, C. Bianchi, D. Decker, F. Morel, *Prog. Org. Coat.* **2001**, 42, 253-266; (*f*) I. Alig, P. A. M. Steeman, D. Lellinger, A. A. Dias, D. Wienke, *Prog. Org. Coat.* **2006**, 55, 88-96.
[21] S. F. Alvarado, S. Barth, H. Bässler, U. Scherf, J.-W. van der Horst, P. A. Bobbert, M. A. J. Michels, *Adv. Funct. Mater.* **2002**, 12, 117-122.
[22] (*a*) M. Chandross, S. Mazumdar, S. Jeglinski, X. Wei, Z. V. Vardeny, E. W. Kwock, T. M. Miller, *Phys. Rev. B: Condens. Matter Mater. Phys.* **1994**, 50, 14702-14705; (*b*) K. Pichler, D. A. Halliday, D. D. C. Bradley, P. L. Burn, R. H. Friend, A. B. Holmes, *J. Phys.: Condens. Matter* **1993**, 5, 7155-7172; (*c*) M. Weiter, V. I. Arkhipov, H. Bässler, *Synth. Met.* **2004**, 141, 165-170; (*d*) J. W. van der Horst, P. A. Bobbert, M. A. J. Michels, H. Bässler, *J. Chem. Phys.* **2001**, 114, 6950-6957; (*e*) D. M. Basko, E. M. Conwell, *Phys. Rev. B: Condens. Matter* **2002**, 66, 155210-155217.
[23] L. Zhang, J. A. Bain, J. G. Zhu, L. Abelmann, T. Onoue, *IEEE Trans. Magn.* **2004**, 40, 2549 - 2551.

4.5. Supplementary Material

All reagents were purchased from Aldrich (Canada) and used as received. Milli-Q water (18 MΩ cm resistivity, Millipore Ltd.) was used to rinse the cell and to prepare solutions. Electrochemical measurements were carried out on a CHI 660B potentiostat using the standard 3-electrode setup. The working, counter and reference electrodes were polycrystalline gold electrode (diameter of 1.6 mm, BASi, IN, USA), Pt wire, and Ag/AgCl, respectively. Before the experiment, each solution was purged with argon for at least 20 minutes and kept under an argon atmosphere throughout the duration of the experiment. All the experiments were carried out at room temperature (22 °C). A BS73-10 OEM laser module (Intelite Inc., NV, USA): laser power 10 mW, wavelength 473 nm and beam diameter 1.5 mm, was used as the laser source.

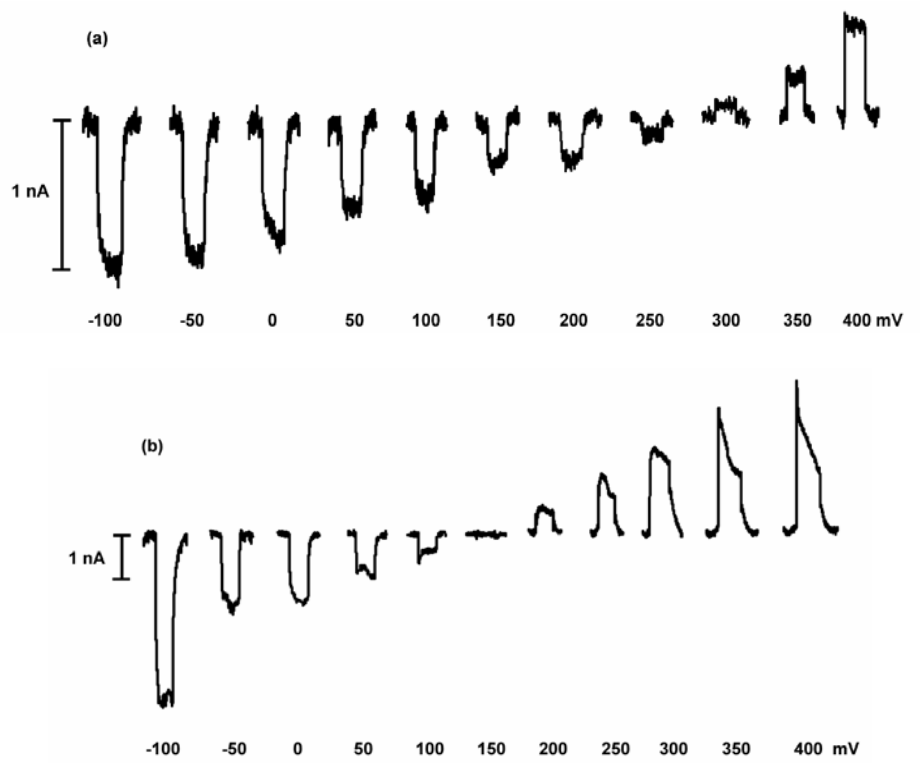

Figure S4.1. Current responses from bare gold electrode in 0.1 M NaF aqueous solution (a), after the addition of 0.4 ml of 0.1 M NaCl aqueous solution to 1 ml of 0.1 M NaF aqueous solution (b).

Both peptides form well packed films on gold from trifluoroethanolic solutions, since cyclic voltammetry measurements for the SAM-modified gold electrodes in a 4 mM ferricyanide/ferrocyanide in 2.0 M $NaClO_4$ aqueous solution showed negligible redox peak compared with a bare gold electrode.

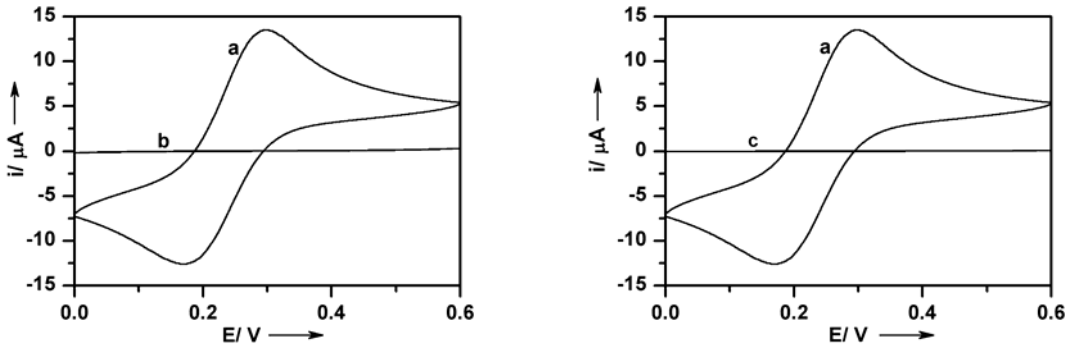

Figure S4.2. Cyclic voltammograms of bare (a), **Ac18L** (b) and **18LAc** (c) modified gold electrodes in 4 mM ferricyanide/ferrocyanide in 2.0 M $NaClO_4$ at a scan rate of 0.1 V/s.

Chapter 5

Effect of the Surface Curvature on the Secondary Structure of Peptides Adsorbed on Nanoparticles

5.1. Connecting Text

The second chapter on potential applications of peptide-modified surfaces focuses on a nano-application. Because of its biological relevance, peptide-protected nanoparticles are becoming very popular for biomedical applications. But, it is well-known that the structure of peptides is notoriously flexible and a peptide can act differently because of structural differences. As we have seen in Chapter 2, the dynamic properties may even govern the observed ET rates of the peptide film. Thus, it is very important that the peptides chosen for a specific function retain the desired structure on the surface of nanoparticles. This chapter describes the structural investigation of an α-helix on the surface of nanoparticles having different sizes. It has been found that the radius of curvature of nanoparticles has a significant consequence on the structure of the adsorbate peptides and thereby, may be a critical factor in nanoparticle-based applications.

 This paper is co-authored by H.-B. Kraatz. The initial idea was suggested by Prof. Kraatz and I performed the experiments. After observing some interesting results, he advised some further experiments. I wrote the first draft of the manuscript and Prof. Kraatz revised it several times. The manuscript will be used *verbatim* in my thesis.

5.2. Introduction

In two-dimensional self-assembled monolayers (2D-SAMs) on flat metal surfaces, the stability and the structure of the adsorbates depend on the interactions among neighboring molecules, for example, in alkanethiolated 2D-SAMs, the adsorbates interact primarily through the intermolecular van der Waals forces and form well-packed and almost defect-free monolayers.[1] On the other hand, in monolayer-protected nanoparticles (3D-SAMs), the inter-chain distance increases as one moves outwards from the core and the adsorbate monolayer becomes progressively less dense, defect-prone and irregular.[2] Recently, peptide-protected gold nanoparticles (GNPs) have received significant attention due to their potential relevance in biomedical applications. Demonstrations of nuclear targeting,[3] molecular recognition[4] and protein-like properties[5] are truly promising. However, the secondary structure of the peptide is known to be highly dependent on the interactions with the surrounding environment,[6] and the effect of the curvature between crystallographic faces of GNPs (which are polyhedral species)[7] on the secondary structure of adsorbate peptides is still an unexplored but potentially a critical issue. In this paper, we report the structural investigation of a 16 amino-acid containing peptide in both 2D- and 3D-SAMs (having increasing core diameters: 5, 10 and 20 nm respectively, and thereby decreasing the curvature between crystallographic faces) on gold surfaces. We have found that the degree of surface curvature has a profound effect on the secondary structure of the peptide and 3D-SAMs (on nanoparticles) does not always resemble to 2D-SAMs.

5.3. Results and Discussion

The Leu-rich peptide **Ac10L** (Ac-KTAL_{10}NPC-NH_2) is a synthetic model for the α-helical conformation observed in natural proteins[8] and possesses a thiol-functionalized Cys residue at the C-terminal (Figure 5.1). A preliminary account of the design, synthesis and characterization of the peptide, and preparation of both 2D- and 3D-SAMs, is provided in the electronic supplementary information (ESI). We have employed[9] Fourier transform infrared (FT-IR) spectroscopy to probe the structure of the peptide, since this technique has been one of the primary tools in understanding the secondary structure of peptides in both 2D- and 3D-SAMs.[10]

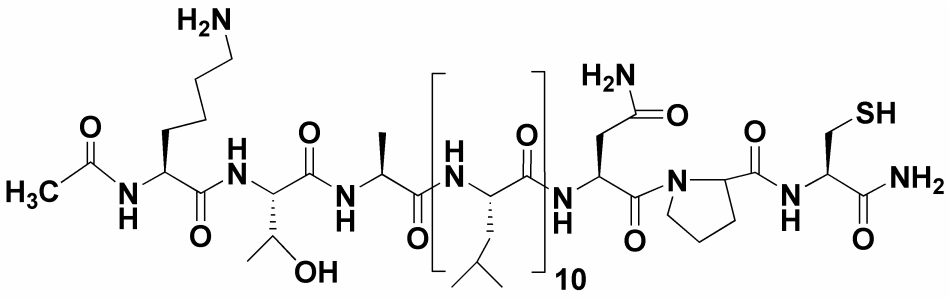

Figure 5.1. Molecular structure of the peptide **Ac10L**.

The amide I band, which is well-known for its sensitivity to the peptide secondary structure, appears at 1659 cm^{-1} for the free peptide in KBr (Figure 5.2a) and indicates that the peptide is α-helical.[11] On flat gold surface (2D-SAM), the peptide remains helical as Fourier transform reflection absorption infrared spectroscopy (FT-RAIRS) shows Amide I band at 1674 cm^{-1} (Figure 5.2e). The band shifts by ~15 cm^{-1} compared to that in KBr, which is not related to any structural change of the α-helix on flat gold surface, but rather due to the so-called optical effects.[10b-d,12] More specifically, this blue shift of the amide I band depends on the orientation of the helix axis relative to

the gold surface; the more vertical the arrangement, the higher is the shift. Similar types of observation and interpretation were reported previously for several helical peptides in 2D-SAMs on gold surfaces.[10 b-d]

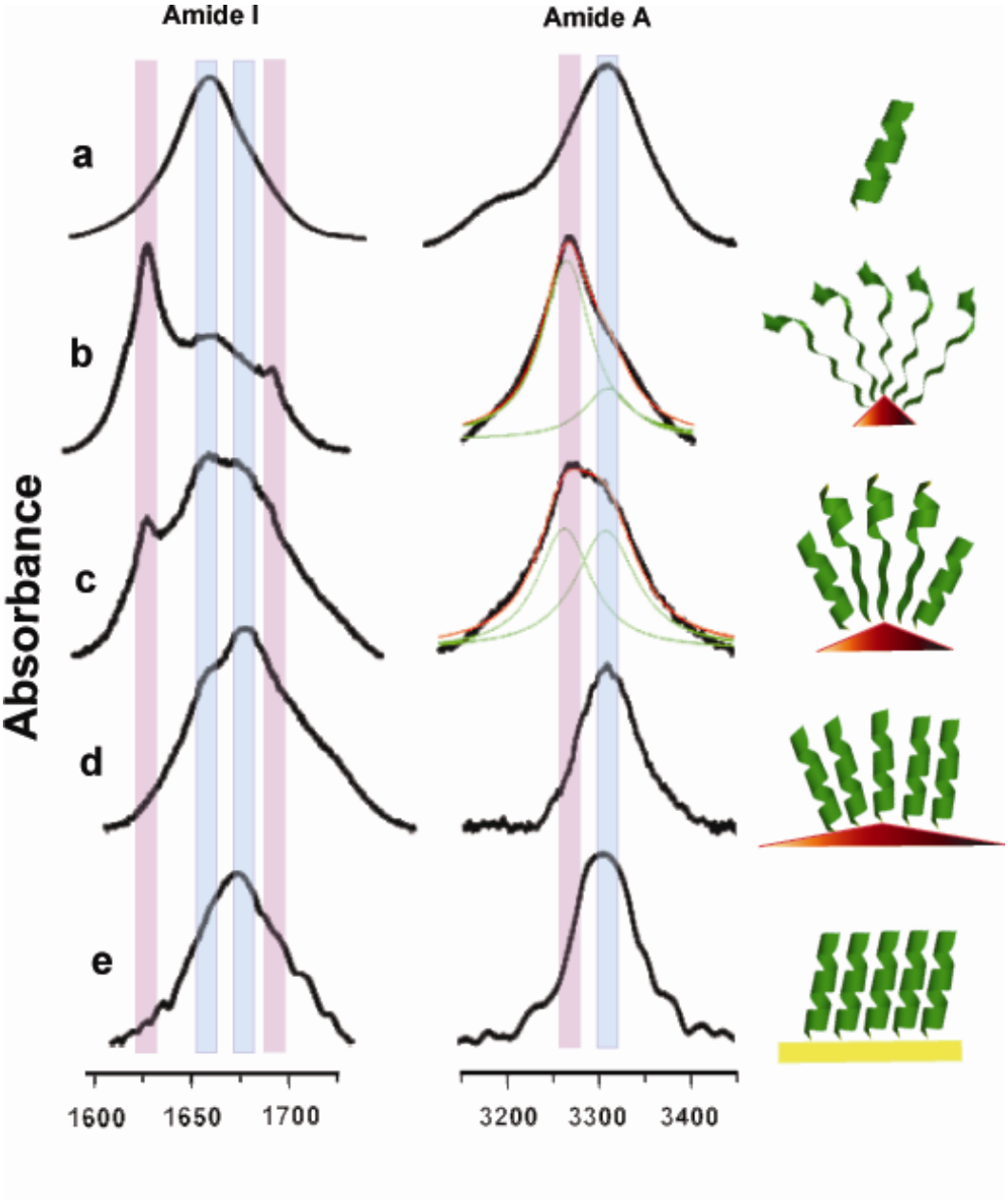

Figure 5.2. FT-IR spectra (KBr) of **Ac10L**: free state (a); on 5, 10 and 20 nm Au-NPCs (b, c and d, respectively); and FT-RAIRS on flat gold surface (e). The light blue and pink shades show regions where absorptions due to α- and β-sheet conformations occur, respectively.

Interestingly, IR spectrum (KBr) of the peptide on 5 nm GNPs (Figure 5.2b) significantly differs from those of the free and 2D states. The amide I region is composed of two additional bands: an intense band at 1627 cm^{-1} and a weak band at 1692 cm^{-1}, which we assign to the presence of a β-sheet conformation of the peptide.[13,14] For 10 and 20 nm GNPs (Figures 5.2c and 5.2d, respectively), a new absorption band appears at 1675 cm^{-1} which is close to the amide I for the peptide on flat gold surface and assigned to the α-helices present on the flat crystallographic faces of the GNPs (shifted due to the optical effects). The band is absent in 5 nm GNPs and the relative intensity of the band is greater in 20 nm GNPs compared to that in 10 nm, which may be correlated to larger amount of faces in larger GNPs.[7c,d] In addition, by comparing the spectra of the peptide on GNPs to that of the free state, we can conclude that the absorption at 1659 cm^{-1} (Figures 5.2b, c and d) is due to the partially folded/intact helical conformation at the edges and corners of GNPs where optical effects are absent.

For 5 nm GNPs, an analogous situation is demonstrated in the amide A region (Figure 5.2b). Two amide A bands are observed which implies the occurrence of two types of hydrogen-bonded N-H groups. A low-energy region (at 3266 cm^{-1}) due to the NH groups involved in β-sheet like H-bonds (C=O···H-N)[2d,14,15] and a high-energy region (at 3307 cm^{-1}) corresponding to the NH groups analogous to the native helix (intra-molecular hydrogen bonds). From the deconvoluted spectrum, it can be shown that the peptide (on 5 nm GNPs) almost exclusively (~ 78 %) adopt β-sheet conformation. In 10 nm GNPs, the relative content of β-sheet is reduced (~ 48 %) and if the size is further increased (20 nm), it completely disappears (Figures 5.2b, c and d).

Table 5.1. α-Helical and β-sheet contents of **Ac10L** in free, 2-D and different 3-D SAMs from the amide A band.

	α-helical content (%)	β-sheet content (%)
Free state	100	0
3D SAMs		
5 nm GNPs	22	78
10 nm GNPs	52	48
20 nm GNPs	100	0
2D SAM	100	0

The decrease in the β-sheet and increase in the α-helical contents with the increase in the GNP size can be rationalized as follows. At the edges and corners of GNPs, the Au-S bond density has been reported to be higher compared to that in the faces because of greater unsaturation of the gold atoms.[7a,b,16] So the peptides bound through the Au-S bond at the edges and corners (of 5 and 10 nm GNPs) are close enough to form inter-molecular H-bond containing β-sheet conformation. At the periphery where inter-chain distance is larger because of the surface curvature, the peptides are unable to form the inter-molecular H-bonds and adopt their native structure (helix). With the increase of the size of the GNPs, the curvature of the faces and the degree of unsaturation of the gold atoms at the edges and corners reduce which results in the decrease of the Au-S bond density and the increase in the intermolecular distance. In 20 nm GNPs, the curvature of the faces is probably negligible and the Au-S bond density is comparable to that in the faces, and the peptides are α-helical even at the edges and corners.

Our IR investigations indicate that the peptide remain helical on flat gold surface, but changes primarily to the β-sheet conformation on 5 nm GNPs and gradually transforms into the native helical structure as the surface curvature is reduced by increasing the size of the GNPs. This is in sharp contrast to that observed for structurally

rigid unnatural amino acid Aib-containing peptides,[10a] in which the native secondary structure (helix) is retained even on smaller GNPs (1.1-2.3 nm). So we speculate that peptide rigidity is also very important to govern the Au-S bond density at the edges and corners of GNPs. For the natural amino acid-containing peptide backbones which are not as rigid as Aib-containing ones, the higher reactivity of the Au atoms (at edges and corners)[7b] dominates and forms denser Au-S bonds, whereas for structurally rigid peptides, bulkiness of the molecule controls the Au-S density.

Since the reactivity of a peptide is related to the secondary structure,[17] any conformational change could seriously alter the overall activity of the peptide-protected nanoparticles and this work may provide a somewhat cautionary note in selecting a particular peptide sequence for nanoparticle based applications just by considering the native structure. In addition, the size of the nanoparticle should also be taken into consideration.

5.4. Acknowledgments

We thank the Natural Science and Engineering Research Council of Canada for funding. H.-B. K. is the Canada Research Chair in Biomaterials.

5.5. Supporting Information Available

Design, synthesis and characterization details, CD and UV-vis absorption spectra, deconvoluted IR spectra with parameters, TEM images.

5.6. References

[1] D. Bain, J. Evall, G. M. Whitesides, *J. Am. Chem. Soc.* **1989**, 111, 7155-7164.

[2] (a) A. C. Templeton, M. J. Hostetler, C. T. Kraft, R. W. Murray, *J. Am. Chem. Soc.* **1998**, 120, 1906-1911; (b) M. J. Hostetler, J. J. Stokes, R. W. Murray, *Langmuir* **1996**, 12, 3604-3612; (c) R. Paulini, B. L. Frankamp, V. M. Rotello, *Langmuir* **2002**, 18, 2368-2373; (d) A. K. Boal, V. M. Rotello, *Langmuir* **2000**, 16, 9527-9532; (e) C. Weeraman, A. K. Yatawara, A. N. Bordenyuk, A. V. Benderskii, *J. Am. Chem., Soc.* **2006**, 128, 14244-14245.

[3] A. G. Tkachenko, H. Xie, D. Coleman, W. Glomm, J. Ryan, M. F. Anderson, S. Franzen, D. L. Feldheim, *J. Am. Chem. Soc.* **2003**, 125, 4700-4701.

[4] E. Katz, I. Willner, *Angew. Chem., Int. Ed.* **2004**, 43, 6042-6108.

[5] R. Levy, N. T. K. Thanh, R. C. Doty, I. Hussain, R. J. Nichols, D. J. Schiffrin, M. Brust, D. G. Fernig, *J. Am. Chem. Soc.* **2004**, 126, 10076-10084.

[6] (a) W. F. DeGrado, J. D. Lear, *J. Am. Chem. Soc.* **1985**, 107, 7684-7689; (b) T. Kiyota, S. Lee, G. Sugihara, *Biochemistry* **1996**, 35, 13196-13204.

[7] (a) A. C. Templeton, W. P. Wuelfing, R. W. Murray, *Acc. Chem. Res.* **2000**, 33, 27-36; (b) E. Roduner, *Chem. Soc. Rev.* **2006**, 35, 583-592; (c) D. A. H. Cunningham, W. Vogel, H. Kageyama, S. Tsubota, M. Haruta, *J. Catal.* **1998**, 177, 1-10; (d) C. Gutiérrez-Wing, J. A. Ascencio, M. Pérez-Alvarez, M M. arín-Almazo, M. José-Yacamán, *J. Cluster Sci.* **1998**, 9, 529-545.

[8] D. J. Barlow, J. M. Thornton, *J. Mol. Biol.* **1988**, 201, 601-619.

[9] Characterization of the 3-D SAMs by CD and 1H-NMR was not possible due to precipitation problem.

[10] (a) L. Fabris, S. Antonello, L. Armelao, R. L. Donkers, F. Polo, C. Toniolo, F. Maran, *J. Am. Chem. Soc.* **2006**, 128, 326-336; (b) Y. Miura, S. Kimura, Y. Imanishi, J. Umemura, *Langmuir* **1999**, 15, 1155-1160; (c) M. Boncheva, H. Vogel, *Biophys. J.* **1997**, 73, 1056-1072; (d) Y. Miura, S. Kimura, S. Kobayashi, M. Iwamoto, Y. Imanishi, Umemura, *J. Chem. Phys. Lett.* **1999**, 315, 1-6.

[11] D. F. Kennedy, M. Crisma, C. Toniolo, D. Chapman, *Biochemistry* **1991**, 30, 6541-6548.

[12] D. L. Allara, A. Baca, C. A. Pryde, *Macromolecules* **1978**, 11, 1215-1220.

[13] (a) E. Benedetti, B. D. Blasio, V. Pavone, C. Pedone, C. Toniolo, G. M. Bonora, *J. Biol. Chem.* **1981**, 256, 9229-9234; (b) C. Toniolo, G. M. Bonora, H. Showell, R. J. Freer, E. L. Becker, *Biochemistry* **1984**, 23, 698-704; (c) C**.** Toniolo, G**.** M. Bonora**,** V. N. R**.** Pillai, M**.** Mutter**,** *Macromolecules* **1980,** 13**,** 772-774.

[14] C. Toniolo, G. M. Bonora, V. Barone, A. Bavoso, E. Benedetti, B. Di Blasio, P. Grimaldi, F. Lelj, V. Pavone, C. Pedone, *Macromolecules* **1985**, 18, 895-902.

[15] (a) S. W. Tam-Chang, H. A. Biebuyck, G. M. Whitesides, N. Jeon, R. G. Nuzzo, *Langmuir* **1995**, 11, 4371-4382; (b) R. S. Clegg, J. E. Hutchison, *Langmuir* **1996**, 12, 5239-5243.

[16] The higher density of the Au-S at the edges and corners of gold nanoparticles could also be partly due to the difference in the local pH and the pK constants in these particular sites compared to those in the flat crystallographic faces.

[17] (a) M. Venanzi, A. Valeri, A. Palleschi, L. Stella, L. Moroder, F. Formaggio, C. Toniolo, B. Pispisa, *Biopolymers* **2004**, 75, 128-139; (b) F. Formaggio, A.

Barazza, A. Bertocco, C. Toniolo, Q. B. Broxterman, B. Kaptein, E. Brasola, P. Pengo, L. Pasquato, P. Scrimin, *J. Org. Chem.* **2004**, 69, 3849-3856.

5.7. Supplementary Information

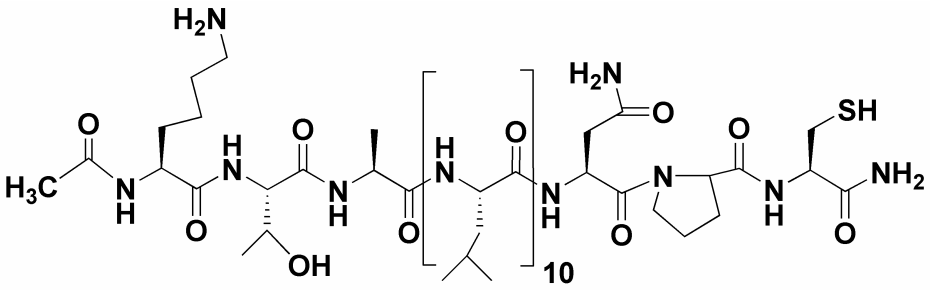

Ac-Lys-Thr-Ala-(Leu)$_{10}$-Asn-Pro-Cys-amide

Figure S5.1. Molecular structure of the peptide **Ac10L**.

5.7.1. Peptide Design

Leucine is the most hydrophobic of all the natural amino acids and it frequently occurs in the helical segments of proteins.[S1] Increased helicity has been reported to be coincident with the number of leucine incorporated in synthetic copolymers[S2] and extensive studies of poly-aminoacids showed that poly(Leu) forms the most stable helix because of the stronger hydrophobic interactions among the Leu residues.[S2] Hydrophobic interaction is generally accepted as the predominant source of free energy change that maintains the folded state of proteins.[S3] We expected that the hydrophobic side chain of leucine would make the peptide (in self assembled monolayers on gold surfaces): 1) well-packed and stable (van der Waals or London interactions among the hydrophobic side chains)[S4] and 2) ordered, since leucine residues align themselves parallel to each other along the helical interface.[S5] The N and C-terminals were

acetylated and amidated respectively to avoid repulsions with the helix dipole. Lysine was introduced because it has been reported to extend away from the helical backbone[S6] and was considered to enhance the solubility of the modified gold nanoparticles by creating a polar surface. Threonine is often found at the N-cap of α-helices;[S7] it helps to stabilize and increase the helicity of short peptides via a N-capping interaction.[S8] We speculated that alanine might bias the threonine residue at the N-cap toward a helical conformation and effective capping. The sequence Asn-Pro at the C-terminal has been shown to increase the helicity of peptides.[S9] The side chain of Asn forms H-bond with the helix main chain CO that is four residues away and thereby, stabilizes the C-terminal. Proline was introduced because of its conformational rigidity and cyclic side chain. It is believed to reduce the entropic penalty associated with the formation of the first helical turn and thereby, assist helix nucleation by confining the first C=O group of the helix into the appropriate position.[S7,S10] Cys was added so that we could assemble the peptide on gold surfaces.

5.7.2. Experimental

5.7.2.1. Materials

Fluorenylmethyloxycarbonyl (Fmoc)-protected L-α-amino acids, 1-hydroxybenzotriazole (HOBt) were purchased from SynPep (Dublin, CA). 5-(4-Fmocaminomethyl-3,5-dimethoxyphenoxy)valeric acid-MBHA (PAL) resin, (1H-benzotriazol-1-yloxy)tris(di- methylamino)phosphoniumhexafluoro phosphate (BOP) were from Advanced ChemTech (Louisville, KY). All other reagents and solvents including; 1,8-diazabicyclo[5.4.0]undec-7-ene (DBU) and diisopropylethylamine (DIPEA) were obtained from Sigma-Aldrich Canada Ltd. and used as received.

5.7.2.2. Synthesis and Characterization

The peptide was synthesized using an Argonaut Technologies Quest 210 semi-automated Organic Synthesizer, following the Fmoc-based strategy with PAL resin (0.4-0.8 mmol/g, 100-200 mesh) at 0.1 mmol scale. Crude peptide was purified using Merk silica gel 60 F254 aluminium preparatory plates. The solvent system used was $CHCl_3$/MeOH/CH_3COOH (85/12/3 v/v/v).

Ac10L: R_f = 0.45. ESI-MS: calcd for $C_{87}H_{158}N_{19}O_{19}S$ = 1805.2 $[M+H]^+$; found: 903.1 $[M+2H]^{2+}$.

Scheme S5.1. Peptide synthesis protocol.

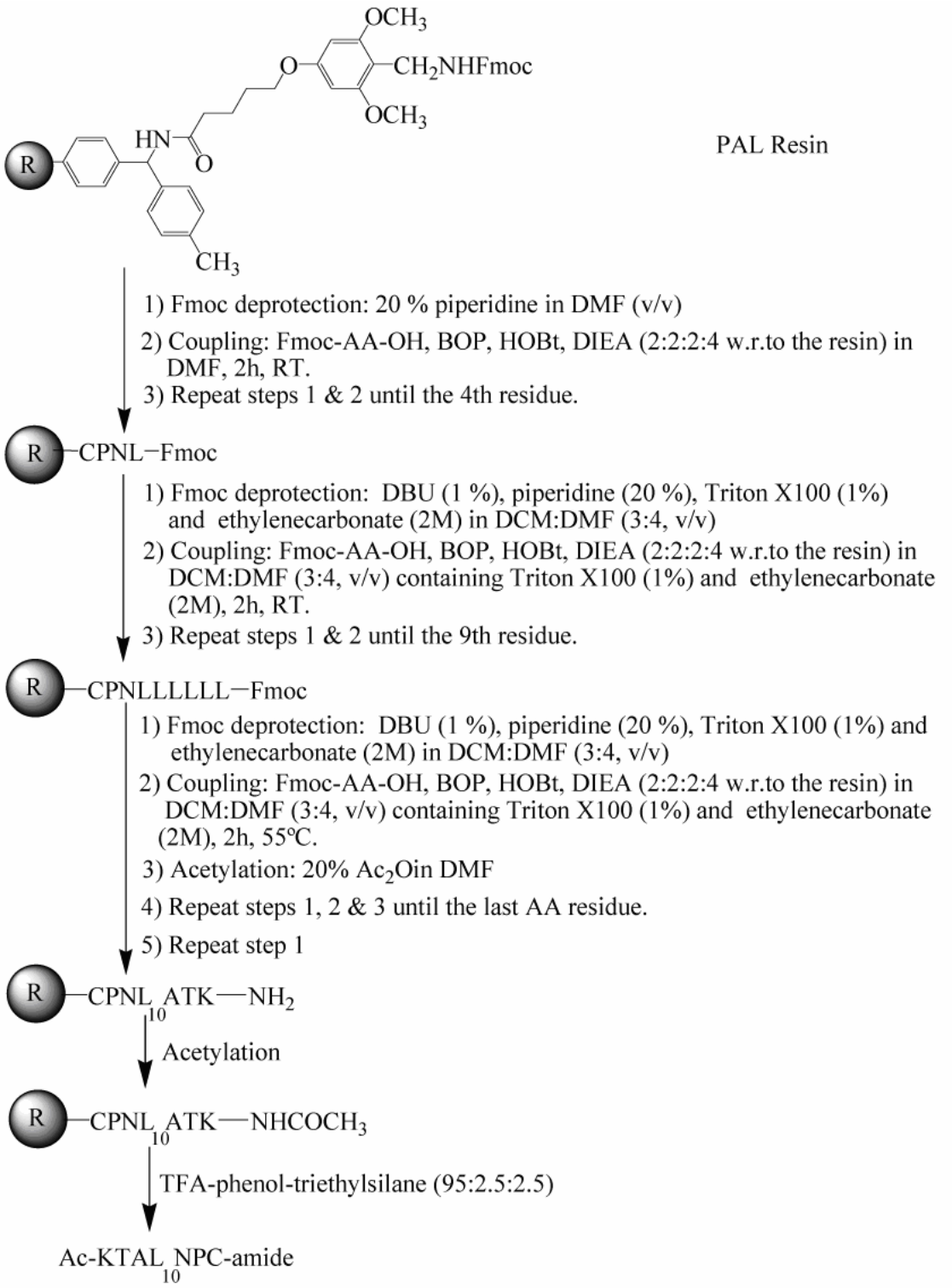

5.7.2.3. Circular Dichroism (CD) Spectroscopy

CD spectrum was taken with an Applied Photophysics π*-180 instrument at 22 ± 1ºC. The spectropolarimeter was calibrated daily with an aqueous solution of recrystallized ammonium camphorsulfonate-10-d. Ellipticity is reported as the mean residue ellipticity (θ, in deg·cm^2·dmol^{-1}) and calculated as, $\theta = \theta_{obs}(\mathrm{MRW}/10lc)$, where θ_{obs} is the ellipticity measured in millidegrees, MRW is the mean residue molecular weight of the polypeptide molecular weight divided by the number of amino acid residues, c is the concentration of the sample in mg/ml, and l is the optical path length of the cell in centimeters. Wavelength scans were performed in a 0.1 mm CD cell. The peptide (in trifluoroethanol) showed an intense maximum at ~190-191 nm and minima at ~206-207 and 220-222 nm, which are generally accepted as the characteristics of the helical structure.[S11]

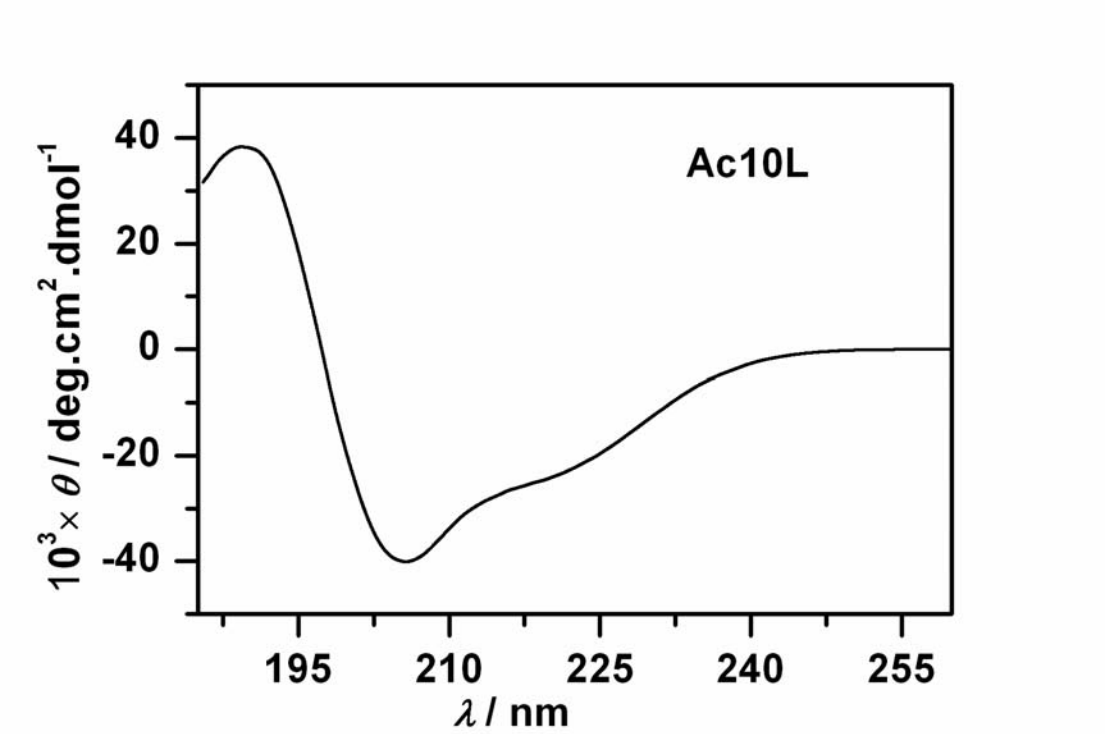

Figure S5.2. CD spectrum of **Ac10L** in trifluoroethanol at 22 ± 1ºC.

5.7.2.4. Peptide-Coated MPCs Synthesis

0.2 ml of citrate-stabilized gold nanoparticles (Sigma-Aldrich Canada Ltd.) was added drop wise to a vigorously stirred trifluoroethanolc solution (4 ml) of **Ac10L** (2 mg) over 10 minutes. Then the solution was stirred at room temperature for 48 hours. The peptide-coated nanoparticles were precipitated by centrifuging the solution at 14000 rpm. The supernatant solution containing unreacted peptides was discarded and 1 ml of TFE was added in the vial, centrifuged and again the supernatant solution was discarded. The process was repeated until the supernatant solution showed the absence of unreacted peptides in ATLC.

5.7.2.5. Preparation of 2D-SAM

To make 2D-SAM, Au on Si (100) (Platypus Technologies, Inc) wafer was incubated in 0.1 mM peptide in trifluoroethanolic solution for 5 days.

5.7.2.6. Infrared Spectroscopy

A Bio-Rad FTS-40 system was used to record the IR spectra. Origin 7.0 (OriginLab Corporation, Northampton, MA) was employed to deconvolute the spectra.

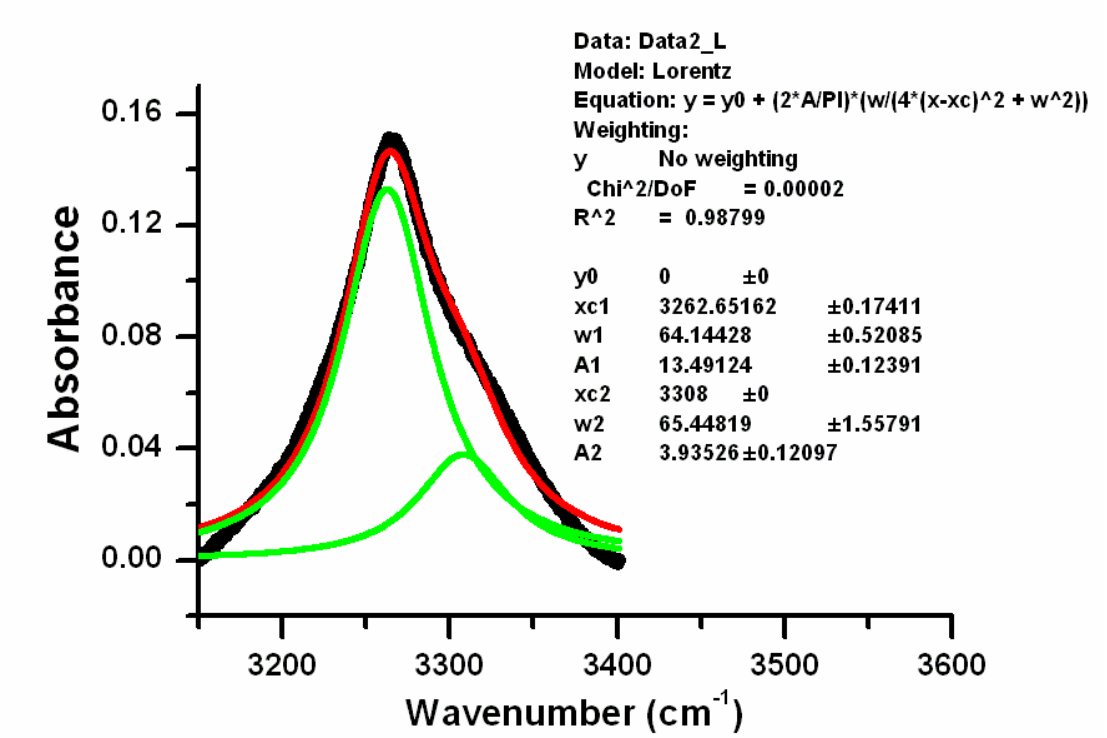

Figure S5.3. Amide A of **Ac10L** modified 5 nm Au-NPCs.

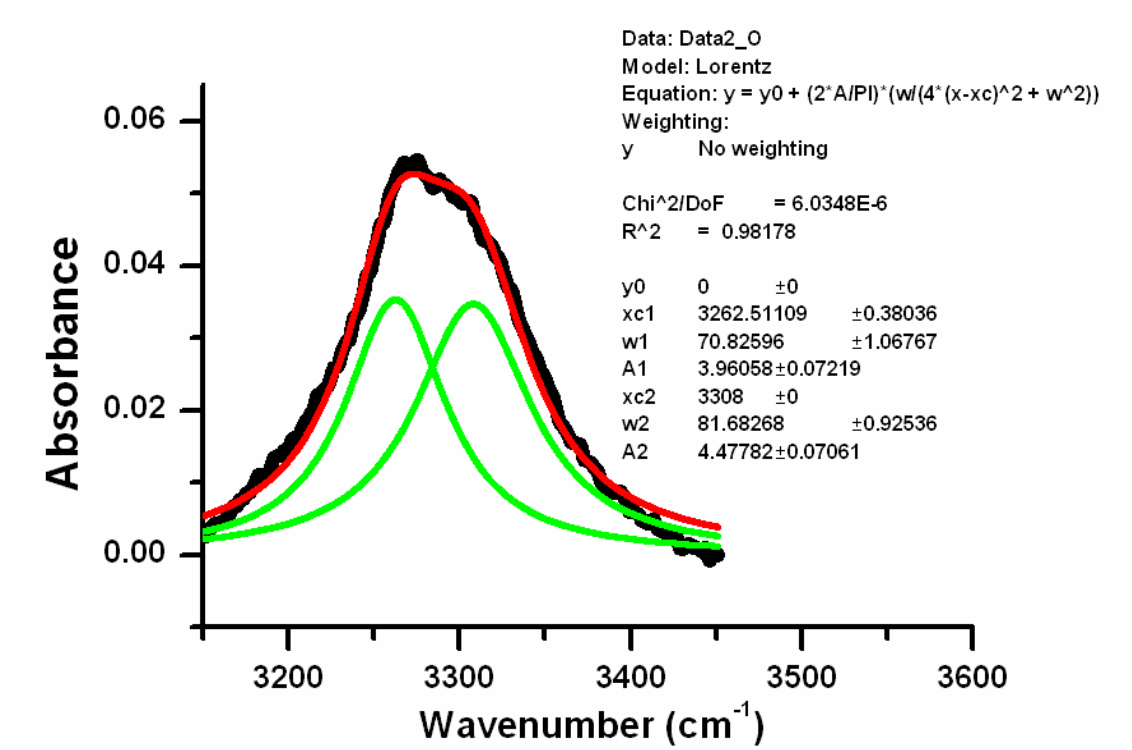

Figure S5.4. Amide A of **Ac10L** modified 10 nm Au-NPCs.

5.7.2.7. UV-Vis Absorption Spectroscopy

UV-vis spectra were taken in TFE solution with a Varian Cary 5 UV-vis spectrophotometer at room temperature.

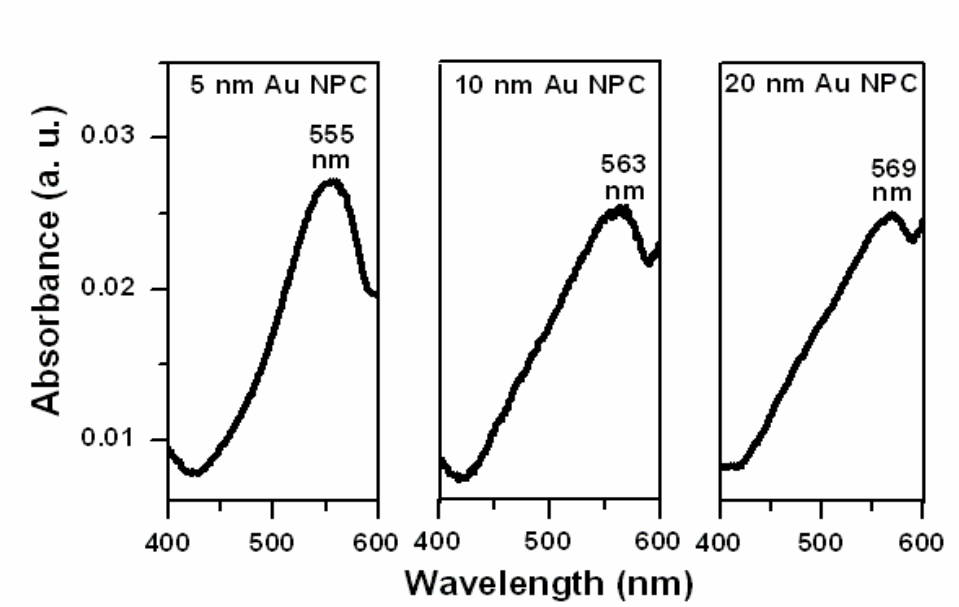

Figure S5.5. UV-vis absorption spectra of **Ac10L** modified Au-NPCs in trifluoroethanolc solution (~1 mg/ml). However, the concentration is not correct because the modified NPCs showed precipitation over time.

5.7.2.8. Transmission Electron Microscopy

TEM phase contrast images were obtained with a Philips TEM 4101 LS.

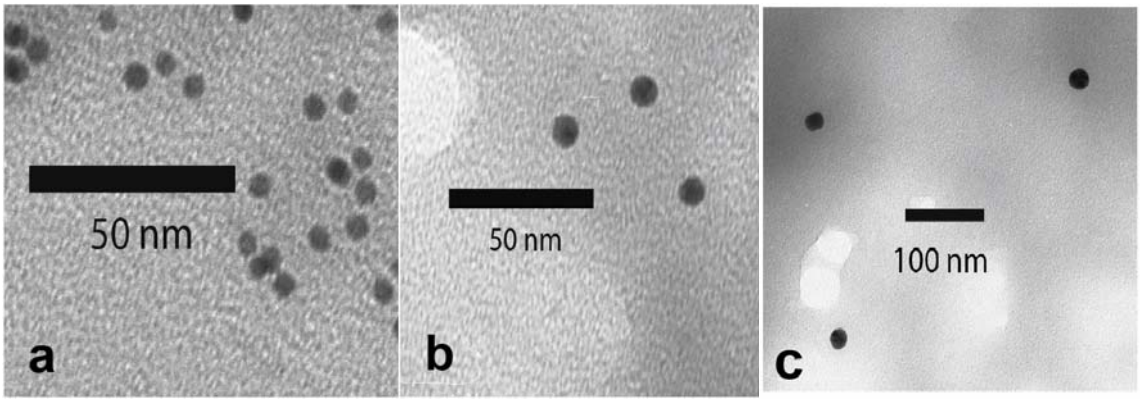

Figure S5.6. TEM images of **Ac10L** modified Au-NPCs: (a) 5 nm, (b) 10 nm and (c) 20 nm.

5.7.3. Supplementary References

S1 S. Padmanabhan, S. Marqusee, T. Ridgeway, T. M. Laue, R. L. Baldwin, *Nature* **1990**, 344, 268-270.

S2 C. R. Snell, G. D. Fasman, *Biopolymers* **1972**, 11, 1723-1744.

S3 S. C. Kwok, R. S. Hodges, *J. Biol. Chem.* **2003**, 278, 35248-35254.

S4 S. K. Burley, G. A. Petsko, *Adv. Protein Chem.* **1988**, 39, 125-189.

S5 E. K. O'Shea, R. Rutkowski, W. F. Stafford, P. S. Kim, *Science* **1989**, 245, 646-648.

S6 J. R. Broughman, L. P. Shank, O. Prakash, B. D. Schultz, T. Iwamoto, J. M. Tomich, K. J. Mitchell, *Membr. Biol.* **2002**, 190, 93-103.

S7 M. Vijayakumar, H. Qian, H.-X. Zhou, *Proteins: Struct., Funct., Genet.* **1999**, 34, 497-507.

S8 D. L. Luisi, W.-J. Wu, D. P. Raleigh, *J. Mol. Biol.* **1999**, 287, 395-407.

S9 H. X. Zhou, P. C. Lyu, D. E. Wemmer, N. R. Kallenbach, *J. Am. Chem. Soc.* **1994**, 116, 1139-1140.

S10 M. J. I. Andrews, A. B. Tabor, *Tetrahedron* **1999**, 55, 11711-11743.

S11 P. Wallimann, R. J. Kennedy, D. S. Kemp, *Angew. Chem. Int. Ed.* **1999**, 38, 1290-1292.

Chapter 6

General Discussions and Conclusions

As discussed in Chapter 1 (section 1.5), the controversy about the electron transfer (ET) phenomenon in helical peptides[1-12] motivated me to investigate this important area of research. A better understanding in this regard is necessary to elucidate the complex biological ET processes and explore the possibility of using this particular structural motif as scaffolds for molecular electronics. In my approach, I studied ET in some synthetic α-helical peptides. The peptides were equipped with a cysteine sulfhydryl group which enabled the formation of thin films on gold surfaces. In Chapter 2, I described the investigation of ET in a redox-active helical peptide (Fc18L) assembled in two types of films which differ by the alignment of the dipole moment of the helices on the surface of gold electrodes: in SAM1, the dipole moments of the peptides were aligned in the same direction, whereas in SAM2, they were opposite. The ET rate for Fc18L, measured electrochemically, was found an order of magnitude lower in SAM2 than that in SAM1. This observation can be rationalized by the difference in molecular dynamics (MD) of the two films. In SAM2, the peptides are more rigid due to the presence of intermolecular dipole-dipole interactions,[13,14] leading to the restriction of MD in this film. I suggest that ET may involve some active conformers which are only accessible if the peptide is dynamic, and the rate of formation of the conformers govern the overall ET efficiency i.e. the faster the dynamics, the faster is the rate of ET.

While Jones II and Vullev suggested [15] the involvement of the dynamic properties of helical peptides before, my studies described in this thesis are the first to demonstrate the involvement directly. My results explain the discrepancy in the literature about the conductivity of the α-helix (note that Batchelder *et al.* reported[10] the α-helix as an excellent conductor whereas Inai *et al.* described[11,12] it as an insulator). Depending on the difference in the amino acid sequences, different helices may have unlike flexibility and dynamic properties. So, according to my findings, ET can vary in different helices of comparable length just because of the difference in their dynamics: helices with more flexibility are expected to show more conductivity due to increased dynamics. In addition, assuming a static scenario i.e. a fixed distance between the donor (D) and the acceptor (A) is also incorrect because of the dynamic properties of the bridging peptide. During the long range ET, the D-A separation may vary and give rise to several conformers which can be different from each other in terms of the D-A separation and/or the coupling efficiency. The models ("distance" by Dutton,[16] "pathway" by Beraton[17]) that are used to interpret and compare the ET rates of different helices reported in the literature,[5,6] consider the D-B-A system static during ET and do not deal with the dynamic nature of the helix. So the comparison of ET rates in different helices having comparable D-A separation is meaningless unless their dynamic properties are proven to be similar under the experimental conditions employed. For example, the work reported by Zheng *et al.*[5] can be mentioned where the intramolecular H-bond was deleted and the ET rate was compared to that of the native structure. This type of comparison is prone to be incorrect as the dynamics of the two will not be the same. My investigations also point out why the ET rates for helices in solutions are orders of magnitude higher[1] than those in films on surfaces.[2] The α-helix is very dynamic in solution,[18] but when

the molecule is assembled in a film, its MD can be visualized to reduce and hence, can give lower ET rates.

The effect of dynamics on ET in the α-helix indicates a more complex picture of ET in proteins which generally contain several helical segments.[19,20] The dynamic nature of proteins is well-established,[21] and there is a high probability that numerous conformational changes may take place at the time scale of the long range ET process and affect the overall ET rates. In fact, as was recently shown,[10] dynamic processes are crucial in ET in proteins. My findings also give a clue why the discussion of ET in proteins is debated. Depending on the nature of the protein and the experimental conditions, the degree of protein dynamics can be different. So, once again, I suggest that comparing ET rates of different proteins which may have similar D-A separation, is not useful because of their difference in dynamics and there is an urgent need to develop improved theoretical models for ET that deal with this inherent property of peptides/proteins.

As a next step in my investigation, the ET kinetics of helical peptides was investigated in detail, for a number of films prepared from α-helical peptides having increasing lengths. The peptides showed a very weak distance dependence of ET and when these rates were compared to those of some published Fc-peptides on surface,[2,22] two distinct ET regimes were clearly evident. For smaller peptides, the ET rate decreases exponentially with the distance (the decay constant $\beta = 1.0$ Å^{-1}), indicating that the ET kinetics are governed by a tunneling mechanism.[23] But after ~2.5 nm, ET decreases very weakly ($\beta = 0.04$ Å^{-1}). Isied observed[24] similar type of transition for the ET in oligoprolines and suggested this as a signature of change in the ET mechanism. He speculated, following some theoretical work[25,26] on long-range ET, that the tunneling of

an electron from the donor to the acceptor becomes energetically unfavorable when the bridge becomes longer. In these cases, a bridge-mediated sequential hopping mechanism takes place which is weakly distant dependent in nature. But my observation of the absence of the redox-activity of Ac-peptides indicates that the peptide backbone itself is not prone to either oxidation or reduction and rules out the hopping mechanism. In addition, electronic structure calculations of the molecular orbitals in an ideal but short model helical peptide revealed an HOMO-LUMO gap of ~ 5 eV, which is much higher than the onset of conduction observed in STS. This indicates that the moving electron from the D to the A does not use the molecular orbital and its transfer follows the tunneling mechanism. I suspect that the transition of the ET rates with the length of the bridge is most likely related to the structural change of the peptide at ~2.5 nm; the peptides become longer and adopt a regular helical structure. I should point out that the oligoprolines studied by Isied also show the change when they adopt the helical polyproline II structure.[27] Newton theoretically predicted[28] that in both the α-helix and the polyproline II structures, the π-π interactions among the neighboring amide groups become possible and ET could be more favorable due to enhanced electronic coupling between the D and the A through the bridging peptide. Furthermore, electronic coupling has been calculated[28] to be stronger in the former (the α-helix) due to the presence of the intramolecular H-bond network (note that oligoprolines lack H-bonds). The importance of the H-bond in electron tunneling has been demonstrated by several groups.[4,29] Beratan and Gray suggested[29] that a H-bond is equivalent to two covalent bonds in mediating ET. This supports Maran's suggestion[4] that with the addition of a new amino acid residue in the helix, a new H-bond is formed which may compensate for the increase in the D-A separation. These also agree with the ET studies[30-32] of

oligoprolines and collagen-mimics (triple helix containing inter-molecular H-bonds)[33] performed in our lab; we observed higher rates in the later (collagen-mimics). Although, the pattern of the H-bond in collagen-mimics is different than that in the α-helix, considering numerous repports[4,29] on the importance of H-bond on ET, we think that the H-bond network in the α-helix is responsible for the weak distance dependence (β = 0.04 $Å^{-1}$). The value of β is weaker than that observed for the longer oligoprolines studied by Isied (β = 0.18 $Å^{-1}$),[24] because of the lack of H-bond in the later. It can also be pointed out that the distance dependence of ET (and thereby the value of β) just signifies the conductive nature of the bridge, for example, saturated alkane chains show β = 1.0 $Å^{-1}$,[23] whereas the highly conductive oligophenylenevinylene (OPV) derivatives have β = 0.06 $Å^{-1}$ for which ET also follows the tunneling mechanism.[34] So change of the β value should not be considered as an indication of a change in the ET mechanism as was suggested by Isied.[24]

One of the major goals of my study was to investigate the nature of the ET active coformers in the α-helix. I found that the peptides exist in solutions as dynamic mixtures of two closely related helical conformers (α and 3_{10}). In the literature, the dynamics of this equilibrium is reported to be very fast (τ ~ ns) in solution.[18] But the dynamics, as shown by Kimura, is reduced when the molecule is in a film (τ ~ 50s).[34b] This time scale agrees well with our ET rates. The 3_{10} conformer is reported to be more conductive than the α-helix because of the shorter and hence, stronger H-bonds (even though the D-A separation in this case is larger).[18] So, I think that 3_{10} is a possible ET active conformer and the the dynamics between the two conformers govern the overall ET rate.

Because of the difference in the H-bonding pattern between the α-helix and the collagen-mimics, it may not be judicial to compare their ET properties from a strict point of view. Nevertheless, they both contain H-bonds. Impedance spectroscopy showed the presence of large diffusion during ET in collagen films,[31] whereas in my studies the diffusion is negligible. These observations, following the findings in Chapter 2, can be correlated to the higher ET rates observed in collagen-mimics[31] compared to the α-helix.

These discoveries, led to the study of photo-electron transfer. Literature reports suggested that photocurrents can be observed in peptides decorated with suitable photoactive moieties.[35-38] However, as was quickly discovered and is reported in Chapter 4, a photocurrent was produced from bare gold and non-chromophore containing helical peptides, and both the direction and the intensity of this signal can be changed by the pH and nature of the electrolyte in solution. The results described in Chapter 4 clearly demonstrate that the photocurrent can be ascribed to the heating of the electrode by the laser and is not due to a "true" photocurrent generated from electron transfer from an excited chromophore to the gold surface as was reported in the literature.[35-38]

Finally in Chapter 5, a short ten leucine containing α-helical peptide was assembled on the surface of gold nanoparticles having different sizes and different degrees of surface curvature. FT-IR studies revealed that changes occur in the peptide secondary structure as a function of nanoparticle size. This is the first observation of its kind outlining an effect of nanoparticle size on an attached peptide. On a 5 nm Au particle, the peptide adopts primarily a β-sheet structure and gradually regains the native helical conformation as the curvature of the surface is reduced by increasing the size of

the nanoparticles. The reasons for these observations are probably the flexibility of the peptide studied and the higher reactivity of the Au atoms at the corners and edges of the nanoparticles.[39,40] In smaller nanoparticles, the curvature is high and the Au atoms at these sites are more reactive because of greater unsaturation. Thus, the density of the Au-S bond at the corners and edges is so high that the bulky helical peptides are forced to adopt a β-sheet conformation which is more stretched in comparison to the compact α-helical structure. With the increase of the nanoparticle size, the reactivity and hence, the Au-S density becomes similar to those at the faces and the peptide can retain their native helical conformation. Previously, Maran studied[41] the structure of some helices containing the unnatural amino acid (AA) Aib on smaller nanoparticles (< 2.5 nm in diameter). Aib-rich helices are structurally very rigid and can retain their native structure on the surface of the nanoparticles. But my studies which involve a flexible α-helix of natural AAs, clearly demonstrates the effect of the nanoparticles on the structure of biomolecules. These findings are important because peptide-protected nanoparticles are suggested to be relevant candidates for biomedical applications.[42-45] According to my investigations, the flexibility of the peptide and the size of the nanoparticles should be considered.

In conclusion, I think that I have achieved the objectives described in Section 1.7 of Chapter 1. By using model peptides, I have shown that the dynamic property plays a cruicial role in ET in helical peptides. These findings along with the work on collagen-mimics performed in our lab and Barton's work[46,47] on DNA may indicate the involvement of a common dynamically modulated ET in these semi-rigid systems. I hope that the results will be useful to understand the highly efficient biological ET processes and may offer a new direction in developing improved theoretical models for

ET. The investigations on photocurrent generation clearly demonstrate the necessity for advanced experimental techniques to explore natural photosystems. Finally, the work on peptide-protected nanoparticles points to the importance of a more in-depth study on the peptide stability and the size of the nanoparticle for efficient biomedical applications.

Reference:

[1] M. A. Fox, E. Galoppini, *J. Am. Chem. Soc.* **1996**, 118, 2299-2300.
[2] T. Morita, S. Kimura, *J. Am. Chem. Soc.* **2003**, 125, 8732-8733.
[3] Y. Inai, M. Sisido, Y. Imanishi, *J. Phys. Chem.* **1990**, 94, 6237-6243.
[4] F. Polo, S. Antonello, F. Formaggio, C. Toniolo, F. Maran, *J. Am. Chem. Soc.* **2005**, 127, 492-493.
[5] Y. Zheng, M. A. Case, J. F. Wishart, G. L. McLendon, *J. Phys. Chem. B.* **2003**, 107, 7288-7293.
[6] M. Sisido, S. Hoshino, H. Kusano, M. Kuragaki, M. Makino, H. Sasaki, T. A. Smith, K. P. Ghiggino, *J. Phys. Chem. B.* **2001**, 105, 10407-10415.
[7] G. Jones II, V. Vullev, E. H. Braswell, D. Zhu, *J. Am. Chem. Soc.*, **2000**, 122, 388-389.
[8] K. J. Kise, B. E. Bowler, *Inorg. Chem.* **2003**, 42, 3891-3897.
[9] J. Watanabe, T. Morita, S. Kimura, *J. Phys. Chem. B.* **2005**, 109, 14416-14425.
[10] T. L. Batchelder, R. J. III Fox, M. S. Meier, M. A. Fox, *J. Org. Chem.* **1996**, 61, 4206-4209.
[11] Y. Inai, M. Sisido, Y. Imanishi, *J. Phys. Chem.* **1991**, 95, 3847-3851.
[12] Y. Inai, M. Sisido, Y. Imanishi, *J. Phys. Chem.* **1990**, 94, 6237-6243.
[13] S. Yasutomi, Y. Imanishi, S. Kimura, *Science* **2004**, 304, 1944-1947.
[14] M. Niwa, M. Morikawa, N. Higashi, *Angew. Chem. Int. Ed.* **2000**, 39, 960-963.
[15] G. Jones II, X. Zhou, V. I. Vullev, *Photochem. Photobiol. Sci.* **2003**, 2, 1080-1087.
[16] C. C. Page, C. C.Moser, X. Chen, P. L. Dutton, *Nature* **1999**, 402, 47-52.
[17] D. N. Beratan, J. N. Betts, J. N. Onuchic, *Science* **1991**, 252, 1285-1288.
[18] S. E. Huston, G. R. Marshall, *Biopolymers* **1994**, 34, 75-90.
[19] D. M. Lawson, C. E.M. Stevenson, C. R. Andrew, and R. R. Eady, *The EMBO Journal* **2000**, 19, 5661–5671
[20] V. I. Vullev, J. II Jones, *Res. Chem. Interm.* **2002**, 28, 795-781.
[21] H. Wang, S. Lin, J. P. Allen, J. C. Williams, S. Blankert, C. Laser, N. W. Woodbury *Science* **2007**, 316, 747-750.
[22] S. Sek, A. Sepiol, A. Tolak, A. Misicka, R. Bilewicz, *J. Phys. Chem. B.* **2004**, 108, 8102-8105.
[23] D. B. Robinson, C. E. D. Chidsey, *J. Phys. Chem. B* **2002**, 106, 10706-10713.
[24] R. A. Malak, Z. Gao, J. F. Wishart, S. S. Isied, *J. Am. Chem. Soc.* **2004**, 126, 13888-13889.
[25] E. G. Petrov, Ye. V. Shevchenko, V. I. Teslenko, V. May, *J. Chem. Phys.* **2001**, 115, 7107-7122.

[26] M. Bixon, J. Jortner, *J. Chem. Phys.* **1997**, 107, 5154-5170.
[27] M. Y. Ogawa, J. F. Wishart, Z. Young, J. R. Miller, S. S. Isied, *J. Phys. Chem.* **1993**, 97, 11456-11463
[28] Y.-g. K. Shin, M. D. Newton, S. S. Isied, *J. Am. Chem. Soc.* **2003**, 125, 3722-3732.
[29] D. N. Beratan, J. N. Onuchic, J. R. Winkler, H. B. Gray, *Science* **1992**, 258, 1740-1741.
[30] M. M. Galka, H.-B. Kraatz, ChemPhysChem **2002, 3**, 356 – 359.
[31] H.-B. Kraatz, I. Bediako-Amoa, S. H. Gyepi-Garbrah, T. C. Sutherland, *J. Phys. Chem. B.* **2004**, 108, 20164-20172.
[32] S. K. Dey, H. S. Mandal, Y.-T. Long, S. Chowdhury, T. C. Sutherland, H.-B. Kraatz, *Langmuir* **2007**, 23, 6475-6477.
[33] A. V. Finkelstein, O. B. Ptitsyn, In *Protein Physics*; Lectures 7. Academic Press: New York, **2002**.
[34] (a) H. D. Sikes, J. F. Smalley, S. P. Dudek, A. R. Cook, M. D. Newton, C. E. D. Chidsey, S. W. Feldberg, *Science* **2001**, 291, 1519-1523; (b) K. Kitagawa, T. Morita, S. Kimura, *Angew. Chem., Int. Ed.* **2005**, 44, 6330-6333.
[35] T. Morita, S. Kimura, S. Kobayashi, Y. Imanishi, *J. Am. Chem. Soc.* **2000**, 122, 2850-2859.
[36] K. Yanagisawa, T. Morita, S. Kimura, *J. Am. Chem. Soc.* **2004**, 126, 12780-12781.
[37] S. Yasutomi, T. Morita, S. Kimura, *J. Am. Chem. Soc.* **2005**, 127, 14564-14565.
[38] S. Yasutomi, T. Morita, Y. Imanishi, S. Kimura, *Science* **2004**, 304, 1944-1947.
[39] A. C. Templeton, W. P. Wuelfing, R. W. Murray, *Acc. Chem. Res.* **2000**, 33, 27-36.
[40] E. Roduner, *Chem. Soc. Rev.* **2006**, 35, 583-592;
[41] L. Fabris, S. Antonello, L. Armelao, R. L. Donkers, F. Polo, C. Toniolo, F. Maran, *J. Am. Chem. Soc.* **2006**, 128, 326-336
[42] J. M. de la Fuente, C. C. Berry, M. O. Riehle, A. S. G. Curtis, *Langmuir* **2006**, 22, 3286-3293.
[43] A. G. Tkachenko, H. Xie, D. Coleman, W. Glomm, J. Ryan, M. F.,erson, S. Franzen, D. L. Feldheim, *J. Am. Chem. Soc.* **2003**, 125, 4700-4701.
[44] E. Katz, I. Willner, *Angew. Chem., Int. Ed.* **2004**, 43, 6042-6108.
[45] R. Levy, N. T. K. Thanh, R. C. Doty, I. Hussain, R. J. Nichols, D. J. Schiffrin, M. Brust, D. G. Fernig, *J. Am. Chem. Soc.* **2004**, 126, 10076-10084.
[46] M. A. O'Neill, J. K. Barton, *J. Am. Chem. Soc.* **2004**, 126, 13234-13235.
[47] M. A. O'Neill, J. K. Barton, *J. Am. Chem. Soc.* **2004**, 126, 11471-11483.

Curriculum Vitae

Himadri S. Mandal
Department of Chemistry
110 Science Place
University of Saskatchewan
Saskatoon, SK S7N 5C9, Canada
Email: hsm420@mail.usask.ca

Education:

2007 (expected)	Ph. D. *"Electron Transfer Mechanism and Potential Applications of α-Helical Peptides"* Supervisor: Prof. H.-B. Kraatz Department of Chemistry University of Saskatchewan, Canada
2000	M. Sc. "*Syntheses and Reactions of some Novel Triosmium Clusters*" Supervisor: Prof. S. E. Kabir Department of Chemistry Jahangirnagar University, Bangladesh
1997	B. Sc. Department of Chemistry Jahangirnagar University, Bangladesh

Publications

(1) S. Piana, **H. S. Mandal** and H. –B. Kraatz, "Understanding the Mechanism of Electron Transfer through α-Helical Peptides", *Submitted*.
(2) **H. S. Mandal** and H.-B. Kraatz, "Effect of the surface curvature on the secondary structure of peptides adsorbed on nanoparticles," *J. Am. Chem. Soc.* **2007**, 129, 6356-6357.
(3) S. K. Dey, Yi-Tao Long, S. Chowdhury, T. C. Sutherland, **H. S. Mandal** and H.-B. Kraatz, "Study of electron transfer in ferrocene-labeled collagen-like peptides," *Langmuir*, **2007**, 23, 6475-6477.
(4) **H. S. Mandal,** I. J. Burgess and H.-B. Kraatz, "Investigation of laser induced photocurrent generation experiments," *Chem. Commun.* **2006**, 4802 – 4804.
(5) **H. S. Mandal** and H.-B. Kraatz, "Electron transfer across α-helical peptides: Potential influence of molecular dynamics," *Chem. Phys.* **2006**, 326, 246-251.
(6) **H. S. Mandal** and H.-B. Kraatz, "Ferrocene-histidine conjugates: *N*-ferrocenoyl-histidyl(im*N*-ferrocenoyl)methylester: synthesis and structure," *J. Organomet. Chem.* **2003**, 674, 32-37.

(7) S. E. Kabir, K. M. A. Malik, **H. S. Mandal**, Md. A. Mottalib, Md. J. Abedin, E. Rosenberg, "Reaction of $Os_3(CO)_9(\mu_3\text{-}\eta^2\text{-}C_7H_3(2\text{-}CH_3)NS)(\mu\text{-}H)$ with diazomethane. The first example of a trimetallic cluster containing a μ-methylidene and a σ-methyl," *Organometallics* **2002**, *21*, 2593-2595.

Permissions

07/24/2007 12:45 FAX 2027768112 001

ACS PUBLICATIONS DIVISION
JUL 10 2007
COPYRIGHT OFFICE

PERMISSION REQUEST FORM

Date: 05/07/2007

~~From~~ To: Copyright Office
Publications Division
American Chemical Society
1155 Sixteenth Street, N.W.
Washington, DC 20036

FAX: 202-776-8112

~~From~~ To: Himadri S. Mandal
Dept. of Chemistry, University of Saskatchewan
110 Science Place, Saskatoon, S7N 5C9, SK.
Canada
Phone No. 1-306-220-8848
Fax No. 1-306-966-4730

I am preparing my PhD thesis entitled:
ELECTRON TRANSFER MECHANISM AND POTENTIAL APPLICATIONS OF

α-HELICAL PEPTIDES

I would appreciate your permission to use the following ACS material in print and other formats with the understanding that the required ACS copyright credit line will appear with each item and that this permission is for only the requested work listed above:

From ACS journals or magazines (for ACS magazines, also include issue no.):

ACS Publication Title Issue Date,	Vol.No.	Page(s)	Material to be used*
J. Phys. Chem. B.; 2003;	107(30);	7288-7292.	**Figure 1**
J. Phys. Chem. B.; 2001;	105(42);	10407-10415	**Figure 7**
J. Am. Chem. Soc.; 2003;	125(29);	8732-8733.	**Figures 1 & 2b**
J. Am. Chem. Soc.; 2004;	126(43);	13888-13889.	**Figures 1**
J. Phys. Chem. B.; 2005;	109(30);	14416-14425.	**Figure 8**
J. Am. Chem. Soc.; 2003;	125(16);	4700-4701.	**Figure 1**

From ACS books: include ACS book title, series name and number, year, page(s), book editor=s name(s), chapter author's name(s), and material to be used, such as Figs. 2 & 3, full text, etc.*

* If you use more than three figures/tabl
will also be required.
Questions? Please call Arleen Courtney

This space is reserved for ACS Copyright Office Use

PERMISSION TO REPRINT IS GRANTED BY THE AMERICAN CHEMICAL SOCIETY

ACS CREDIT LINE REQUIRED. Please follow this sample: Reprinted with permission from (reference citation). Copyright (year) American Chemical Society.

APPROVED BY: C. Arleen Courtney 7/11/07
ACS Copyright Office

☐ If box is checked, author permission is also required. See original article for address.

Science
AAAS

Permissions Letter

Ref # 07-22708

DATE: Monday, July 09, 2007

TO: Himadri Mandal
Dept. of Chemistry, University of Saskatchewan
110 Science Place
Saskatoon, SK S7N 5C9
Canada
FROM: Elizabeth Sandler, Rights and Permissions
RE: Your request for permission dated 07/05/07

Regarding your request, we are pleased to grant you non-exclusive, non-transferable permission to use the AAAS material identified below in your dissertation or thesis identified below, but limited to the formats identified below, and provided that you meet the conditions / requirements below. Such permission is for one time use and therefore does not include permission for future editions, revisions, additional printings, updates, ancillaries, other formats, translations, or promotional pieces, unless otherwise permitted below. This permission does not apply to figures / artwork that are credited to non-AAAS sources. This permission does not include the right to modify AAAS material.

The following credit line must be printed along with the AAAS material: "From [Insert Full Reference Citation]. Reprinted with permission from AAAS."

This permission covers the use of the AAAS material identified herein in the following format versions of your dissertation/thesis:
[x] print
[x] microform
[x] Digitized / electronic versions , provided the reprinted AAAS material remains in situ and is not made digitally available separated from your dissertation/thesis

AAAS agrees that ProQuest/UMI may supply copies of the dissertation/thesis on demand.

If the requested material is sourced to or references non-AAAS sources, you must obtain authorization from that source as well.

Permission fees are waived in this instance. AAAS reserves the right to charge for reproduction of AAAS controlled material in the future.

AAAS must publish the full paper prior to use of any text.

AAAS does not supply photos or artwork. Use of the AAAS material must not imply any endorsement by the American Association for the Advancement of Science. This permission is not valid for the use of the AAAS and/or SCIENCE logos.

Permission is valid for use of the following AAAS material only:
Fig 1 and Fig. 4(A) from Yasutomi et al., SCIENCE 304:1944-1947 (6/25/2004)
In the following work only:
"Introduction", ELECTRON TRANSFER MECHANISM AND POTENTIAL APPLICATIONS OF A-HELICAL PEPTIDES published by University of Saskatchewan

Thank you for writing. If you have any questions please call me at (202) 326-6765 or write to me via fax at (202) 682-0816. For international calls, +1 is the country code for the United States.

Headquarters:
1200 New York Avenue, NW, Washington, D.C. 20005 USA

University of Saskatchewan Webmail

INBOX Compose Folders Options Search Help Address Book Logout Open Folder

INBOX: RE: Obtain Permission (34 of 170)

Move | Copy

Delete | Reply | Reply to All | Forward | Redirect | Blacklist | Message Source | Save as | Print

Back to INBOX

Date: Tue, 03 Jul 2007 14:40:20 +0100

From: "Watts, James (ELS-OXF)" <J.Watts@elsevier.com>

To: hsm420@mail.usask.ca

Subject: RE: Obtain Permission

Part(s): 1.2 unnamed text/html 8.69 KB

This message was written in a character set other than your own. If it is not displayed correctly, click here to open it in a new window.

Dear Dr. Mandal

We hereby grant you permission to reprint the material detailed below at no charge in your thesis subject to the following conditions:

1. If any part of the material to be used (for example, figures) has appeared in our publication with credit or acknowledgement to another source, permission must also be sought from that source. If such permission is not obtained then that material may not be included in your publication/copies.

2. Suitable acknowledgment to the source must be made, either as a footnote or in a reference list at the end of your publication, as follows:

"This article was published in Publication title, Vol number, Author(s), Title of article, Page Nos, Copyright Elsevier (or appropriate Society

name) (Year)."

3. Your thesis may be submitted to your institution in either print or electronic form.

4. Reproduction of this material is confined to the purpose for which permission is hereby given.

5. This permission is granted for non-exclusive world English rights only. For other languages please reapply separately for each one required. Permission excludes use in an electronic form other than submission. Should you have a specific electronic project in mind please reapply for permission.

6. This includes permission for the Library and Archives of Canada to supply single copies, on demand, of the complete thesis. Should your thesis be published commercially, please reapply for permission.

Yours sincerely

Clare Truter

Rights Manager

-----Original Message-----
From: hsm420@mail.usask.ca [mailto:hsm420@mail.usask.ca]
Sent: 27 June 2007 20:20
To: Rights and Permissions (ELS)
Subject: Obtain Permission

This Email was sent from the Elsevier Corporate Web Site and is related to Obtain Permission form:

Product: Customer Support
Component: Obtain Permission
Web server: http://www.elsevier.com
IP address: 10.10.24.148
Client: Mozilla/4.0 (compatible; MSIE 7.0; Windows NT 5.1; iebar; .

NET CLR 2.0.50727)
Invoked from: http://www.elsevier.com/wps/find/obtainpermissionform.cws_home?isSubmitted=yes&navigateXmlFileName=/store/prod_webcache_act/framework_support/obtainpermission.xml

Request From:
Himadri Shekhar Mandal
Department of Chemistry
110 Science Place
S7N 5C9
Saskatoon
Canada

Contact Details:
Telephone: (306) 220-8848
Fax: (306) 966-4730
Email Address: hsm420@mail.usask.ca

To use the following material:
ISSN/ISBN:
Title: Chemical Physics
Author(s): Himadri S. Mandal and Heinz-Bernhard Kraatz
Volume: 326
Issue: 1
Year: 2006
Pages: 246 - 251
Article title: Electron Transfer across á-Helical Peptides:

How much of the requested material is to be used:
whole, verbatim

Are you the author: Yes
Author at institute: Yes

How/where will the requested material be used: In a thesis or dissertation

Details:

I'd like to reproduce the paper verbatim in my PhD thesis entitled "Electron Transfer Mechanism and Potential Applications of á-Helical Peptides"

Additional Info: I would highly appeciate if permission is granted as soon as possible. Thanks in advance.

```
- end -

For further info regarding this automatic email, please contact:
WEB APPLICATIONS TEAM  ( esweb.admin@elsevier.co.uk )


This email is from Elsevier Limited, a company registered in England and
Wales with company number 1982084,
whose registered office is The Boulevard, Langford Lane, Kidlington,
Oxford, OX5 1GB, United Kingdom.
```

2 image001.gif image/gif 2.23 KB

3 image002.jpg image/jpeg 1.95 KB

University of Saskatchewan Webmail

INBOX Compose Folders Options Search Help Address Book Logout Open Folder

Search Results: RE: Permission Request Form: Himadri Shekhar Mandal (1 of 1)

Move | Copy

Delete | Reply | Reply to All | Forward | Redirect | Blacklist | Message Source | Save as | Print

Back to Search Results

Date: Thu, 28 Jun 2007 07:23:14 +0100

From: "CONTRACTS-COPYRIGHT (shared)" <Contracts-Copyright@rsc.org>

To: hsm420@mail.usask.ca

Subject: RE: Permission Request Form: Himadri Shekhar Mandal

Part(s): 2 unnamed text/html 15.89 KB

This message was written in a character set other than your own. If it is not displayed correctly, click here to open it in a new window.

Dear Himadri Shekhar Mandal

The Royal Society of Chemistry (RSC) hereby grants permission for the use of your paper(s) specified below in the printed or microfilm version of your thesis. You may also make available the PDF version of your paper (s) that the RSC sent to the corresponding author(s) of your paper(s) upon publication of the paper(s) in the following ways: in your thesis via any restricted internal website that your university may have for the deposition of theses, via your university's Intranet or via your own personal website. We are unable to grant you permission to include the paper(s) in any publicly available database/website, including the ProQuest Dissertation Abstracts Database. The Royal Society of Chemistry is a signatory to the STM Guidelines on Permissions (available on request).

Please note that if the material specified below or any part of it appears with credit or acknowledgement to a third party then you must also secure permission from that third party before reproducing that

material.

Please ensure that the published article states the following:

Reproduced by permission of The Royal Society of Chemistry

Regards

Gill Cockhead

Contracts & Copyright Executive

Gill Cockhead (Mrs), Contracts & Copyright Executive

Royal Society of Chemistry, Thomas Graham House

Science Park, Milton Road, Cambridge CB4 0WF, UK

Tel +44 (0) 1223 432134, Fax +44 (0) 1223 423623

http://www.rsc.org <http://www.rsc.org/> and http://www.chemsoc.org <http://www.chemsoc.org/>

-----Original Message-----
From: hsm420@mail.usask.ca [mailto:hsm420@mail.usask.ca]
Sent: 27 June 2007 20:00
To: CONTRACTS-COPYRIGHT (shared)
Subject: Permission Request Form: Himadri Shekhar Mandal

Name : Himadri Shekhar Mandal

Address :

Department of Chemistry

University of Saskatchewan

110 Science Place

Saskatoon, SK S7N 5C9 Canada

Tel: (306) 966-4655 Fax: (306) 966-4730

Tel : (306) 966-4655

Fax : (306) 966-4730

Email : hsm420@mail.usask.ca

I am preparing the following work for publication:

Article/Chapter Title : Electron Transfer Mechanism and Potential Applications of á-Helical Peptides

Journal/Book Title : PhD thesis, University of Saskatchewan, CANADA

Editor/Author(s) : Himadri Shekhar Mandal

Publisher :

I would very much appreciate your permission to use the following material:

Journal/Book Title : Chem. Comm.

Editor/Author(s) : Himadri S. Mandal, Ian J. Burgess and Heinz-Bernhard Kraatz

Volume Number : 46

Year of Publication : 2006

Description of Material : the whole article

Page(s) : 4802-4804

Any Additional Comments :

I'd like to reproduce the paper verbatim in my PhD thesis.

University of Saskatchewan Webmail

INBOX Compose Folders Options Search Help Address Book Logout Open Folder

Search Results: Re: permission for the Chem. Comm. paper (1 of 1)

Move | Copy

Delete | Reply | Reply to All | Forward | Redirect | Blacklist | Message Source | Save as | Print

Back to Search Results

Date: Tue, 01 May 2007 12:24:49 -0600

From: Ian Burgess <ian.burgess@usask.ca>

To: "Himadri S. Mandal" <HIMADRI.MANDAL@usask.ca>

Subject: Re: permission for the Chem. Comm. paper

Absolutely Himadri.

Ian

Himadri S. Mandal wrote:
> Dear Dr. Burgess,
> I'm writing my manuscript-based thesis and for that I need your permission to
> include the following paper as one the chapters.
>
> "Investigations of Laser Induced Photocurrent Generation Experiments. Chemical
> Communications. 2006, 46. 4802-4804".
>
> Could you please give me the permission (a positive e-mail response is fine for
> this purpose).
>
> Thanks in advance.
> Sincerely,
> Himadri
> Department of Chemistry
> 110 Science Place
> University of Saskatchewan
> Saskatoon, SK S7N 5C9, Canada
> Email: hsm420@mail.usask.ca
> Phone: (306) 966-1636

American Chemical Society

Publications Division
Copyright Office

1155 Sixteenth Street, NW
Washington, DC 20036
Phone: (1) 202-872-4368 or -4367
Fax: (1) 202-776-8112 E-mail: copyright@acs.org

FAX: 306-966-4730 DATE: July 2, 2007

TO: Himadri S. Mandal, Department of Chemistry, University of Saskatoon
110 Science Place, Saskatoon, SK S7N 5C9, Canada

FROM: C. Arleen Courtney, Copyright Associate C. Arleen Courtney

Thank you for your request for permission to include **your** paper(s) or portions of text from **your** paper(s) in your thesis. Permission is now automatically granted; please pay special attention to the implications paragraph below. The Copyright Subcommittee of the Joint Board/Council Committees on Publications approved the following:

Copyright permission for published and submitted material from theses and dissertations
ACS extends blanket permission to students to include in their theses and dissertations their own articles, or portions thereof, that have been published in ACS journals or submitted to ACS journals for publication, provided that the ACS copyright credit line is noted on the appropriate page(s).

Publishing implications of electronic publication of theses and dissertation material
Students and their mentors should be aware that posting of theses and dissertation material on the Web prior to submission of material from that thesis or dissertation to an ACS journal may affect publication in that journal. Whether Web posting is considered prior publication may be evaluated on a case-by-case basis by the journal's editor. If an ACS journal editor considers Web posting to be "prior publication", the paper will not be accepted for publication in that journal. If you intend to submit your unpublished paper to ACS for publication, check with the appropriate editor prior to posting your manuscript electronically.

If your paper has **not** yet been published by ACS, we have no objection to your including the text or portions of the text in your thesis/dissertation in **print and microfilm formats**; please note, however, that electronic distribution or Web posting of the unpublished paper as part of your thesis in electronic formats might jeopardize publication of your paper by ACS. Please print the following credit line on the first page of your article: "Reproduced (or 'Reproduced in part') with permission from [JOURNAL NAME], in press (or 'submitted for publication'). Unpublished work copyright [CURRENT YEAR] American Chemical Society." Include appropriate information.

✳ If your paper has already been published by ACS and you want to include the text or portions of the text in your thesis/dissertation in **print or microfilm formats**, please print the ACS copyright credit line on the first page of your article: "Reproduced (or 'Reproduced in part') with permission from [FULL REFERENCE CITATION.] Copyright [YEAR] American Chemical Society." Include appropriate information.

Submission to a Dissertation Distributor: If you plan to submit your thesis to UMI or to another dissertation distributor, you should not include the unpublished ACS paper in your thesis if the thesis will be disseminated electronically, until ACS has published your paper. After publication of the paper by ACS, you may release the entire thesis (**not the individual ACS article by itself**) for electronic dissemination through the distributor; ACS's copyright credit line should be printed on the first page of the ACS paper.

Use on an Intranet: The inclusion of your ACS unpublished or published manuscript is permitted in your thesis in print and microfilm formats. If ACS has published your paper you may include the manuscript in your thesis on an intranet that is not publicly available. Your ACS article cannot be posted electronically on a publicly available medium (i.e. one that is not password protected), such as but not limited to, electronic archives, Internet, library server, etc. The only material from your paper that can be posted on a public electronic medium is the article abstract, figures, and tables, and

07/03/2007 10:59 FAX 2027768112 002/002

Karen Buehler

From: Himadri S. Mandal [hsm420@mail.usask.ca]
Sent: Wednesday, June 27, 2007 3:53 PM
To: Copyright
Subject: permission to reproduce my published paper in PhD thesis

Dear Sir/Madam,
I'd like to reproduce one of my published papers (including the electronic supplementary information) verbatim in my PhD thesis entitled "Electron Transfer Mechanism and Potential Applications of á-Helical Peptides".

Title of the requested article:"Effect of the Surface Curvature on the Secondary Structure of Peptides Adsorbed on Nanoparticles"
Authors: Himadri S. Mandal and Heinz-Bernhard Kraatz, Journal title: J. Am. Chem. Soc.
Year: 2007
Volume: 129,
pages: 6356-6357

Is it enough if I just print "Reproduced with permission from J. Am. Chem. Soc. 2007, 129, 6356-6357, Copyright [2007] American Chemical Society." on the first page of my chapter, or do I have get permission for this? Print the credit line on the first page of the ACS article, not on the first page of the chapter. ✱
I would highly appeciate if you could kindly clarify this to me. Thanks in advance.
Sincerely,

Himadri S. Mandal
Department of Chemistry
110 Science Place
University of Saskatchewan
Saskatoon, SK S7N 5C9, Canada
Email: hsm420@mail.usask.ca
Phone: (306) 220-8848
Fax: (306) 966-4730